การเพิ่มการยึดติดระหว่างพอร์ซเลนวีเนียร์และโครงเซอร์โกเนียด้วยชั้นแก้วเซรามิกส์

นางสาวกมลพร วัฒนเสริมกิจ

วิทยานิพนธ์นี้เป็นส่วนหนึ่งของการศึกษาตามหลักสูตรปริญญาวิทยาศาสตรดุษฎีบัณฑิต
สาขาวิชาทันตชีววัสดุศาสตร์ (สหสาขาวิชา)
บัณฑิตวิทยาลัย จุฬาลงกรณ์มหาวิทยาลัย
ปีการศึกษา 2556

IMPROVEMENT OF BONDING BETWEEN VENEERING PORCELAIN AND ZIRCONIA SUBSTRATE WITH GLASS-CERAMIC INTERLAYER

Miss Kamolporn Wattanasirmkit

A Dissertation Submitted in Partial Fulfillment of the Requirements
for the Degree of Doctor of Philosophy Program in Dental Biomaterials Science
(Interdisciplinary Program)
Graduate School
Chulalongkorn University
Academic Year 2013

Thesis Title	IMPROVEMENT OF BONDING BETWEEN VENEERING PORCELAIN AND ZIRCONIA SUBSTRATE WITH GLASS-CERAMIC INTERLAYER
By	Miss Kamolporn Wattanasirmkit
Field of Study	Dental Biomaterials Science
Thesis Advisor	Associate Professor Supatra Jinawath, Ph.D.
Thesis Co-Advisor	Assistant Professor Dr. Viritpon Srimaneepong, Ph.D.
	Associate Professor Dr. Kanchana Kanchanatawewat, DSc.

Accepted by the Graduate School, Chulalongkorn University in Partial Fulfillment of the Requirements for the Doctoral Degree

.....Dean of the Graduate School

(Associate Professor Amorn Petsom, Ph.D.)

THESIS COMMITTEE

.....Chairman

(Associate Professor Dr. Pasutha Thunyakitpisal, Ph.D.)

.....Thesis Advisor

(Associate Professor Supatra Jinawath, Ph.D.)

.....Thesis Co-Advisor

(Assistant Professor Dr. Viritpon Srimaneepong, Ph.D.)

.....Thesis Co-Advisor

(Associate Professor Dr. Kanchana Kanchanatawewat, DSc.)

.....Examiner

(Assistant Professor Dujreutai Pongkao Kashima, Ph.D.)

.....Examiner

(Assistant Professor Sirithan Jiemsirilers, Ph.D.)

.....External Examiner

(Naruporn Monmaturapoj, Ph.D.)

.....External Examiner

(Professor Serena Michelle Best, Ph.D.)

กมลพร วัฒนเสริมกิจ : การเพิ่มการยึดติดระหว่างพอร์ซเลนวีเนียร์และโครงเซอร์โกเนียด้วยชั้นแก้วเซรามิกส์. (IMPROVEMENT OF BONDING BETWEEN VENEERING PORCELAIN AND ZIRCONIA SUBSTRATE WITH GLASS-CERAMIC INTERLAYER) อ.ที่ปรึกษาวิทยานิพนธ์หลัก: รศ. ดร. สุพัตรา จินาวัฒน์, อ.ที่ปรึกษาวิทยานิพนธ์ร่วม: ผศ. ทพ. ดร. วิริทธ์พล ศรีมณีพงศ์, รศ. ทญ. ดร. กาญจนา กาญจนทวีวัฒน์, , หน้า.

ลิเทียม ไดซิลิเกตกลาสเซรามิกส์ถูกนำมาใช้เป็นชั้นระหว่างโครงเซอร์โกเนียกับพอสเลนส์ฉาบผิว เพื่อวัตถุประสงค์ ลอกเลียนลักษณะการใช้งานจริงในทางทันตกรรม ซึ่งมีการเผาซ้ำหลายรอบ ชิ้นตัวอย่างการทดสอบที่เคลือบผิวด้วยพอสเลนส์ ซึ่งถูกเตรียมด้วยกระบวนวิธีที่ผู้ผลิตแนะนำซึ่งใช้กับระบบเซอร์โกเนียร์ เพื่อให้มีศักยภาพ ค่ากำลังยึดเฉือน มีค่าเป็นไปตามกำหนด เพื่อเปรียบเทียบ ผลลัพธ์ของคุณสมบัติเชิงกล ค่ากำลังยึดเฉือน ค่าความแข็งผิวชนิดวิกเกอร์ และความทนต่อการแตกหักที่ตำแหน่งรอยต่อการเชื่อมยึด ถูกนำมาวิเคราะห์ ในแง่สัมพันธ์คุณสมบัติทางฟิสิกส์ เช่นลักษณะทางกายภาพและ โครงสร้างผลึก รวมถึงพื้นผิวภายหลังการแตกหักของรอยต่อการเชื่อมยึด โดยการตรวจสอบด้วยภาพจากกล้องจุลทรรศน์อิเล็กตรอนแบบส่องกราด อุปกรณ์วิเคราะห์ธาตุเชิงพลังงาน กล้องจุลทรรศน์ชนิดสเตอริโอและ อุปกรณ์วิเคราะห์การเลี้ยวเบนรังสีเอ็กซ์ นอกจากนี้ยังศึกษา ความเข้ากันได้ทางชีวภาพ และการทดสอบด้วยรอบน้ำร้อน-เย็น จากชิ้นตัวอย่างที่เลือกสรร เพื่อให้มั่นใจว่าเหมาะสมกับการใช้งานทางคลินิก จากการศึกษานี้ ค่ากำลังยึดเฉือนที่วัดได้จากกลุ่มที่มีลิเทียมไดซิลิเกตที่เผาที่อุณหภูมิที่เหมาะสม มีค่าสูงกว่ากลุ่มพอสเลนส์ฉาบผิวที่ใช้อยู่ ณ ปัจจุบันซึ่งเป็นแก้วเซรามิกส์ชนิดลูไซด์ และกลุ่มที่ปราศจากชั้นกลาสเซรามิกส์ อย่างมีนัยสำคัญ นอกจากนี้ คุณสมบัติต่างๆที่เหนือกว่าในด้านเชิงกล เชิงความเข้ากันได้ทางชีวภาพ เชิงความทนทาน และค่าสัมประสิทธิการขยายตัวความร้อนที่เสถียรกว่าเป็นต้น ทำให้ ลิเทียมไดซิลิเกตกลาสเซรามิกส์ ได้รับการยืนยันว่าเป็นวัสดุ ที่มีคุณสมบัติโดยรวมเหนือกว่าลูไซด์กลาสเซรามิกส์

สาขาวิชา ทันตชีววัสดุศาสตร์ ลายมือชื่อนิสิต .....

ปีการศึกษา 2556 ลายมือชื่อ อ.ที่ปรึกษาวิทยานิพนธ์หลัก .....

ลายมือชื่อ อ.ที่ปรึกษาวิทยานิพนธ์ร่วม .....

ลายมือชื่อ อ.ที่ปรึกษาวิทยานิพนธ์ร่วม .....

5187751520 : MAJOR DENTAL BIOMATERIALS SCIENCE
KEYWORDS: ZIRCONIA / LITHIUM DISILICATE / SHEAR BOND STRENGTH / GLASS CERAMIC

KAMOLPORN WATTANASIRMKIT: IMPROVEMENT OF BONDING BETWEEN VENEERING PORCELAIN AND ZIRCONIA SUBSTRATE WITH GLASS-CERAMIC INTERLAYER. ADVISOR: ASSOC. PROF. SUPATRA JINAWATH, Ph.D., CO-ADVISOR: ASST. PROF. DR. VIRITPON SRIMANEEPONG, Ph.D., ASSOC. PROF. DR. KANCHANA KANCHANATAWEWAT, DSc, pp.

Lithium disilicate glass-ceramic was introduced as interlayer between zirconia substructure and veneering porcelain. To simulate dental practice which involved multiple firings, the experimental samples of porcelain veneer were prepared following the veneering procedure recommended by suppliers of zirconia system and to assess the performance, mean shear bond strengths (SBS) of porcelain veneers consisted of lithium disilicate glass-ceramic and commercial glass-ceramic liners were determined in comparison. The obtained mechanical results of SBS, Vickers hardness and fracture toughness at the bonding interface are discussed in relation to physical properties, i.e. morphologies and crystal phases of the fired porcelain veneers including fracture surfaces respectively investigated by SEM, EDX, XRD and stereomicroscope. Moreover, biocompatibility and thermocycling tests were also performed on the selected specimens to assure clinical viability. It is found that the SBSs of porcelain veneers consisted of lithium disilicate glass-ceramic of which were fired at optimal conditions are significantly higher than those of porcelain veneers consisted of the current commercial leucite glass-ceramic liners and without glass-ceramic liner. In addition to good mechanical properties, biocompatibility, durability and the better CTE stability over that of leucite glass-ceramic, lithium disilicate glass-ceramic has been proved to be a potent glass-ceramic liner for porcelain veneer.

Field of Study:	Dental Biomaterials Science	Student's Signature .....
		Advisor's Signature .....
Academic Year:	2013	Co-Advisor's Signature .....
		Co-Advisor's Signature .....

ACKNOWLEDGEMENTS

I would like to thank my advisors and mentors, Associate Professor Dr. Kanchana Kanchanathawewat, Assistant Professor Dr. Viritpon Srimaneepong and Associate Professor Dr. Supatra Jinawath for their guidance, help, and knowledgeable advice throughout my research. I really appreciate their concern about the quality of my work, my academic and professional goals. I would also like to thank Professor Dr. Serena Best, Director of the Cambridge Centre for Medical Materials for useful discussions and guidance with laboratory work, as well as continuous help and opportunities she kindly provided for my experiment at the Department of Materials Science and Metallurgy, University of Cambridge, U.K. I would also like to gratefully thank Dr Naruporn Monmaturapoj for her valuable suggestions and kindness in preparing me the lithium disilicate glass-ceramic. I would also like to thank Associate Professor Dr. Pasutha Thunyakitpisal and the staff of Dentistry Department and the Graduate School, Chulalongkorn University, for their administrative support. I am also indebted to the Office of the Higher Education Commission, Ministry of Education of Thailand, for granting me the financial support under the project "Strategic Scholarships for Frontier Research Network". Last, but not least, I would like to thank assistant Professor Dr. Wantanee Buggalcupta, my friends and my family for their support, patience, and confidence.

CONTENTS

Page

Page

LIST OF FIGURES

LIST OF TABLES

Chapter 1
Introduction

"Zirconia", the most modern dental ceramic in this century, has been used in the medical field as the bearing surfaces in hip transplant prosthesis because it has good mechanical properties such as wear resistance and fracture toughness and good biocompatibility with many cell types. In dentistry, zirconia was first used as filler particles for strengthening dental all-ceramic crown substructures. The pleasant white color and transformation toughening properties have led to the wide spread use of zirconia as a major component of all ceramic crown substructures or a dental implant abutments.

There are 3 different types of zirconia that have been used in dental applications: yttrium doped tetragonal zirconia polycrystal (Y-TZP), Magnesium doped partially stabilized zirconia (Mg-PSZ) and zirconia toughened alumina (ZTA). All ty pes are suitable for dental applications but the use of each zirconia system depends on a company's freedom to operate base on the patent landscape. These patents cover not only the component design, but also the protection of processing and sintering schdules which are unique for each system. The fully sintered disc belongs to Zircon company while there are many product systems produced as partially sintered blank such as the Lava system and the VITA Zahnfabrik block system. Some companies (i.e. Katana system) produce only isostatic pressed blocks without sintering process, hence the block is soft. The main reason is to reduce milling time while processing. When milling the block, the soft unsintered ones can be process/shaped easily, so the milling time is short. However, the dimension of the softer one changes significantly after sintering. In contrast, there is no further dimensional change for the fully sintered block but it is hard to mill and results in a long fabrication time.

After preparation, the zirconia substructure has to be masked with veneering porcelain to make it look like natural teeth. Mechanism of bonding between veneering porcelain and zirconia substructure is still controversial. However, in clinical studies, chipping of the veneering porcelain from the zirconia substructure

after fixing and functioning in the oral cavity has been a major problem. Acording to Sailer [1], there was a failure rate to 15% after 2 years [2, 3] and 13% after 3 years [1]that porcelain chipped off from zirconia substructure. Therefore, some researchers claimed that only a micromechanical bond exists between the zirconia substructure and the porcelain veneer [2], while others argued that both mechanical and chemical bonds could be formed between these two materials.[4, 5] So far there has been no solid proof as to whether zirconia can or cannot form a chemical bond with porcelain. However, zirconia is still useful and attractive in the field of dentistry.

Of all the methods reported to improve bonding, the chemical/mechanical means, by applying an optional liner material between the zirconia core and veneer seems to be the most interesting and several systems of glass or glass-ceramic have been developed and modified to this end.

Research question

At present, there is still controversy among dentists on whether using a commercial glass or glass-ceramic as an intermediate layer lining between zirconia and the veneering porcelain would improve bond strength. These ideas are based on the assumption that melted glass would penetrate and form a micromechanical interlock with the zirconia surface while also forming a chemical bond with porcelain.

Objective

This study is an attempt to answer the above question by determining the shear bond strength and studying the fracture surface of composite specimens with and without a glass-ceramic liner. Inaddition, a novel lithium disilicate glass-ceramic has been investigated to explore whether the lower CTE and crystal morphology, would enhance the bonding between a zirconia substructure and veneering porcelain in comparison with commercial glass liner and hence favour long term clinical success of this all-ceramic type of veneer/restoration.

Research hypothesis

The bonding between the zirconia core and veneering porcelain may be significantly improved by employing interlayer of glass or glass-ceramic having suitable crystal morphology for micromechanical interlocking and high CTE stability.

Scope of research

1. To fabricate composite specimens of all ceramic crowns composed of a zirconia core veneered with leucite porcelain.
2. To enhance the adhesive bonding strength between the zirconia core and the veneering porcelain by a liner material (glass or glass-ceramic) between the zirconia core and the veneering porcelain**.**
3. To characterize the chemical, physical and mechanical properties of the starting materials and the composite specimens. In addition to perform a thermocycling test of the composite. An *In vitro* biological study of the glass-ceramic liners will also be performed to respectively simulate the oral environment in terms of durability and biocompatibility.

Research conditions

Specimens employed in this study are designed according to ISO standard

1. ISO No. 11405 for shear bond strength testing
2. ASTM C 1372 for Vickers' indentation test
3. ASTM E112-10 for Average grain size analysis

Limitation:

The biocompatibility study was carried at a laboratory scale *(in vitro)* and cannot fully mimic real oral cavity environment, to reproduce condition such as, occlusal force, temperature and acid-base variation.

Advantages

Experience from this study will throw some light on the possible to improve bonding between the zirconia substructure and the porcelain veneer for long term clinical success, thus reducting the likelyhood of failure as a result of delamination of the veneering porcelain from the substructure. Moreover, since there has not been any research relevant to this topic reported from any dentistry institutions in Thailand and elsewhere, this study will provide benefit in terms of academic and clinical information.

Chapter 2
Literature Review

Zirconia frameworks substructure provide good mechanical properties, a pleasant color and high level of biocompatibility. These favorable characteristics make it sue wide spread and increasingly popular in dentistry. Apart from usage of crowns and bridges, It has been used in prefabricated post and core ceramic systems such as Cosmo post (Vivadent), Snow post (Danville), implant fixture [6] and implant abutment [7].

Zirconia or Zirconium oxide (ZrO_2) was first reported by the German chemist, Martin Heinrich, in 1789. These materials were formed after heating some jewels. A long time ago, it was used as a ceramic pigment to blend with rare earth oxides and could be used as additive to enhance the properties of other oxides in term of refraction[8].

For biomedical applications, zirconia was manufactured as a ball head in hip prosthesis to replace the more brittle alumina [9]. The most favorable prominent property of zirconia is “transformation toughening” which makes the zirconia have higher resistance to crack propagation and inhibit crack growth by taking energy from the crack and promoting dimensional change. This phenomenon will compress the crack around the object. This leads to the development of a compressive strength and increase the energy required for crack propagation. Furthermore other mechanisms such as microcrack toughening and contact shielding can also to be used to toughen zirconia [10].

Zirconia occurs in three crystallographic forms: monoclinic (M), tetragonal (T) and cubic (C). At room temperature pure zirconia, the most stable phase is the monoclinic crystal structure and this remains the case up to 1170 ^{0}C. At higher temperatures, the monoclinic phase transforms a tetragonal phase which then transforms into a cubic phase when the temperature reaches 2730 ^{0}C. In contrast, the transformation from the cubic phase to the monoclinic phase happens during cooling and is always accompanied by volume expansion. The volume expansion from the cubic to the tetragonal phase is about 2.31 % and from the tetragonal phase to the monoclinic phase is 4.5 %. Ruff et al. found that small amount of CaO could stabilize Cubic phase down to room temperature[11]. Gravie and Nicholson also reported that the addition of a "stabilizing oxide" in small amounts such as calcia (CaO), magnesia (MgO), labria (La_2O_3) and yttria (Y_2O_3) could result in the retention of the cubic and tetragonal structure at lower temperatures [12]. 8 mol% of Y_2O_3 or MgO can stabilize fully cubic zirconia while partially stabilized zirconia (PSZ) can occur with a contration of 2-5 mol% of dopant[13]. Gravie and Nicholson also observed that the metastable tetragonal phase (T) was able to transform into the monoclinic phase (M) when mechanical energy was put into the system (stress). In that situation, the strain generated by volume expansion due to the phase transformation will act against the driving force promoting crack propagation. Therefore the object is more tough because the energy driving crack propagation is absorbed by the T to M transformation mechanism and compressive strain due to volume expansion [12]. This phenomena is called "Transformation toughening" by Piconi and Maccauro in 1999 [8].

The metastable phase of zirconia are prone to aging in moist environments (water or vapor, body fluid or during stream sterilization) and are sensitive to lower temperature degradation. Aging is a slow process, happening especially at surfaces that are in contact with moisture. This results in the degradation of the mechanical properties[8, 14].

Chevalier explained that the T to M transformation starts at the surface grains first and leads to phase instability. This transformation is a continuing process beginning step by step from one grain to another grain. The strain generated by volume expansion acts on the neighboring grain so that a microcrack is formed, water can then penetrat down by microleakage and the surface can lift in a dome like shape and finally surface grain can pull out[15]. Catastrophic failure of metastable zirconia could occur following this degradation of the mechanical properties[8]. The variability of aging depended on the sintering process[15] (temperature and time, etc.) while Liiley has explained that microstructural parameters (yttria concentration and distribution), grain size, flaw population and distribution of the materials additional factors might also have a strong influence on the aging mechanism[16].

In 1991, Swab described TZP aging in the following ways[17] :

(1) The most critical temperature range was 200-300 ^{0}C.

(2) The effects of aging were a reduction in strength, toughness and density, and an increase in monoclinic phase content.

(3) Degradation of mechanical properties was due to the T to M transition, taking place with micro and macro-cracking of the material.

(4) T to M transition started on the surface and progressed into the material bulk.

(5) Reduction in grain size and/or increase in concentration of stabilizing oxide reduced the transformation rate.

(6) T to M transformation was enhanced in water or in vapour.

Haraguchi was the first person to report that the surface degradation of zirconia was caused by phase transformation. He found that 20-30 % monoclinic content in 3-6 year old zirconia implants were associated with increase surface roughness[18]. Catledge et al. studied the degradation of surface properties by investigating nano-identation hardness and found that the hardness dropped from 18 to 11 GPa in the transformd area with monoclinic content ranging from 0-78 %[19].

According to Denry and Kelly, dental zirconia was classified into three types. First is zirconia toughened alumina (ZTA). The second is magnesium cation doped partially stabilized zirconia (Mg-PSZ) and the other one is yttrium cation doped tetragonal zirconia polycrystals (3Y-TZP) [20].

Glass-infiltrated zirconia-toughened alumina (ZTA) is commercially available on only one zirconia system called “In-ceram ®zirconia” (Vident™, Brea, Ca)” In-ceram contains 33 vol% of 12 mol% Ceria-stabilized zirconia (12 Ce-TZP) in composition of Inceram-alumina. There are two steps for fabricating a crown substructure. The first one is a slip-casting process and the second step is a glass infiltration process. The initial temperature for sintering after the slip casting process is 1,100 $^{\circ}$C for 2 hours. After the first sintering, the substructure looks like an egg shell

with an interconnected pore structure. After that the glass infiltration process will strengthen the substructure. The advantage of the technique is that shrinkage from the sintering process can be limited. However the porosity resulting from this method is greater than that of 3Y-TZP and hence mechanical properties are lower. Improvement the properties of this type of material can be achived by dispersing fine grain of zirconia toward alumina matrix at the stage of raw material powder preparation [21-23].

The second type of dental zirconia, Partially stabilized zirconia (PSZ), has a large grain size (30-60 μm.) with generalized porosity[8]. The amount of magnesium dopant (Mg) is approximately 8-10 mol%. Because of the high sintering temperature about 1600°C-1800°C and long range for cooling down, the temperature must be strictly controlled. The example of this system is Denzer-M (Dentronic AB)[24].

TZP is a system of zirconia ceramic which consists of only the tetragonal phase at room temperature, and contains Y_2O_3 approximately 2-3 % as dopant. For clinical application, green blocks, presenter blocks and fully sintered blocks of 3Y-TZP are most frequently used for fabricating dental crowns and fixed partial dentures [25].

The mechanical properties of 3Y-TZP are affected by grain size, sintering conditions and fraction of dopant content. Some studies reported that a large grain size is formed at high temperatures and long sintering times and T to M transformation occurs more easily than for small grain sizes[26-28]. The small grain size is formed at lower sintering temperatures and short sintering times prevent/suppress transformation and lead to a reduced fracture toughness in the

substructure[29]. Reverse transformation from the monoclinic phase to the tetragonal phase can occur when reheating at 900^{0}C- 1000 ^{0}C for 1 min. Gupta et al. reported that the strength of materials depends on the amount of tetragonal phase present, hence a higher content of tetragonal phase provides a higher strength materials[30].

3Y-TZP has density of about 6 g/cm^{3} with porosity below 0.1 % and a bending strength of approximately 900-1200 MPa. Compressive strength is 2000 MPa and Young modulus is 21 GPa. Fracture toughness (K_{1C}) is 7-10 MPa/$m^{1/2}$. Coefficient of thermal expansion (CTE) is 10 x 10^{-6} K^{-1} with thermal conductivity of 2 Wm/K and hardness of 1200 HV.

There are three types of block used in dental field: green stage block (milled by dry carbide bur), pre-sintered block (milled by diamond with cooling liquid) and fully sintered block (milled with the same technique and instrument with pre-sintered block).

Today, there are at least two zirconia systems of fully sintered block such as Denzir® (Cadesthetics AB) and DC-Zirkon® (DSC Dental AG) prepared by the following method[31]. The block is pre-sintered at a temperature below 1500 ^{o}C until its density is near 95 % theoretical density. After that the block is processed by Hot Isostatic Press (HIP) at 1400 ^{o}C -1500 ^{o}C in an inert atmosphere to achieve 99 % of theoretical density. The advantage of this fully sintered block is dimensional stability and hence no more changes occur during final fully sintering of substructure is fabricated. The disadvantages of this block type are high hardness, low machinability, long milling times and wear of milling burs[32]. Blue reported that fully sintered Y-TZP block was significantly harder than fully sintered alumina block when measured

using milling rate[33]. In 1999, Kosmač reported that grinding fully sintered blocks with a bur had less effect on the T to M transformation than a sandblasting procedure[34].

The second type of block is pre-sintered block or partially fired zirconia block. This block is milled by computer aided machining and is then fully sintered at high temperature to make it strong enough to support the crown. The prepared block of this type consists of spray-dried agglomerates of powder and binder about 60 μm in diameter and the binder is eliminated in the pre-sintering step. These two compositions are manufactured by cold isostatic pressing that creates a pre-sintered block with approximately 20-30 nm in pore size. The density of each blank is measured in order to calculate and compensate for shrinkage at the final step. The generalized final density of the pre-sintered block is about 40 % of theoretical density. For the exact compensation, each block has a barcode containing the density for that block[32]. Then the block is milled using diamond bur and cooling liquid into an oversized crown form and shaded by immersing into metal salt. Therefore the color will be developed during final sintering stage but some system can be individualized through adding some oxide to the green stage framework (e.g. Vita shade concept, Vita Zahnfabrik, Bad Sackingen, Germany)[31]. The sintering process should be done in an ambient furnace, the sintering temperature is increased from 1000 $^{\circ}$C until reaching the final temperature at 1350°C-1550°C range. Then the crown form is held at this temperature for 2-5 hours until densified density reaching 99 % of theoretical density with an approximate 25-30 % of volume shrinkage. Once the sintering process is complete, the zirconia substructure is ready for a veneering porcelain, to make the final restoration[20]. The examples of this

block system are YZ cube for Cerec in lab®(vident™); Zs-blank, Everestt; Hint-ELsZirkonTZP-W, DigiDent; DC-Shrink, Precident[31].

The third type of block is green stage block. This block can be milled with a carbide bur in a dry environment without water cooling. Product examples of this group are Cercon®(Dentsply International) and Lava™(3M™ESPE™).[31]

Veneering porcelain is used to improve aesthetics of framework substructures. Ingeneral, dental porcelain is an inorganic structure bonding together with strong covalent forces that gives its properties: a high elastic modulus, and susceptibility to brittle fracture and including chemical inertness.

The main compositions of dental porcelain are quartz, kaolin and feldspar. Quartz is one form of silica with a high melting point and it functions like a framework of porcelain giving strength and reducing translucency in high concentration. Kaolin is one form of clay that is used in very low concentration (4 % or no use) in dental porcelain because of its ability to provide opacity property.

Feldspar or alkali metal ions such as sodium or potassium function as a flux by breaking down or interrupting the bond between silicon atom and oxygen atom during the firing stage. In this way the structure of silica network may be changed from a tetrahedral structure into a linear chain, able to move more easily at temperatures below the melting point and increase in coefficient of thermal expansion. When both Na_2O (Soda) and K_2O (potash) feldspar are fired with various metal oxides at high temperature, a crystal phase called “leucite” can be formed.

Leucite is crystalline structure of potassium-aluminium-silicate (K_2O-Al_2O_3-SiO_2) with a large CTE (28 $\times 10^{-6}$ K^{-1})[35]

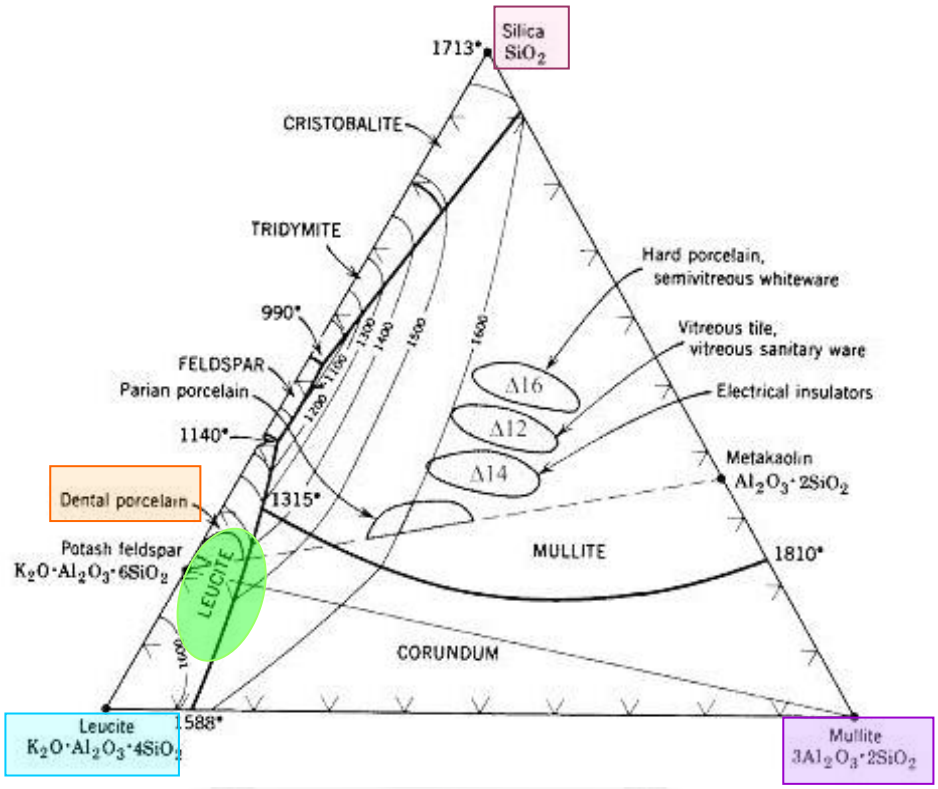

Figure 2.1 Composition of dental porcelain containing only 4 % or no kaolin while content of feldspar is high as 75 %-81 % for its properties of light reflection and translucency like natural teeth

The coefficient of thermal expansion (CTE) of dental porcelain depends primarily on the content of leucite crystals in the glass matrix. The leucite crystal concentration by heating the porcelain and holding at final temperature for long time or leaving it slowly cool after firing or firing the porcelain for many cycles may be generate many crystals of leucite and change the CTE of porcelain, cause of

thermal mismatch between porcelain and substructure. In addition tensile stress can be generated during cooling down and causes microcrack and delamination of porcelain from substructure. In general, the CTE of veneering porcelain must be lower than substructure material, approximately $0.5x10^{-6}$ K^{-1} or less, to generate compressive stress during cooling or compression bonding. Therefore, fracture from CTE mismatch dose not occurr because of the good “thermal compatibility” [36]

Guazzato et al. found that the CTE mismatch between core and veneering porcelain caused cracks to initiate and propagate along the interface of the veneering porcelain. They indicated that zirconia had lower CTE than most other ceramic materials[37]. Therefore low CTE veneering porcelain has been developed to reduce these problems. A study by Saito et al. on bonded zirconia with 5 brands of veneering porcelain investigated the relationship between CTE and shear bond strength. Finally, they concluded that shear bond strength was affected by strong discrepancies in CTE[38].

However, there were some reports of clinical failure. Vult Von Steyern et al. reported that veneering porcelain chipped from zirconia substructures at a rate of 15 % in 24 months in service[3] while the chipping of porcelain was 13 % in 36 months[1] and 25 % in 31 months Pjeturson et.al[39]. Quinn et.al. compared edge chipping between veneered zirconia and porcelain fused to metal specimens, it was found that both types of specimens had similar resistance to chipping. The chip detached and did not penetrate into the substructure when they reached the interface[40].

Yin et al. reported that shear bond strengths of 3Y-TZP (Chinese block) and 4 brands of veneering porcelain (Vita VM9, Shofu vintagezr, IPS e.max ceram and Cercon ceram Kiss) were not significantly different within the ceramic groups and metal ceramic system (Ni-Cr alloy/Vita VMK 95) with an adhesive failure mode at the interface [41]. Özkurt et al. tested shear bond strengths of 4 types of zirconia (Zirkonzahn, Cercon, Lava, DC Zirkon) bonded to veneering porcelain and concluded that bond strength differed according to type of zirconia and manufacturer-recommended veneering porcelain. The mode of failure was predominantly adhesive failure[42].

The cause of adhesive failure is bonding problems. Bonding between two substrates can be classified into several divisions. The basic mechanisms of bonding for porcelain fused to metal crown are mechanical bond, chemical bond and compression bond. Mechanical bond is an interlocking bond on the interface. Many methods are used to achieve this, such as grinding, sandblasting and electro-plating to produce or modify a rough irregular surface of substructure that serves as a retainer for dissolved fired porcelain.

The chemical bonding of porcelain fused to metal substructure occurs due to fusion at the interface and holding electrons to produce a bonding force. Glass, has the major component SiO_2 which forms a tetrahedral structure by Si atoms which are located in the center and surrounded by oxygen atoms. Many types of metal oxide which have been formed on metal surface such as SnO_2, In_2O_3 and Fe_2O_3 could dissolve in molten glass and bond to Si atoms by substitution of an oxygen atom, leading to relaxation of glass network and a decrease in internal energy. This glass

phase with low internal energy in the molten state makes contact with metal. The bond between metal and glass may be achieved easily. Additionally, oxygen free radicals from the silica network are oriented toward the metal base and can establish a chemical bond between the metal and glass.

Bonding from compressive forces is caused by differences in the CTE between two substrates. The values of compressive forces are of the order of 70-80 kg.f /cm^2 which is different and independent from chemical and mechanical bonds.

Unlike porcelain fused to a metal crown, the surface treatment of ZrO_2 such as grinding, polishing, sandblasting and treatment to produce a mechanical bond is still controversial. All surface treatments cause some degree of T to M transformation. Grinding increases the strength of metastable zirconia because the process including T to M transformation generates surface compressive strain by volume expansion [43]. The lattice strain and T to M transformation were confirmed by Reed and Lejus[44]. Ruiz and Ready in 1996 and Kitano et al. in 1988 suggested that rhombohedral phase on ground zirconia surface was formed from tetragonal phase transformation under stress[27, 45]. The T to M transformation occurred after surface grinding and sandblasting, and the compressive stress was generated by volume expansion leading to increase in strength of zirconia[46]. In conclusion, strength of this material depends on amount of transformed M phase, metastability of T to M transformation, grinding severity and developed temperature[47].

Kosmač showed that the critical flaw size was decreased about 30 % when using water spray during grinding and Weibull modulus of the ground zirconia dropped by about one-third to one-half of the initial value[34].

The sandblasting technique has been reported to be able to promote transformation of the zirconia substructure because the particle of sand damages the surface of zirconia including generate erosive wear and microcracks[47]. However, Kosmač et al. found that sandblasting after grinding could reduce flaw size of the ground zirconia surface[34].

Nakamura et al. studied tensile bond strength between tooth-colored porcelain and sandblasted zirconia framework and concluded that after sandblasting the zirconia framework with a pressure of 0.4 MPa., it developed a highest strength bond with tooth-colored porcelain[48]. This is in contrast with Fischer who investigated the shear bond strength of zirconia and veneering porcelain and concluded that the increase in surface roughness of zirconia did not enhance shear bond strength and regeneration firing decreased shear bond strength[5].

Another technique for modifying bonding between these two substrates is a pressing technique. Alnasar et al. compared the shear bond strength between press on porcelain and layering veneer porcelain bonded to the zirconia substructure and found that conventionally layering applied porcelain had a higher bond strength than the press on to porcelain technique [49]. On the contrary, Aboushelib found that press on porcelain veneer showed less crystallization compared with the layering porcelain veneer which had higher Na^{+} and K^{+}. The high concentration of alkaline ions could generate a high CTE and produce a residual tensile stress between the zirconia substructure and veneering porcelain interface leading to interfacial failure[50].

Aboushelib et al. investigated effect of an liner material between the zirconia core and veneer and found that use of liner with layered veneer increased bond strength, except “Nobel Rondo” by Nobel Biocare, and decreased in bond strength for pressable veneers and also observed that application of a liner decreased adhesive failure for layered porcelain but increased it for pressable veneer porcelain[51].

Yin et al. reported that after investigating the mode of failure of 3Y-TZP bonded to VM9 by EDS, they found that element of silicon diffused into the 3Y-TZP material[41]. Saito et al. also claimed the that mode of failure between ZrO_2 and Cercon ceramkiss was a cohesive failure in veneering porcelain and by XRD analysis of interfaces revealed that amorphous glasses can diffuse into the zirconia surface but no amorphous glasses were shown on air-borne particle abrasion surface[38].

The glass-ceramic liner composition is feldspathic porcelain. First, glass application is used to modify the color of the substructure. Nowadays, this approach is thought to enhance adhesive bonding to the zirconia substructure by creating mechanical and chemical bonds. In addition, melting flowable glass should seal the zirconia surface from moisture and reduce the chance of low temperature degradation[52, 53].

Glass-ceramics are composed of two phases: a crystal phase and a glassy matrix. The chemical composition and thermal history are major keys to control the glass-ceramic formation process.

Forming of the glass-ceramic is achieved by two major mechanisms: a nucleation process and a crystal growth process. At the beginning, glass is melted

beyond its melting point, then the temperature is use to control the nucleation and precipitation of the crystal in the amorphous glass matrix.

After that, the crystal growth process is controlled by heating the temperature beyond the maximum nucleation rate but below the melting point which allows the mechanism to begin.

Physical and mechanical properties of the glass-ceramic such as density, chemical durability and coefficient of thermal expansion are dependent on the proportion of crystal phase: remaining residues glass matrix. In addition, the microstructure of the glass plays an important role on chemical, mechanical and thermal properties.

The nucleation process is the major factor to control, following the crystallization process and also the properties of glass-ceramic. This mechanism divided in two subtypes: surface nucleation and volume nucleation. At first, some atoms arrange together known as embryos, Larger and more stable embryos form the nuclei of crystals. Later, the process of crystal growth occurs and will stop when crystals contact to each other. This mechanism is called 'volume nucleation'. In contrast, surface nucleation begins at the surface without internal nucleation process and this results in distortion.

The nucleation rate and crystal growth rate are controlled by two factors. The first one is a thermodynamic factor and the second one is a kinetic factor. At higher temperatures beyond the melting point, crystals are dissolved. The nucleation rate and crystal growth rate have a negative value. While at the melting point, the crystal growth rate is equal to zero and no crystals are formed. The nucleation rate is driven by only kinetic factors. However, when the temperature range is below the melting

point, the nucleation rate and growth rate of the crystals are controlled by thermodynamic factors.

Glass-ceramics with low thermal expansion and glass-ceramics with high mechanical strength (zirconia-containing glass-ceramics and lithium disilicate glass-ceramics) are examples of the application of nucleation and crystallization control. Glass-ceramics derived from silica-alumina-potash feldspar (SiO_2-Al_2O_3-K_2O) system can be generated by surface nucleation and crystallization. The process begins at the grain surface and runs into the bulk of the glass during the sintering process. When using glass dusts as seeding particle, the nucleation rate is higher with two dimensional crystal growths. In contrast, if let it growth without seeding particle, the nucleation was low with anisotropic growth crystal[54]. The main crystal phase of silica-alumina-potash feldspar system is leucite (K_2O-Al_2O_3-$4SiO_2$). This type of glass-ceramic is generally used for dental restoration as veneering materials of porcelain fused to a metal crown. In addition, it can be shaped by lost wax with heat press technique or CAD/CAM technique to produce inlay and core materials of all ceramic crown (IPS Empress® System: Ivoclar-Vivadent, Schaan, Liechtenstein)[55]. This type of glass cerammic has good optical properties and good sinterability even though the coefficient of thermal expansion is high.

Lithium metasilicate and lithium orthophosphate, formed by volume crystallization, was discovered in the 1990s. by Headley and Loehman. They claimed that this type of glass-ceramic has 65 % by volume of crystal content and is strong enough to be used as crown or anterior 3-units bridges substructure[56].

At the first stage lithium metasilicate is formed at the lower temperature, then lithium disilicate is formed later during the heat treatment process. HÖland et al. found that over a range of the temperatures between 530-700 $^{\circ}$C, lithium metasilicate crystals were fast growing, and at higher temperatures, lithium orthophosphate crystal phase (Li_3PO_4) began to form and growth at 700 $^{\circ}$C. At higher temperatures (above 700°C) lithium disilicate crystals began to form and then grew in size to approximately 0.5-3 μm at the heat treatment temperature of 850°C[55].

Seeding particles, P_2O_5 were used as nucleating agents during the crystallization process of this type of glass, helping to control surface crystallization and nucleation[55].

All of the powder-based glass is produced in the form of a cylinder ingot. When fabricating a crown, the ingot will be heated and transformed into a viscous state. Then pressure of about 10^5-10^6 Pa is applied to press the melted glass at 920 $^{\circ}$C for 5-10 min in special furnace to form the crown substructure. Finally, the crown or bridge substructure will be covered and veneered with fluoroapatite porcelain[54].

A glass-ceramic with needle-like fluorapatite crystals was developed by Schweiger (2002). The nucleation mechanism of this glass-ceramic is very fast. After heat treatment at 700 $^{\circ}$C, crystals of needle-like fluorapatite grow along C-axis direction with diameter 60 nm and 300 nm in length. This type of glass-ceramic has good chemical durability and translucence and is used as a highly aesthetic material to veneer on the lithium disilicate glass substructure.

However, there are two studies investigating glass-ceramics applied for adhesive bonding to zirconia substructure. Zang and Kim tried to improve the aesthetics and bonding properties of zirconia substructure by applying a new family

of glass in the SiO_2–Al_2O_3–K_2O–Na_2O–CaO–Tb_4O_7 system to infiltrate Y-TZP. Finally, they found that the mechanical properties of infiltrated Y-TZP were higher than the control group and bonding between the zirconia and glass was a micromechanical bond. They called layer of bond a “graded layer” and concluded that using a combined glass infiltration/densification technique offered the infiltrated Y-TZP better resistance to immediate flexural damage, better aesthetics, and potentially better veneering and cementation properties over homogeneous Y-TZP.[53] The other study was performed by Ntala in 2010. Who tried to develop multi-phase glaze coatings for zirconia, so that the surface could be etched and adhesive bonded. The result revealed that the application of 20 wt% IPS Empress 2 glass-ceramic mixing with 80 wt% IPS e.max Ceram glaze containing lithium disilicate phase might improve the bond strength of zirconia substructure[57].

Chapter 3
Matrerials and Methods

3.1. Materials

Two commercial zirconia systems and lithium disilicate glass-ceramic [prepared in-house by National Metal and Materials Technology Center (MTEC)] were used in this experiment.

Each commercial zirconia system is commonly provided as pre-sintered block with commercial glass-ceramic liner and veneering porcelain. The detailed chemical compositions disclosed by the manufacturers are shown in Error! Reference source not found.

Table 3.1 Zirconia systems and sintering schedules

Core materials (pre-sintered)	manufacturer	Lot No.	Compositions	Sintering Temperature, ^{O}C	Sintering time, hrs	CTE $x10^{-6} K^{-1}$
Lava™ zirconia block	3M™ESPE™, Seefeld, Germany	386993	96 wt% ZrO_2, 3 wt% Y_2O_3, < 0.25 wt% Al_2O_3	1,480 ^{O}C	7.5 hrs.	10.5
VITA In-Ceram® YZ for inLab®	VITA Zahnfabrik, Bad Säckingen, Germany	10730	95 wt% ZrO_2, 5 wt% Y_2O_3, <3 wt% HfO_2, <1 wt% Al_2O_3 and SiO_2+other oxides	1530^{O}C	8 hrs.	10.5

Table 3.2 Properties of glass-ceramic liners

Lining material	manufacturer	Lot No.	Composition	CTE $x10^{-6} K^{-1}$
Lava™ Ceram Frame-Work Modifier (Commercially recommended liner)	3M™ESPE™, Seefeld, Germany	7888G	95-100 wt% ceramic powder 5 wt% pigment	10.5
VITA VM® 9 Effect Bonder (Commercially recommended liner)	VITA Zahnfabrik, Bad Säckingen, Germany	17810	confidential	8.8-9.2
Lithium disilicate glass-ceramic	National Metal and Materials Technology Center (MTEC)		60 wt% SiO_2, 30 wt% Li_2O, 2 wt % Al_2O_3, etc [58]	9.3

Table 3.3 Properties of feldspathic veneering porcelain

Veneering Porcelain	Manufacturer	Lot No.	compositions	CTE $X10^{-6} K^{-1}$
Lava™ Ceram Dentin	3M™ ESPE™, Seefeld, Germany	8615G	Ceramic powder 95-100 wt% Pigment 5 wt%	10
VITA VM® 9 Base dentine	VITA Zahnfabrik, Bad Säckingen, Germany	20470	60–64 wt% SiO_2, 13–15 wt% Al_2O_3, 7–10 wt% K_2O, 4–6 wt% Na_2O, 3–5 wt% B_2O_3	8.8-9.2
VITA VM® 9 Transparent Dentine	VITA Zahnfabrik, Bad Säckingen, Germany	16340	60–64 wt% SiO_2, 13–15 wt% Al_2O_3, 7–10 wt% K_2O, 4–6 wt% Na_2O, 3–5 wt% B2O3	8.8-9.2

3.2. Methods

3.2.1 Characterization of starting materials

a) Mineral phase analysis of zirconia substructure

Specimens with a thickness of 2 mm from pre-sintered zirconia specimens of VITA In-Ceram ® YZ for inLab®and Lava™ zirconia block were prepared using an ISOMET (Isomet, Buehler, Lake Bluff, IL) cutting machine. All of the specimens were then fully sintered in a furnace according to the manufacturers' recommendations until a density of 99% of theoretical density was reached. Fully sintered zirconia specimens were investigated for crystalline phases using X-ray diffractometry (D8, Bruker, Germany) in the range between 5° and 80° 2θ with a step width of 0.01° 2θ. Identification of mineral phases of the specimens was achieved by comparing the obtained diffraction patterns with International Center for Diffraction Data Standard (ICDD).

b) Average grain size and morphology of fully sintered zirconia

After polishing and cleaning using an ultrasonic cleaner, both fully sintered specimens of VITA In-Ceram ® YZ for inLab®and Lava™ zirconias were gold-coated using an ion sputtering device for microstructure observation using SEM (6400, JEOL, Japan) at a magnification of 10,000X and an access 15 kV, then the average grain size was measured according to ASTM E112-10 [59]

c) Mineral phases and morphology of glass-ceramic liners

Specimen preparation for characterization of bulk glass-ceramic liners was carried out as follows: Pastes of VITA commercial glass-ceramic, Lava commercial glass-ceramic and lithium disilicate glass-ceramic powders were each mixed with liquid and formed into pellets of 3 mm diameter and 2 mm thickness in an acrylic mold. The number of specimens for VITA, Lava and lithium disilicate glass-ceramic were 2, 2 and 14 pieces, respectively.

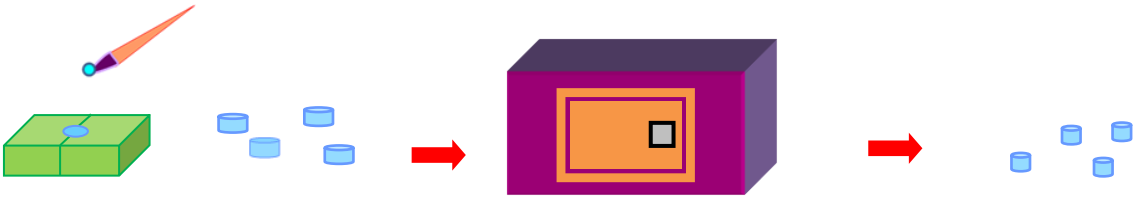

Figure 3.1 Schematic representation of glass-ceramic pellet preparation

Then specimens of commercial glass-ceramic were fired according to the specified firing conditions recommended by the manufacturers **Error! Reference source not found.** Since lithium disilicate glass-ceramic powder obtained from National Metal and Materials Technology Center (MTEC) was selected as liner material in this experiment, it was necessary to find a suitable firing schedule to obtain good adherence with the zirconia substrate. The preliminary firing schedule of lithium disilicate glass-ceramic to form a glass melt with suitable flow to wet the zirconia surface was investigated and evaluated in terms of shear bond strength, crystal phase and morphology of the glass-ceramic. Lithium disilicate glass-ceramic specimens were divided into 2 groups based on zirconia system, VLi and LLi. The VLi group comprises specimens VLi800, VLi850 and VLi900 in duplicate, while the LLi group comprised of duplicate specimens LLi800, LLi850, LLi900 and LLi950. Their firing schedules are designed as shown in **Error! Reference source not found.**

Table 3.4 Firing schedule of commercial-glass-ceramic

specimen	°C →	Min. →	°C ↗	Min. ↗	→ °C	→ Min.	vacuum	
							on	off
VG980	500	6.00	80	6.00	980	1	500	6.00
LG810	450	6.00	45	8.00	810	1	450	8.00

Table 3.5 Firing schedule of lithium disilicate-glass-ceramic

specimen	°C →	Min. →	°C ↗	Min. ↗	→ °C	→ Min.	vacuum	
							on	off
VLi 800	500	6.00	80	3.45	800	1	500	3.45
VLi 850	500	6.00	80	4.22	850	1	500	4.22
VLi 900	500	6.00	80	5.00	900	1	500	5.00
LLi 800	450	6.00	45	7.46	800	1	450	7.46
LLi 850	450	6.00	45	8.53	850	1	450	8.53
LLi 900	450	6.00	45	10.00	900	1	450	10.00
LLi 950	450	6.00	45	11.06	950	1	450	11.06

After being fired according to each schedule, the specimens were polished with SiC papers ranging from No. 600, 800 and 1,000, respectively, and then finished with diamond paste, size 9, 6, 3 and 1 μm, respectively. All specimens were later cleaned in an ultrasonic cleaner, and then coated with gold by ion sputtering for microstructure observation and chemical composition (wt%) determination by SEM and EDX (ISIS 300, Oxford, England), respectively.

All specimens were also investigated for crystalline phases using X-ray diffraction in the 2θ range 5° to 80° with a step width of 0.01° 2θ. Identification of minerals phases of the specimens before and after firing at 800°C, 850°C, 900°C and 950°C was achieved by matching the obtained diffraction patterns with those of International Center for Diffraction Data Standard (ICDD).

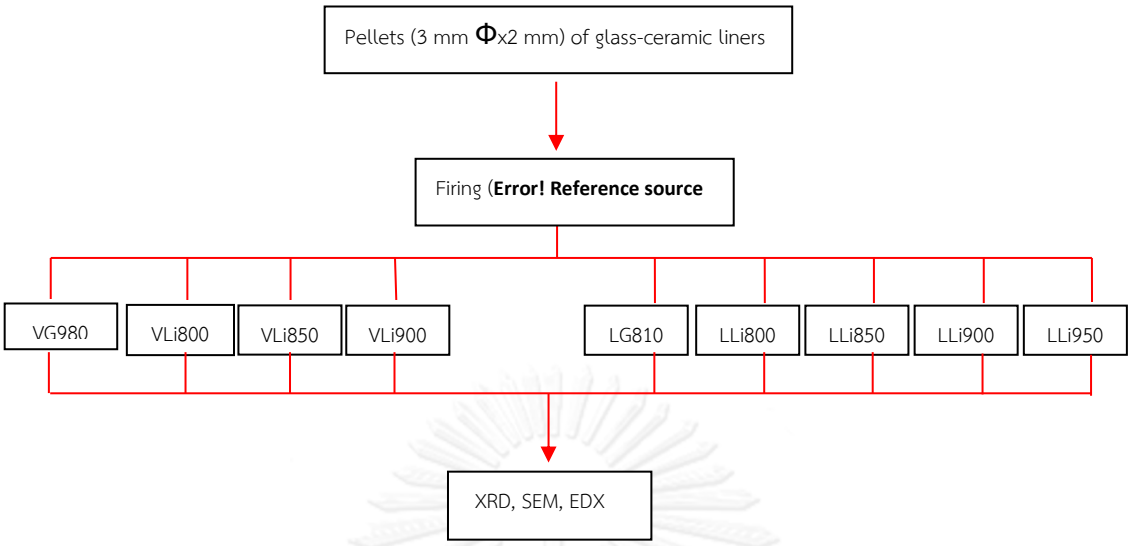

Figure 3.2 Flow chart for characterization of glass-ceramic liners

3.2.2 Characterization of bonding interface

To study properties of the interface between zirconia substructure and veneering porcelain, the fabricated veneering porcelain restoration specimens, were prepared and the preparation method was described according to type of characterization. A fabricated veneering porcelain restoration specimen (in this report) was a composite, composed of a zirconia substrate/glass liner/ veneering porcelain. For simplicity, in this report, this will be refered to the 'composite specimen'.

a) Shear bond strength between zirconia substructure and veneering porcelain

From the results of the firing schedule for lithium disilicate glass-ceramic liners in **Error! Reference source not found.**, the optimal firing schedule of lithium disilicate glass-ceramic could be determined by performing shear bond strength tests on the composite specimens fired at the conditions in **Error! Reference source not found.** and **Error! Reference source not found.** Composite specimen preparation for shear bond strength test between the zirconia substrate and veneering porcelain with- and without an intermediate layer of glass-ceramic liner was performed as follows:

Each zirconia specimen was cut from the pre-sintered block using ISOMET machine into a square of 10 x 10 x 2 mm thickness. After that all the specimens were fully sintered in a furnace according to the manufacturers' recommendations until the density reached 99% of theoretical density. A piece of plastic tape (3.0 mm in diameter) was positioned on top of each zirconia specimen to mark the bonding area. The first single thin layer of glass-ceramic liner was applied in the hole of the tape. The tape was then removed from the zirconia surface and the composite specimens were fired in a programmable vacuum porcelain furnace (Vita Vacumat 4000T, Vita Zahnfabrik, Bad Säckingen, Germany) following the firing schedule **Error! Reference source not found.** and **Error! Reference source not found.** VITA zirconia specimens were prepared into 5 composite specimens with 8 pieces/specimen, and 6 composite specimens with 8 pieces/specimen for Lava zirconia, hence the total composite specimens of VITA and Lava were 40 and 48 pieces, respectively

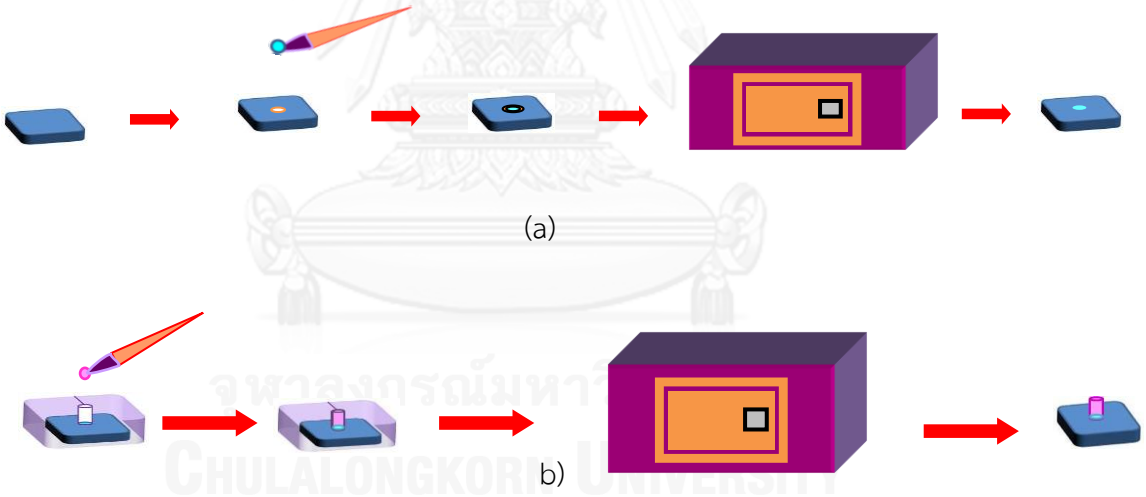

Figure 3.3 Schematic representation of composite specimen preparation: (a) applying layer of glass liner on zirconia surface (b) an acrylic mold was secured on the zirconia surface to act as a template and thickness controller for applying veneering porcelain (dentin) layer

After firing the glass-ceramic liner (Figure3.3 (a)), the zirconia substrate was secured with an acrylic mold with a cylindrical drilled hole of 3 mm diameter and 2

mm thickness and paste of the 1st veneering porcelain layer (primary dentin) was veneered on the zirconia surface then the veneer specimen was fired according to the firing schedule recommended by manufacturers (**Error! Reference source not found.** and **Error! Reference source not found.**). To complete the veneering, a paste of the 2nd (secondary dentin) and the 3rd veneering porcelain layers were each added and fired at lower temperatures to maintain the shape of the first layer according to its firing schedule. The final thickness of the veneer (before the last firing) was controlled at 2 mm.

Table 3.6 Firing schedules of veneer specimens in Lava group

LaVa		°C →	Min. →	°C ↗	Min. ↗	→ °C	→ Min.	vacuum	
								on	off
Glass –ceramic layer	LG810	450	6.00	45	8.00	810	1	450	8.00
	LLi 800	450	6.00	45	7.46	800	1	450	7.46
	LLi 850	450	6.00	45	8.53	850	1	450	8.53
	LLi 900	450	6.00	45	10.00	900	1	450	10.00
	LLi 950	450	6.00	45	11.06	950	1	450	11.06
Veneering porcelain layer	1ry dentin firing	450	6.00	45	8.00	810	1	450	8.00
	2ry dentin firing	450	6.00	45	7.46	800	1	450	7.46

Table 3.7 Firing schedule of veneer specimens in VITA group

VITA		°C →	Min. →	°C ↗	Min. ↗	→ °C	→ Min.	vacuum	
								on	off
Glass-ceramic layer	VG980	500	6.00	80	6.00	980	1	500	6.00
	VLi 750	500	6.00	80	3.07	750	1	500	3.07
	VLi 800	500	6.00	80	3.45	800	1	500	3.45
	VLi 850	500	6.00	80	4.22	850	1	500	4.22
	VLi 900	500	6.00	80	5.00	900	1	500	5.00
Veneering porcelain layer	Base dentin	500	6.00	55	7.49	930	1	500	7.49
	1ry dentin firing	500	6.00	55	7.27	910	1	500	7.27
	2ry dentin firing	500	6.00	55	7.16	900	1	500	7.16

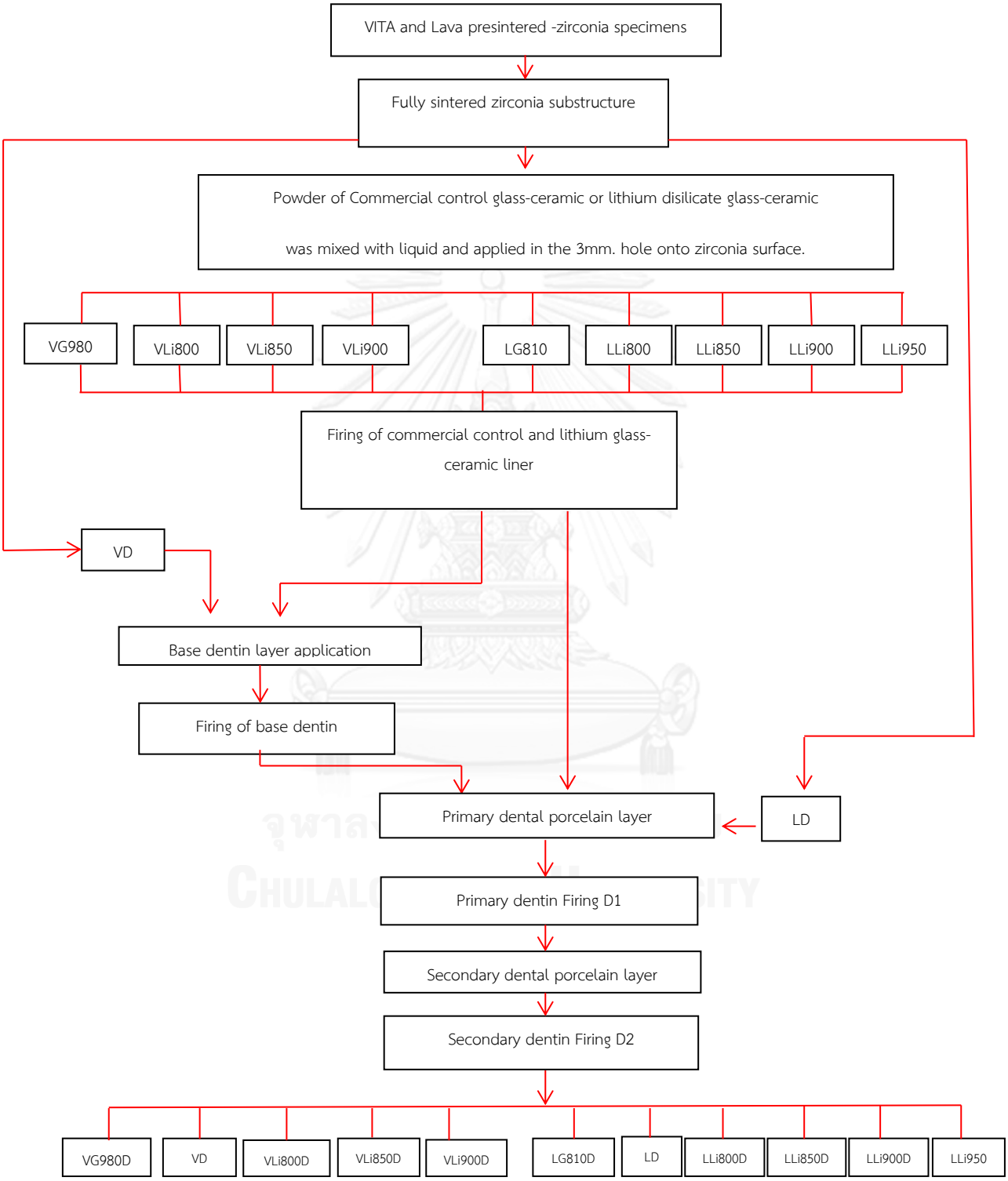
VITA and Lava presintered -zirconia specimens
Fully sintered zirconia substructure
Powder of Commercial control glass-ceramic or lithium disilicate glass-ceramic
was mixed with liquid and applied in the 3mm. hole onto zirconia surface.
VG980
VLi800
VLi850
VLi900
LG810
LLi800
LLi850
LLi900
LLi950
Firing of commercial control and lithium glass-ceramic liner
VD
Base dentin layer application
Firing of base dentin
Primary dental porcelain layer
LD
Primary dentin Firing D1
Secondary dental porcelain layer
Secondary dentin Firing D2
VG980D
VD
VLi800D
VLi850D
VLi900D
LG810D
LD
LLi800D
LLi850D
LLi900D
LLi950

Figure 3.4 Flow chart for characterization of composite specimens

Mounting of specimens for shear bond strength test

The completed specimen was insert into on a stainless steel mold with a 5-mm–diameter opening and fixed in position using double glue surface tape. A PVC ring, 28 mm in diameter and 30 mm in height, was placed over the specimen on the metal mold and held in position with outer metal ring. A PMMA resin was mixed and poured into the ring to fix the specimen. All of them were stored in water at 37 $^{\circ}$C for 24 hours before testing.

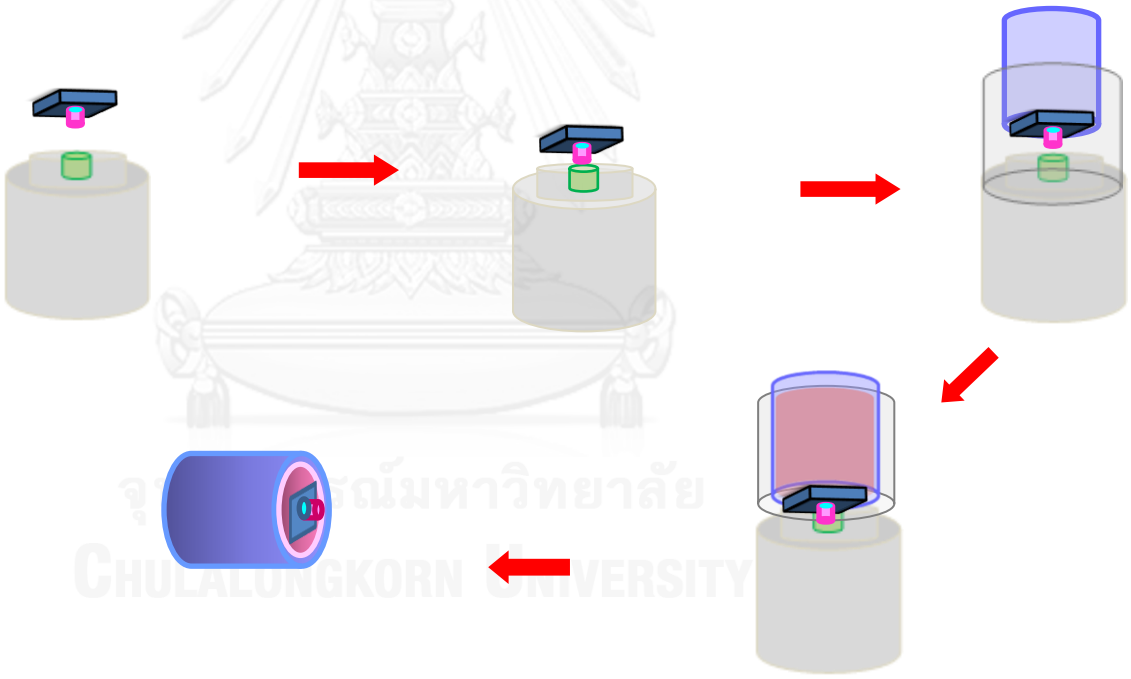

Figure 3.5 Mounting of specimen to PVC ring by embedding in PMMA resin

Testing procedure

Each specimen was mounted in a metal holder on the universal Shimadzu Compact Tabletop (EZ-L/EZ-S Series) testing machine and the load was applied with the jig that had a diameter corresponding to the diameter of the veneering porcelain. Each specimen was tightened and stabilized to ensure that the edge of the shearing jig was touching the core surface and was positioned as close to the veneer-core interface as possible. A shear load was applied at a crosshead speed of 0.50 mm/min until failure. The ultimate load to failure was recorded by the system's software in Newton (N). Average shear strengths (MPa.) were calculated by dividing the load (N) at which failure occurred by the bonding area (mm^2):

$$\text{Shear stress (MPa.)} = \text{Load (N)} / \text{Area } (mm^2)$$

The mean of shear bond strength or failure load and the standard deviation (SD) for each group of specimen were calculated. Fractographic analyses of the fracture surface was also performed using stereoscopic microscope and SEM.

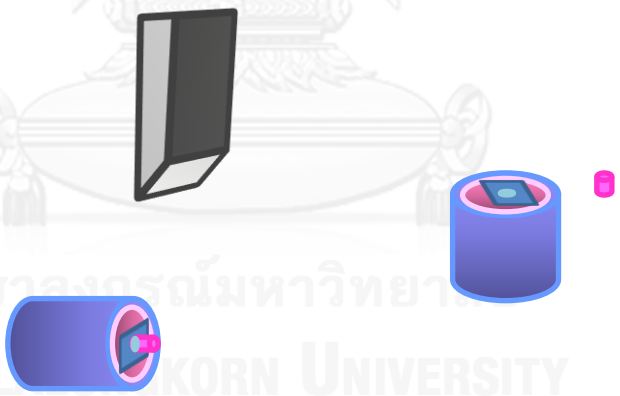

Figure 3.6 Shear bond strength: loading with knife edge blade of universal testing machine.

Fractographic analyses

All specimens were visually analyzed (after having been fractured) using a stereoscopic microscope (Meiji, ML9300, Japan) at a magnification of 15x. Images of the fracture surfaces were plotted and scanned to a computer. The failure modes were classified into six types: cohesive fracture within the veneering porcelain; adhesive failure at the glass-ceramic liner and veneering porcelain interface; cohesive failure within the glass-ceramic liner; adhesive failure at the glass-ceramic liner and the zirconia substructure interface; cohesive failure within the zirconia substructure; and mixed or combined failure (a mixture of adhesive and cohesive failures).

A scanning electron microscope, operated in back scattered mode at 15 kv with 35x magnification, was used to further investigate the fractographic analyses. High contrast between the white zirconia substructure and the grey glass-ceramic liner or veneering porcelain remaining on the zirconia surface was used to assess failure mode.

Statistical analysis

Statistical analysis was carried out using statistical software. The data were analyzed using a one-way analysis of variance test (One-way ANOVA) to determine whether significant differences existed between the values of shear bond strength within the 6 groups of Lava zirconia and 5 groups of Vita Zirconia. Also, a multiple comparisons test was used to assess the differences among the specified materials.

b) Thermocycling test

To assure the durability of the veneering porcelain in service, the composite specimens with highest shear bond strength, Vita zirconia and Lava zirconia with lithium disilicate glass-ceramic liner were selected for thermocycling experiments were composed and their shear bond strengths (after test) to those of commercial products (Vita zirconia with Vita glass-ceramic liner and Lava zirconia with lava glass-ceramic liner). Eight veneer specimens from each group were prepared using the method described previously, but without mounting in a PVC ring. They

were dropped into the water bath of a thermocycling machine which was operated at 5000 and 10,000 cycles. The mean shear bond strength and mode of failure of specimens after test were investigated. For the group 0 cycle, specimens were only stored in distilled water at 37 ^{O}C for 24 hours before shear bond strength test to provide baseline data for comparative purposes. For the groups tested at 5,000 cycles and 10000 cycles, specimens were stored in water between 5 $\pm$ 2 ^{0}C and 55 $\pm$ 2 ^{0}C for 125 hours, and 250 hours, respectively. After that they were each mounted in PVC ring and then stored in distilled water at 37 ^{0}C for 24 hours before testing.

During the thermocycling test, the dwel time for the specimens in each well was 30 seconds, and the transfer time between the wells was 30 seconds. Two cycle times for thermocycling were used. One was to measure the effects on bond strength of short and long time exposure to moisture at oral temperature and the other was to simulate accelerated aging by thermally induced stresses. After that all specimens were each mounted onto the jig of a Shimadzu Compact Tabletop (EZ-L/EZ-S Series) testing machine and tested for shear bond strength. The results were analyzed with ANOVA and fracture surfaces were also analyzed.

c) Mineral phases and morphology of lithium disilicate glass-ceramic liner after multiple firings

Practically, the veneering process involves multiple firings in the order, 1st layer firing (glass liner), primary dentin firing followed by secondary dentin firing, and in the manner that the next maximum firing temperature for veneering porcelain is a little lower than the previous one to maintain the shape of porcelain veneer. Thus to complete a veneering process, required at least 3-4 firing cycles. The repetitive firings to different temperatures might affect the mineral phases and morphology of the glass-ceramic interlayer, therefore the lithium disilicate glass-ceramic specimens which contribute the highest shear bond strengths, LLi950D and VLi850D (**Error! Reference source not found.** and **Error! Reference source not found.**) were chosen for investigation of mineral phases XRD and morphology by SEM. Specimens of VLI850 and LLi950 were prepared into pellets of 5 mm diameter and 1 mm thickness, fired according to the firing schedule based on zirconia system, **Error!**

Reference source not found. and **Error! Reference source not found.** Then the specimens were each mounted in a PVC mold using pink self-curing acrylic resin and polished by polishing machine with sand paper discs, numbers 400, 600 and 1200, respectively with polishing machine. Then they were removed from acrylic resin and mounted on stubs preparing for SEM observation.

Table 3.8 Multiple firing schedule of lithium disilicate glass-ceramic liner (based on VITA zirconia system)

VLi sample		°C →	Min. →	°C ↗	Min. ↗	→ °C	→ Min.	vacuum	
								on	off
1	VLi 850	500	6.00	80	4.22	850	1	500	4.22
2	VLi 850	500	6.00	80	4.22	850	1	500	4.22
		500(base dentin temp)	6.00	55	7.49	930	1	500	7.49
3	VLi 850	500	6.00	80	4.22	850	1	500	4.22
		500(base dentin temp	6.00	55	7.49	930	1	500	7.49
		500(1ry dentin temp)	6.00	55	7.27	910	1	500	7.27
4	VLi 850	500	6.00	80	4.22	850	1	500	4.22
		500(base dentin temp)	6.00	55	7.49	930	1	500	7.49
		500(1ry dentin temp)	6.00	55	7.27	910	1	500	7.27
		500(2ry dentin temp)	6.00	55	7.16	900	1	500	7.16

Table 3.9 Multiple firing schedule of lithium disilicate glass-ceramic liner (based on Lava zirconia system)

LLi sample		°C →	Min. →	°C ↗	Min. ↗	→ °C	→ Min.	vacuum	
								on	off
1	LLi 950	450	6.00	45	11.06	950	1	450	11.06
2	LLi 950	450	6.00	45	11.06	950	1	450	11.06
		450 (1ry dentin temp)	6.00	45	8.00	810	1	450	8.00
3	LLi 950	450	6.00	45	11.06	950	1	450	11.06
		450 (1ry dentin temp)	6.00	45	8.00	810	1	450	8.00
		450 (2ry dentin temp)	6.00	45	7.46	800	1	450	7.46

d) Vickers microhardness and fracture toughness of glass-ceramic liner and interface between zirconia substructure and veneering porcelain.

Glass-ceramic liners

Five specimens (pellets of 3 mm diameter and 1 mm thickness) of glass-ceramic liners from each of the two suppliers (LG810 and VG980) and 2 lithium disilicate glass-ceramics (VLi 850 and LLi950) were prepared and fired to the secondary dentin temperature as previously described.

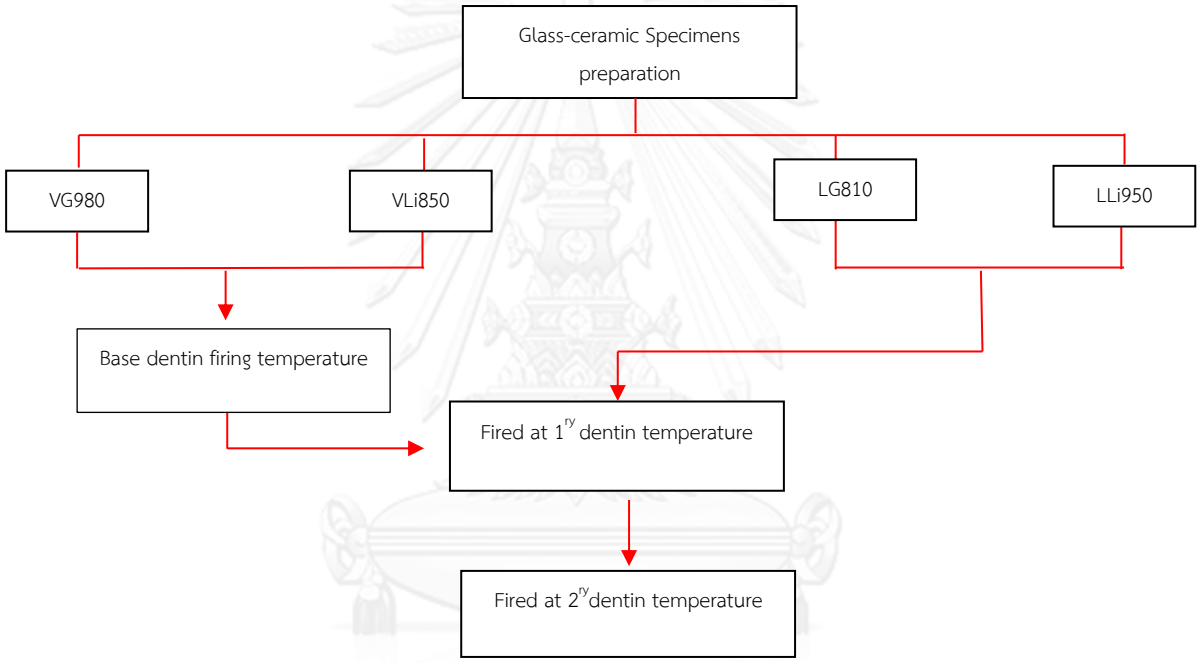

Figure 3.7 Flow chart of glass-ceramic liner specimen preparation for EDX and Vickers microhardness test

Procedure for Vickers microhardness test

Each of the 4 glass-ceramic liner specimens (VG980, VLi850, LG810, LLi950) was pressed with 300 gf. The rate of the indenter motion to contact with the specimen was 0.015-0.070 mm/s and the time of application of full test load should be 10 s (± 2). The mean of these 5 points represents the Vickers hardness of one specimen.

The Bonded interfacial areas between the veneering porcelain and the zirconia substrate of specimens VG980D, VLi850D, LG810D, LLi950D were each located and indented along the interface of the zirconia substrate and glass-ceramic liner using the same conditions as described previously.

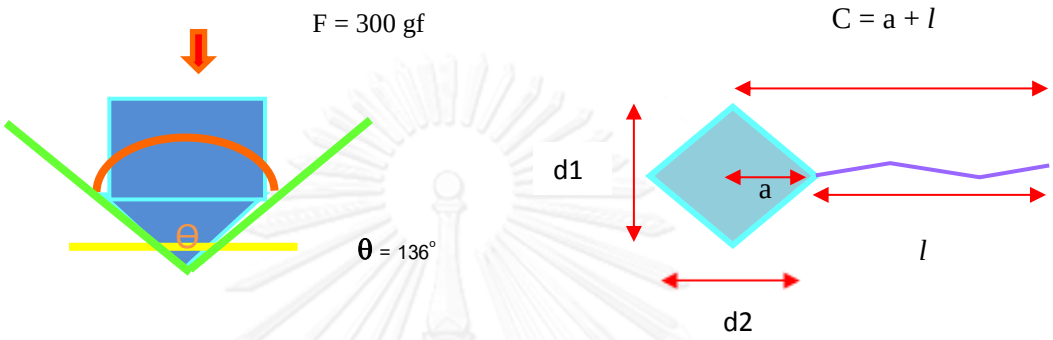

Figure 3.8 diagram of vickers microhaedness and measurement

Microhardness was tested by Vickers' indentation test according to ASTM C 1372 [60]. and fracture toughness (K_{IC}: MPa√m) was calculated by

$$K_{IC} = 0.824 \frac{P}{C^{3/2}}$$

Where P is applied load (N.) and C is crack length from the center of the indentation to the crack end.

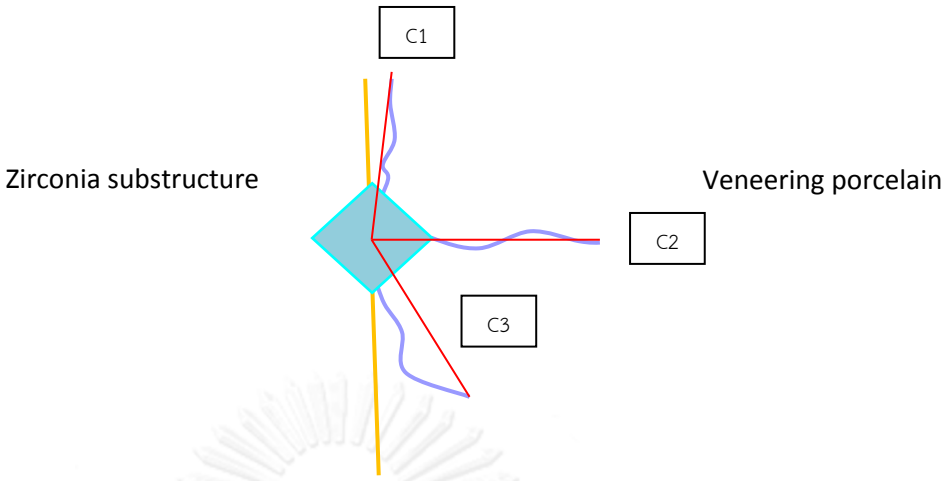

Figure 3.9 Measurement of C-line at interface

C1 is the upper crack length that is parallel to the interface between the zirconia substrate and the glass-ceramic interface

C2 is the crack length which is perpendicular to the interface which penetrates through the glass-ceramic interlayer into the veneering porcelain

C3 is the lower crack length that is parallel to the interface between the zirconia substrate and the glass-ceramic interface

Where (C1 plus C3) means the total crack length that appears along or parallel to the interface

e). Interface analysys between zirconia substructure and veneering porcelain

Specimens VG980D, VLi850D, LG810D and LLi950D were prepared as previously described. Then each specimen was cut in half using an ISOMET machine. The cut surface was polished with SiC papers ranging from No. 600, 800 and 1,000, respectively and then respectively finished with diamond pastes: size 9, 6, 3 and 1 μm. All specimens were later cleaned in an ultrasonic cleaner.

For the high resolution SEM and linear EDX investigations, one specimen was randomly chosen and coated with carbon particle for detailed investigation of the interfaces between the zirconia substrate, glass-ceramic liner and veneering porcelain. The interfaces were studied using a high resolution SEM (JEOL 6340-FE Scanning Electron Microscope, JEOL Ltd., Tokyo, Japan). Another specimen was

coated with gold by sputtering for linear EDX investigation (Oxford Isis 300, Oxfordshire, United Kingdom).

3.2.3 Biocompatibility test of lithium disilicate glass-ceramic

a) MTT assay

Toxicity study for MTEC lithium disilicate glass-ceramic compared to commercial glass-ceramic liners using storage solution technique

The cells used in this study were human gingival fibroblast cells obtained from a periodontist, through collaboration with the Department of Periodontal, Faculty of Dentistry, Chulalongkorn University. The method in brief was as follows: Cells to be tested were plated in a volume at 20,000 cells/well in 48-well microtiter plates using a micro pipette. The plates were incubated at 37 °C for of 24 h allowing cells to re-attach and re-equilibrate. The 1, 3 and 7 day storage of lithium disilicate glass-ceramic and commercial glass-ceramic liners solutions with different concentrations (1:1000, 1:100 and 1:10) of storage solution per total medium volume were added and incubated at 37 °C under 5 v% of carbon dioxide atmosphere for 1 day. 200 µl of MTT solution (7 mg/ml in medium) was added in each well and incubated for 20 min. Next the solution from the well was discarded and formazan was found as solid residue. 400 µl of DMSO solution was dropped into the well. The plates were shaken for 20 min and optical density measurement of the purple solution on spectrophotometer at 570 nm wave length was carried out.

b) Direct contact technique

All of the test specimens were laid down in the 24-well microtiter plate. Human gingival fibroblast cells were plated onto the 4 specimens (VG810, VLi850, LG810, and LLi950) and incubated at 37 °C under 5 v% of carbon dioxide atmosphere for 1day. Then all specimens were prepared for SEM investigation.

Chapter 4

Results

4.1 Result of characterization of starting materials

a) Result of mineral phase analysis of zirconia substrate by X-ray diffraction of zirconia

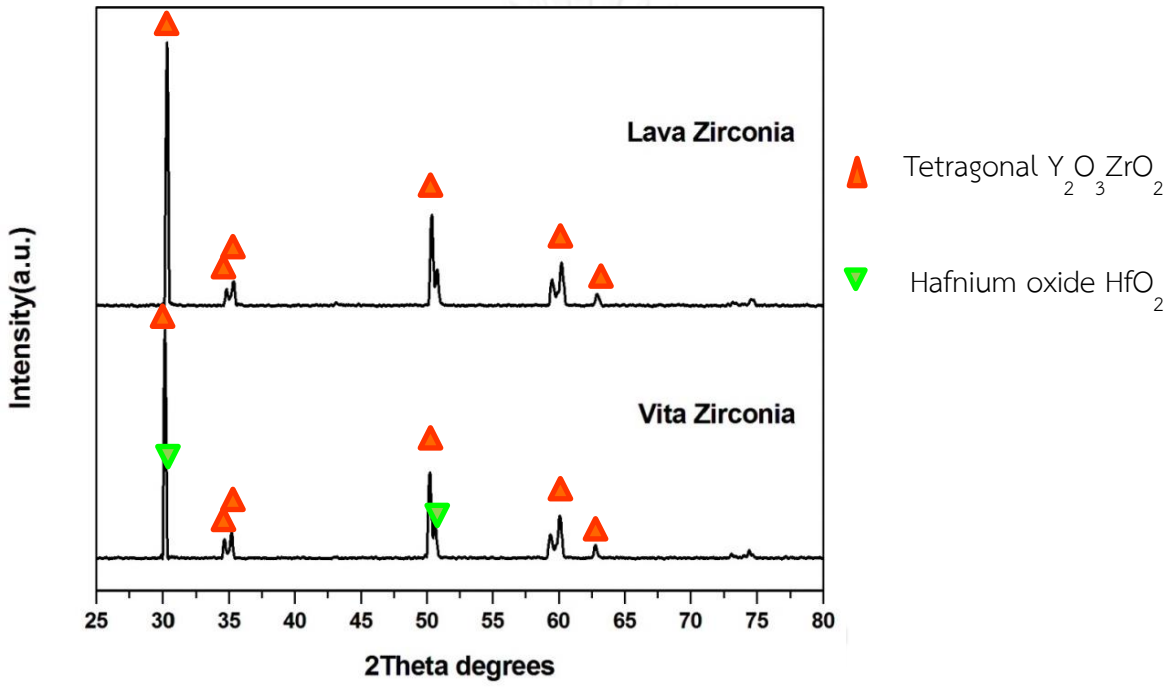

Figure 4.1 XRD result of VITA zirconia and Lava zirconia

It was found that the main composition of these two zirconias was quite similar. They contained zirconium oxide (ZrO_2), zirconium yttrium oxide and corundum (Al_2O_3) but hafnium oxide (HfO_2) was found only in VITA zirconia.

b) Result of average grain size and morphology of fully sintered zirconia

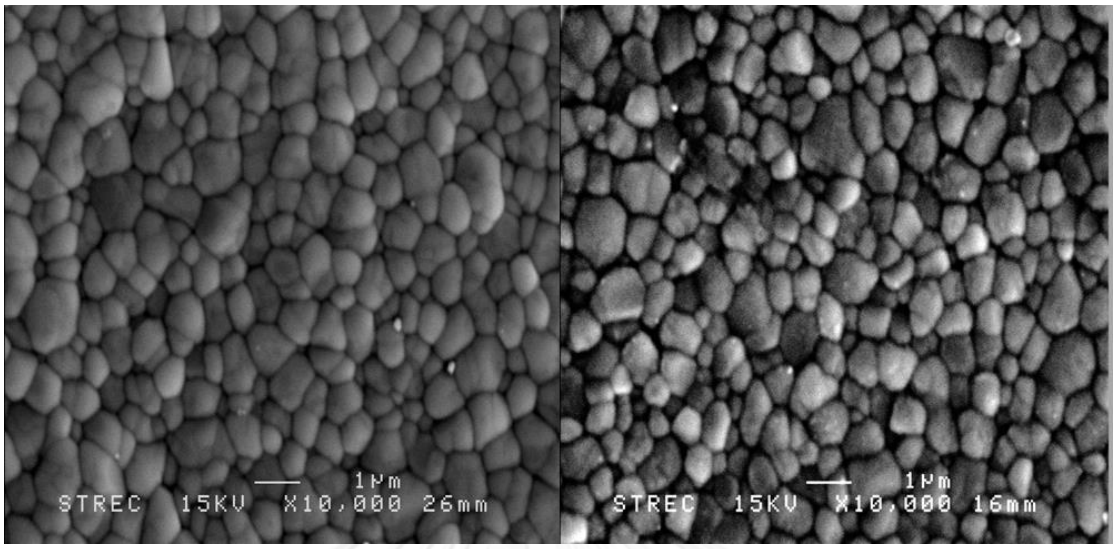

Figure 4.2 SEMs of Lava zirconia(a) and VITA zirconia (b)

From the SEM images, different grain sizes were detected, Vita zirconia had smaller average grain size measured according ASTM E112-10

c) Result of mineral phases and morphology of glass-ceramic liners

- Mineral phase analysis by X-Ray Diffraction of lithium disilicate glass-ceramic powder

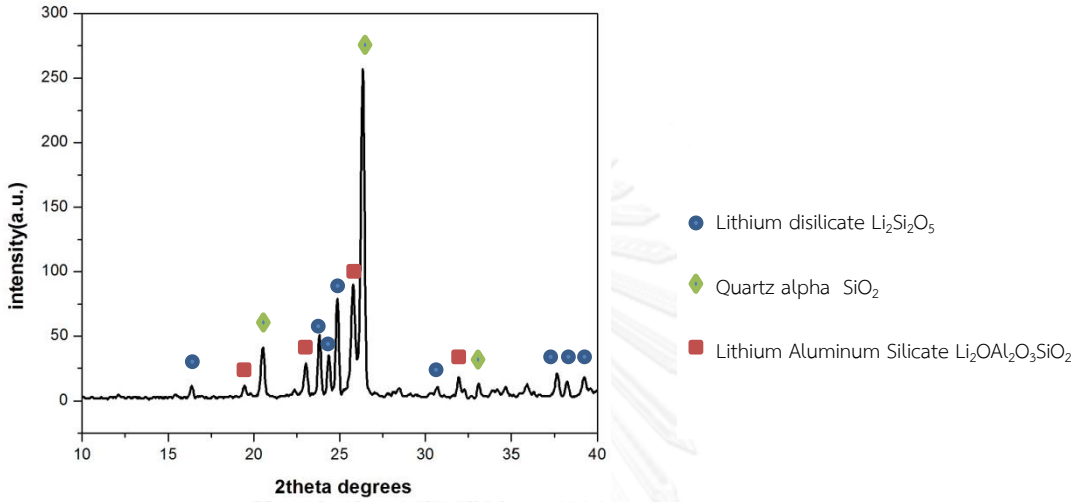

Figure 4.3 XRD of lithium disilicate glass-ceramic powder

-Mineral phase analysis by X-Ray Diffraction of fired glass-ceramic bulk analysis

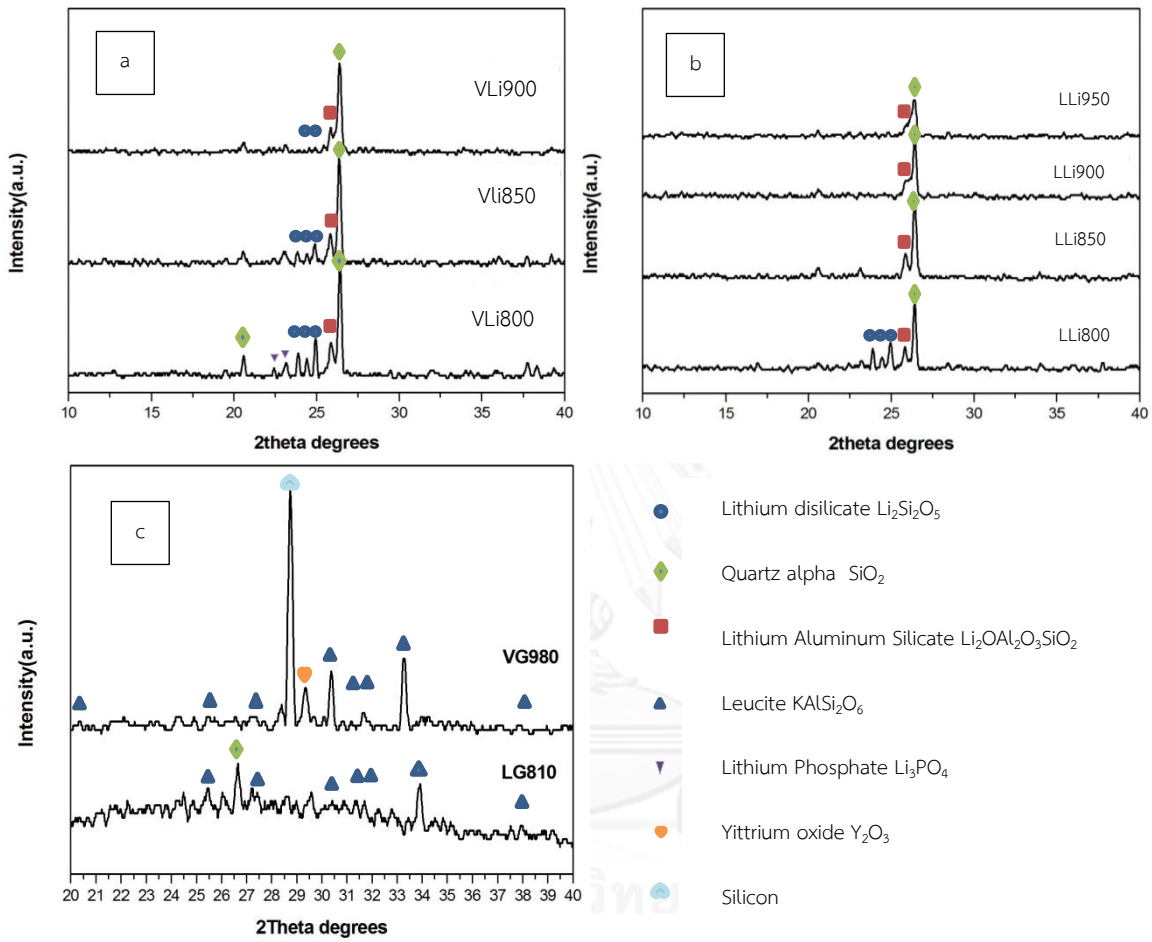

Figure 4.4 XRD of lithium disilicate glass-ceramic powder XRDs of VLi800,VLi850,VLi900 (a) LLi800, LLI850,LLi900, LLi950(b) and VG980, LG810(c)

Figure 4.4 shows the mineral phases of the commercial glass-ceramic and lithium disilicate glass-ceramic liners after being fired at the assigned 1st layer temperature following the firing schedules of VITA and Lava systems. **Figure. 4.4 (a)** shows that the mineral phases of VLi800, VLi850 and VLi900 are composed of **α**-SiO_2 as the major phase followed by $Li_2Si_2O_5$, $Li_2OAl_2O_3SiO_2$ and Li_3PO_4, respectively. The contents of all crystalline phases decreased with increasing firing temperature. **Figure**

4.4 (b) shows that LLi800, LLi850, LLi900, and LLi950 are composed of the same phases as VLi but contents of crystalline phases rapidly decreased with increasing firing temperature which suggests the progressive melting of the glass. **Figure 4.4 (c)** shows that VG980 is composed mainly of Si (resulting from the reduction of SiO2 under vacuum firing condition), leucite and Y_2O_3 as main phases while those of LG810 are microcrystalline leucite and α-SiO_2. The detection of Si (2θ= 28.49°) in VG980 probably results from the reduction of SiO_2 under vacuum firing condition by C from the volatile organic solution (commercial) used during forming of the glass pellet specimens.

Morphologies of glass-ceramic liners observed by SEM

Effect of firing duration and temperature

Microstructures of lithium disilicate glass-ceramic after 1st layer firing are shown in **Figure. 4.5** The firing duration and heating ramp were calculated from the basic Lavaceram veneering porcelain firing schedule. The starting temperatures was assigned as 800°C, 850°C, 900°C and 950°C.

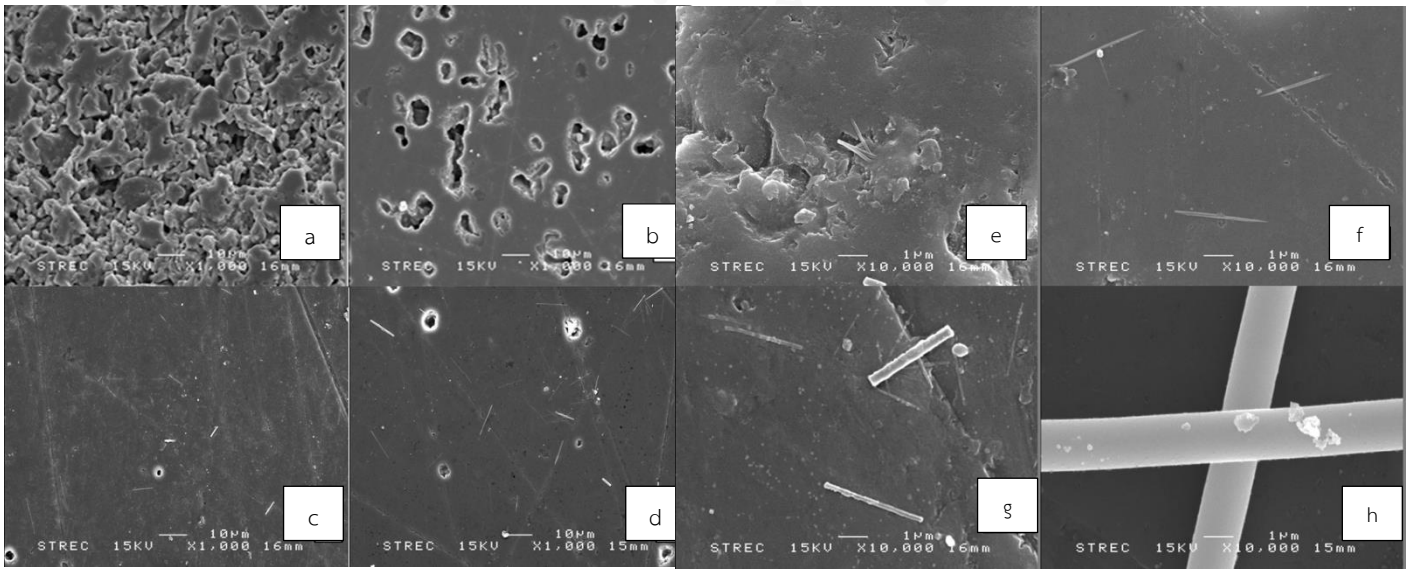

Figure 4.5 Microstructures of lithium disilicate glass-ceramic after being fired at 800°C(a,e), 850°C(B,f), 900°C(c,g) and 950°C(d,f) following the firing Table 3.5

From the microstructures shown in the above **Figure 4.5**, it was found that after firing at 800°C **Figure (a,e)**, LLi800 still shows clusters of the original lithium disilicate glass-ceramic particles which suggests that a higher temperature is needed to melt into glass.

After firing at a higher temperature (850°C), the particles began to melt and link to each other, thus glass matrix was formed and fine needle-like crystals of $Li_2Si_2O_5$ are visible. Porosity decreases with increasing firing temperature. At firing temperatures of 900°C and 950°C, needle-like crystals of $Li_2Si_2O_5$ which grow larger with increasing temperature are observed and the glass matrix looks more homogeneous due to low porosity or small pores.

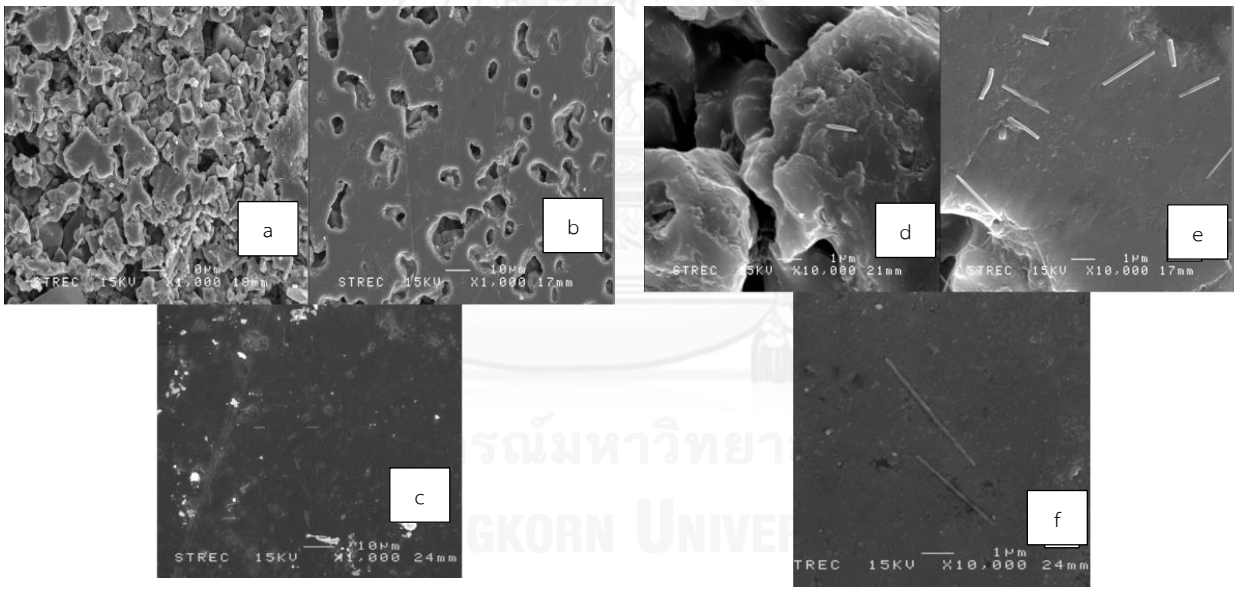

Figure 4.6 Microstructures of lithium disilicate glass-ceramic after being fired at 800°C(a,d), 850°C(b,f) and 900°C(c,f) following the firing schedule of VITA (VM9) zirconia system Table 3.5

From the micrographs it was found that VLi800 behaves in a similar manner to LLi800. It does not adequately melt, thus retains the morphology of the clusters of lithium disilicate glass-ceramic particles. The microstructure of VLi850 is similar to

LLi850, full with evenly distributed large closed pores and fine needle-like crystals in the glass matrix. After being fired at a higher temperature (900°C), the microstructure of VLi900 is similar to LLi900, but with finer and longer needle-like crystals of $Li_2Si_2O_5$.

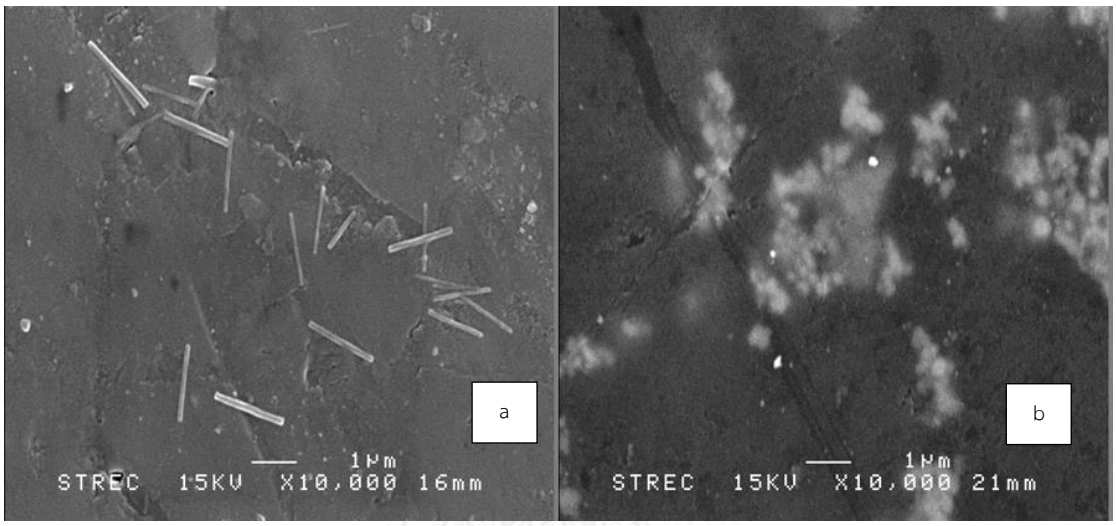

Figure 4.7 SEMs of LG810 (a) and VG980(b) x10000

Figure 4.7 shows the microstructures of the commercial glass-ceramic liners, LG and VG fired according to the recommended 1st layer firing schedules. The needle-like crystals in the dense glass matrix of LG810 cannot be identified due to the undisclosed information of its chemical compositions. However, in the XRD patterns, Fig.4.3C, besides microcrystalline leucite (2θ =27.27°), α-SiO_2 (2θ = 26.4°) is also detected. The round shaped crystals of leucite are observed in the microstructure of VG980 which corroborates well with the XRD result.

-Mineral phase analysis by EDX of glass-ceramic bulk analysis

An example of specimens in the VLi850 group is shown in Error! Reference source not found. **and Figure** 4.8 (a) EDX of matrix area of VLi850, (b) EDX of crystal of VLi850

The rest EDX results of the other samples are shown in the appendices.

Table 4.1 EDX Result of VLi850 group

	VLi850			
Matrix	Elmt	Spect Type%	Element%	Atomic
	O K	ED	45.87	60.07
	Na K	ED	0.68	0.62
	Mg K	ED	1.13	0.97
	Al K	ED	3.14	2.44
	Si K	ED	45.58	34.00
	K K	ED	1.48	0.80
	Ca K	ED	2.11	1.10
		Total	100.00	100.00
crystal	O K	ED	47.74	62.03
	Na K	ED	0.57	0.52
	Mg K	ED	0.83	0.71
	Al K	ED	3.00	2.31
	Si K	ED	43.27	32.03
	K K	ED	1.42	0.75
	Ca K	ED	3.17	1.65
		Total	100	100.00

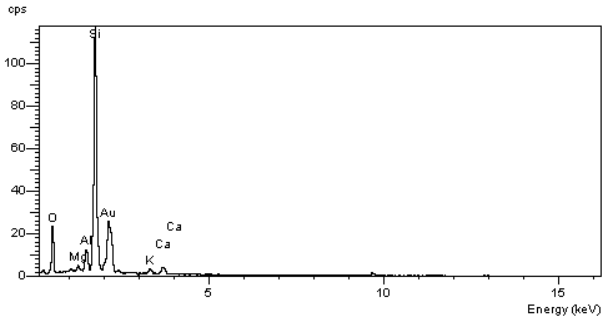

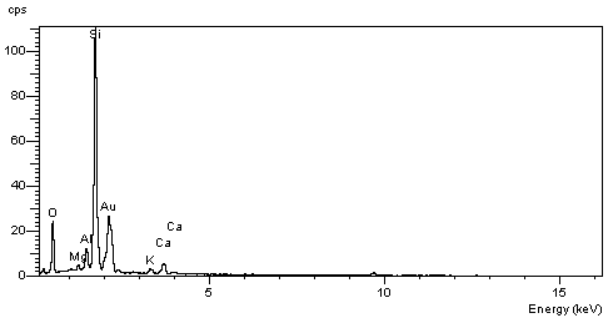

Figure 4.8 (a) EDX of matrix area of VLi850, (b) EDX of crystal of VLi850

4.2 Result of characterization of bonding interface

a) Result of shear bond strength between zirconia substrate and veneering porcelain

Shear bond strengths of the samples of Lava and VITA groups were measured using a Shimadzu compact tabletop testing machine. Mean shear bond strengths of the samples of Lava groups are **shown in Figure 4.9** and those of VITA groups in **Figure 4.11**

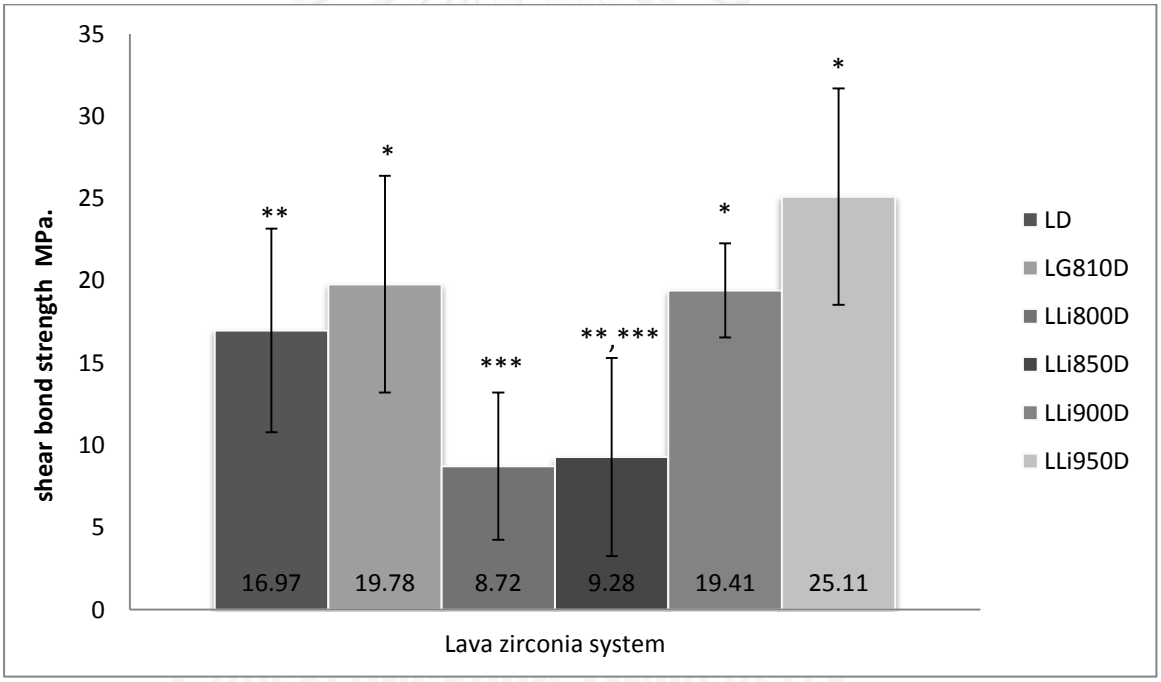

Figure 4.9 Mean shear bond strengths of Lava groups

From the data obtained, it was found that the mean shear bond strength of the LG810D was higher than the LD group but the difference is statistically insignificant. The LLi900D and LLi950D gave higher mean shear bond strengths than that of the Lava group with the commercial glass liner. It is worth noting that the mean shear bond strength of LLi950D just attains the critical acceptable strength limit of 25 MPa.

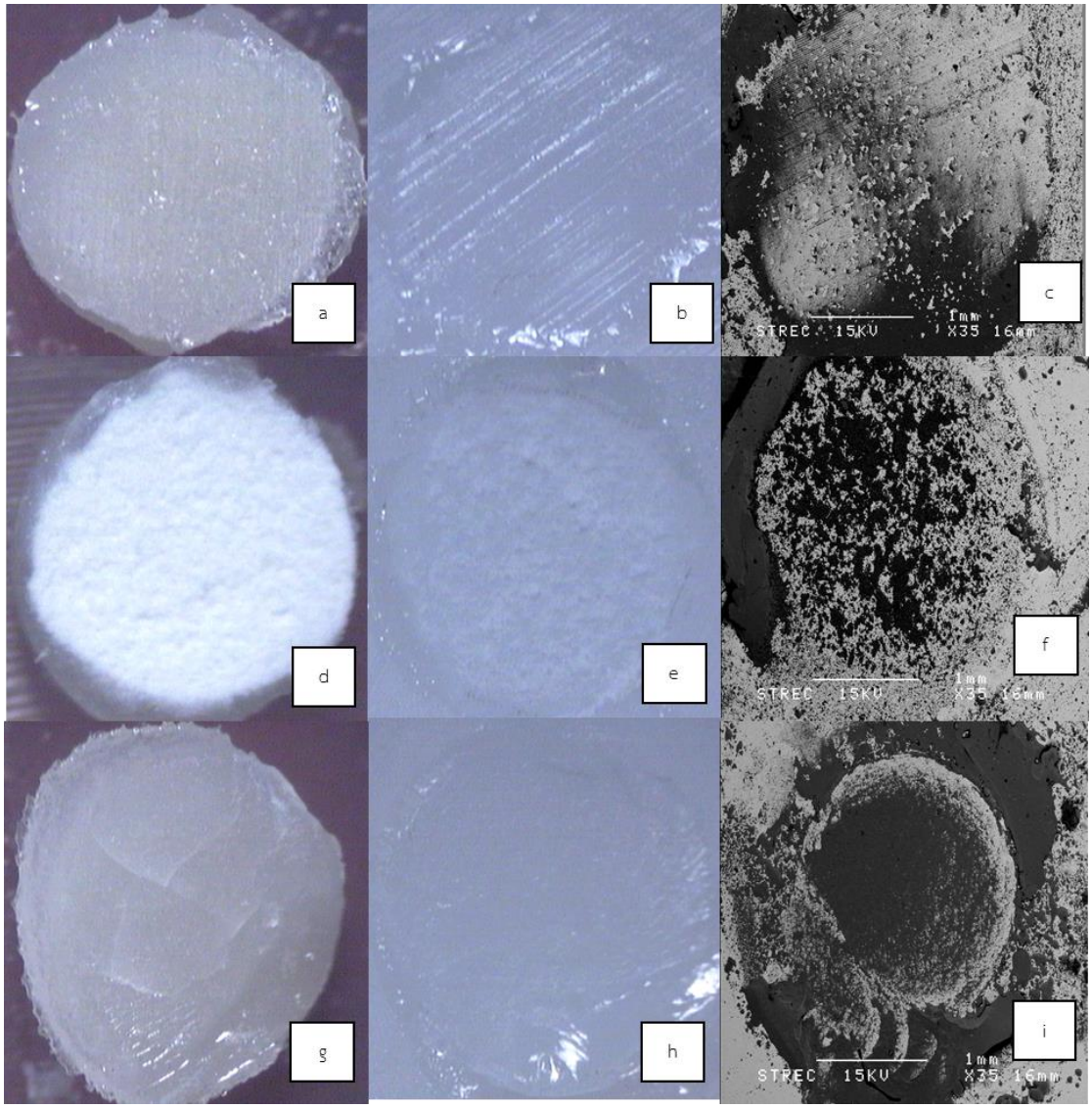

Figure 4.10 SEM micrographs showing modes of failure of Lava groups Porcelain side of LG810D (a), zirconia side of LG810D (b), zirconia side of LG810D (back scattered mode) (c), porcelain side of LLi850D (d), and zirconia side of LLi850D (e), zirconia side of LLi850D (back scattered mode) (f), porcelain side of LLi950D (g), and zirconia side of LLi950D (h), zirconia side of LLi950D (back scattered mode) (i).

Generally, modes of failure are classified according to type of failure as adhesive and cohesive. From the images of the fracture surfaces of Lava groups (a, b, c), the failure between glass interlayer and zirconia surface of Lava with commercial glass liner can be identified as adhesive failure mode. The remaining of some traces of glass on the zirconia surfaces of LLi850D (d, e, f) and LLi950D (g, h, i) indicate a mixed interfacial failure between adhesive and cohesive. LLi950D, with the highest mean shear bond strength shows some typical glass crack lines on the porcelain surface and more traces of glass liner remain while there are some clusters of non-melted glass liner on both zirconia and porcelain surfaces of LLi800D. The information obtained from back scattered mode of SEM correlates well with that from stereomicroscope, there are some traces of glass liner (black color) retained on the zirconia surfaces (white background) in LLi850D LLi850D and LLi950D.

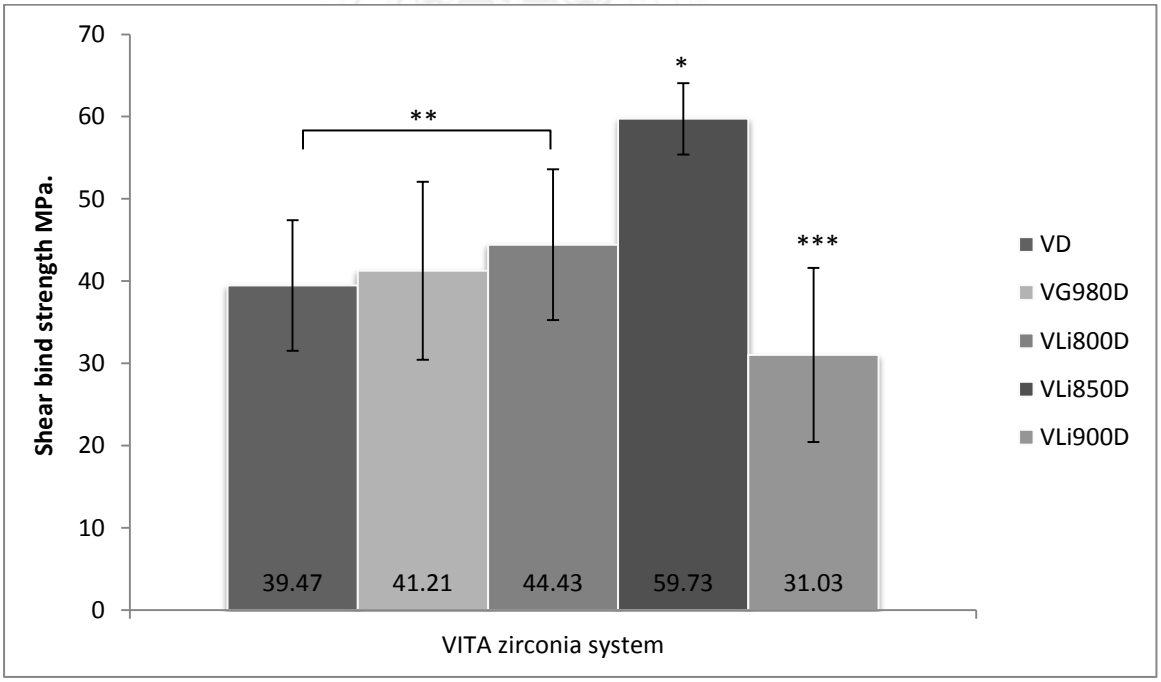

Figure 4.11 Mean shear bond strength of VITA groups

The mean shear bond strengths of VITA groups are shown in **Figure 4.11 Error! Reference source not found.**VLi850D gives highest mean shear bond strength of 59.73 MPa and VLi900D gives the lowest value of 31.03 MP. The mean shear bond

strength of VG980D is a little higher than the VD group but substantially lower than VLi800D and VLi850D. However, all VITA groups show value of shear bond strength of over 25 MPa.

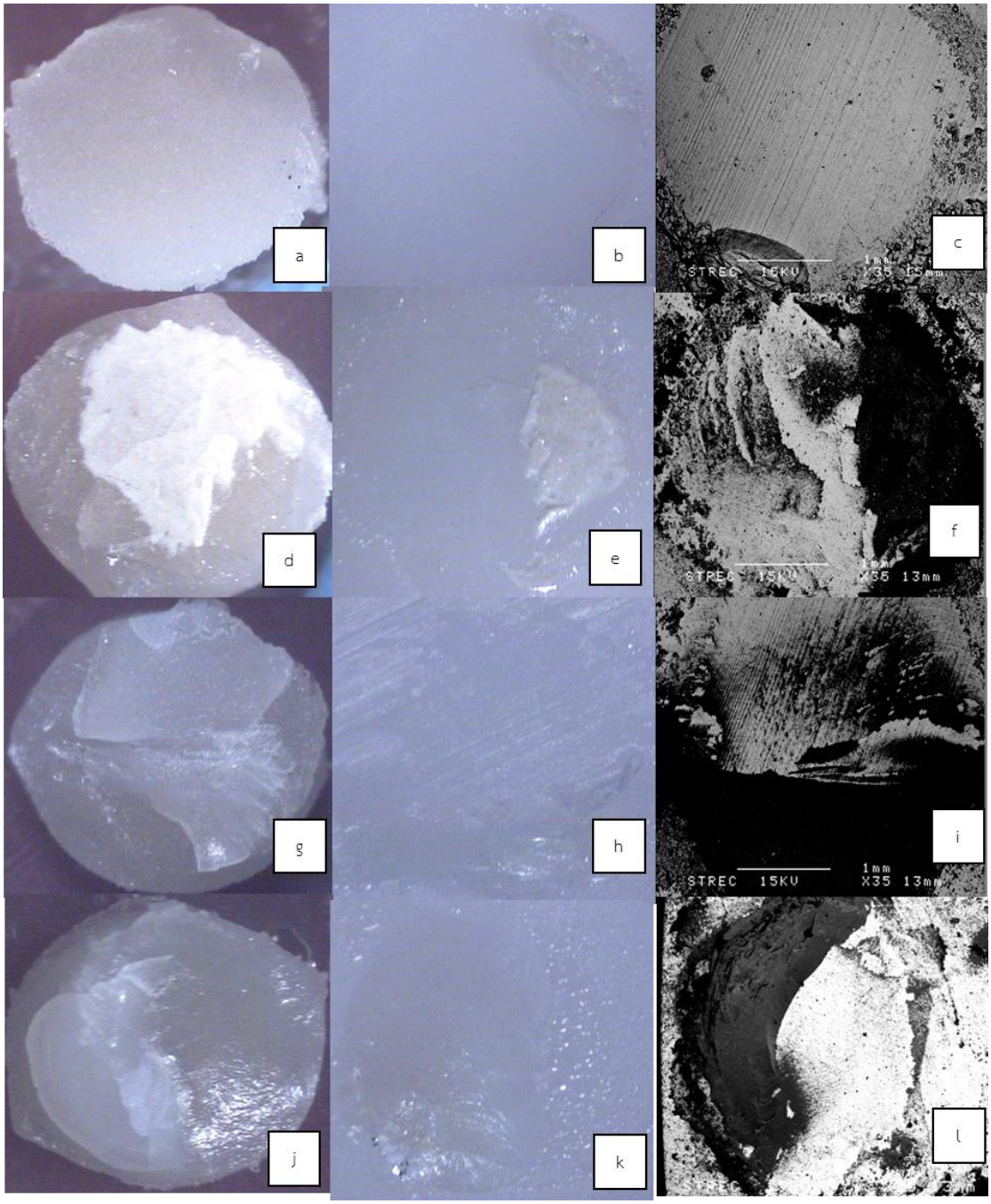

Figure 4.12 Streio and SEM micrographs showing modes of failure of VITA groups porcelain side of VD (a), zirconia side of VD (b), zirconia side of VD (back scattered) (c), porcelain side of VG980D (d), zirconia side of VG980D (e) zirconia side of VG980D (back scattered) (f), porcelain side of VLi850D (g), zirconia side of VLi850D (h), zirconia side of VLi850D (back scattered) (i) porcelain side of VLi900D (j), zirconia side of VLi900D (k), zirconia side of VLi900D (back scattered) (l).

Adhesive failure was detected in all specimens in the VD group. Some traces of commercial glass were retained on both the zirconia surface and the porcelain surface, hence the failure mode was .....to be mixed interfacial failure mode, which is the same as VLi800D, VLi850D, and VLi900D. As expected, there were considerable of glass traces on VLi850D, which had the highest mean shear bond strength. It was noted from these results that the adhesive failure mode was typical for the VD group, hence the application of glass liner in porcelain veneering enhances shear bond strength by reducing adhesive failure. Thus the combination of adhesion and cohesion determines the overall bonding effectiveness since the adhesive bond will fail if the glass liner separates from the substrate or there is internal break-down of the glass liner (cohesive failure). Specimens with a good balance between adhesive and cohesive failures should exhibit a high shear bond strength.

b) Results of thermocycling test

The Lava group with highest mean shear bond strength, LLi950D, was selected to run thermocycling tests and results were compared with the LG810D group.

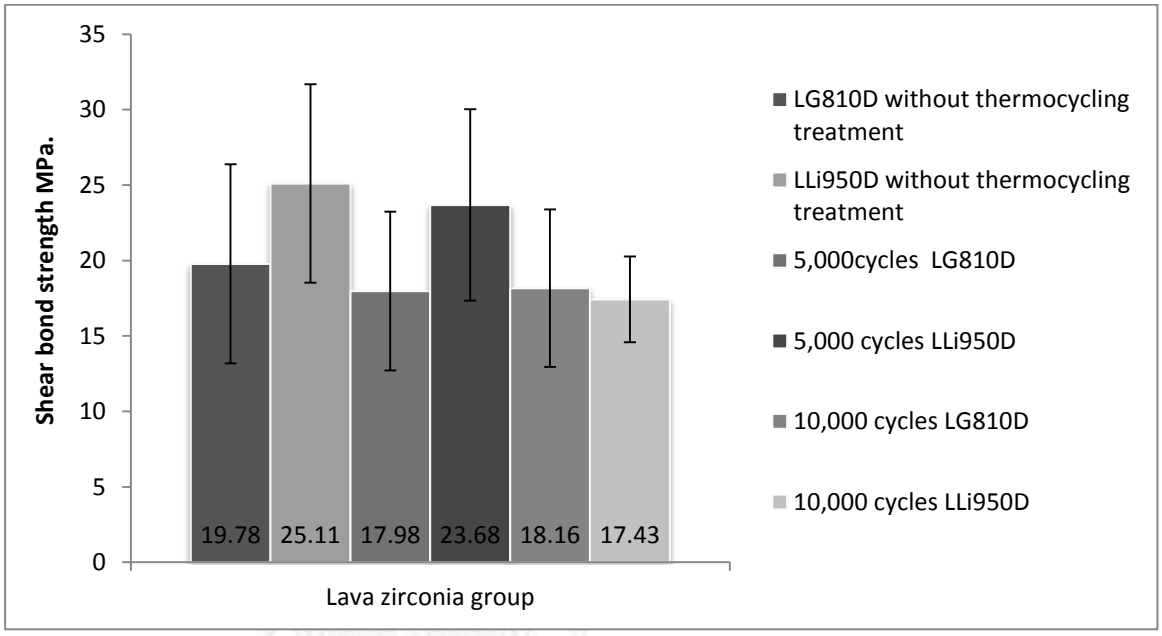

Figure 4.13 Mean shear bond strengths of LLi950D after thermocycling at 5,000 cycles and 10,000 cycles.

From the data obtained, the mean bond strength of LG810D before thermocycling treatment was to be 19.78 MPa and after the treatment the result were 17.98 MPa and 18.16 MPa at 5,000 cycles and 10,000 cycles, respectively. For the LLi950D group the mean shear bond strength before thermocycling treatment is 25.11 MPa and after the treatment at 5,000 cycles decreased to 23.68 MPa which is slightly higher than that of LG810D at the same temperature. However, after being treated for 10,000, the mean shear bond strengths further decreased to 17.43 MPa which is not significant when compared with 18.16 MPa of LG810D at the same temperature. However, there is no statistically significant difference in thermocycling results between the 6 groups.

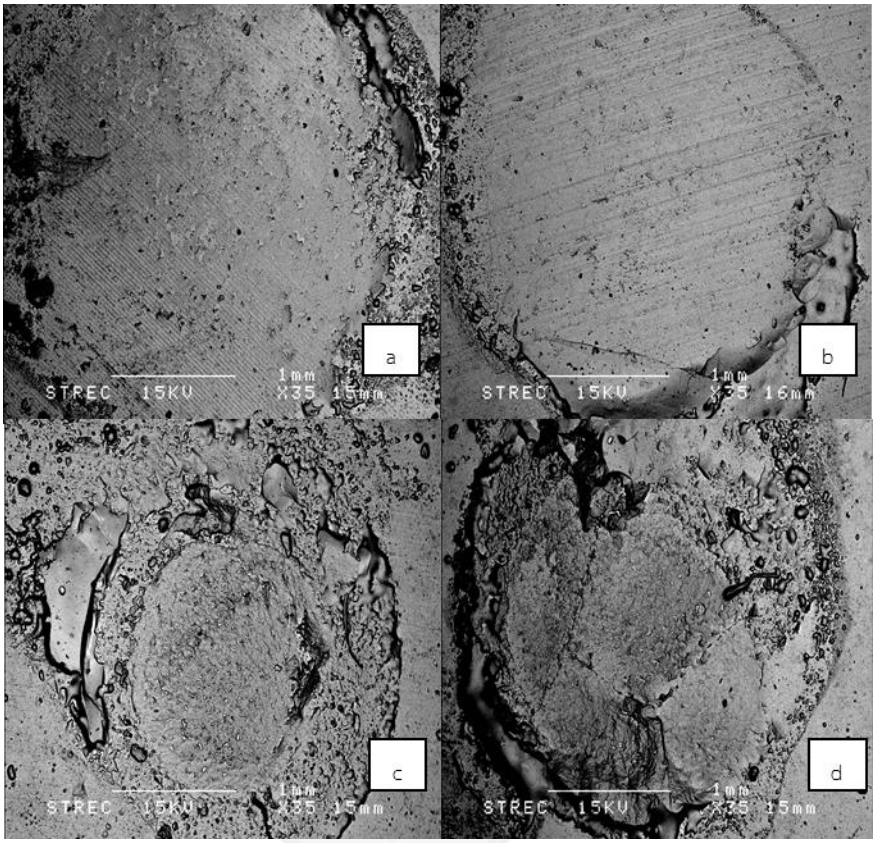

Figure 4.14 Fracture surfaces of LG810D and LLi950D after thermoycling tests, LG810D at 5,000 cycles (a), 10,000 cycles (b), LLi950D at 5,000 cycles (c), 10,000 cycles (d).

From the SEM micrographs, the fracture surfaces of LG810D at 5,000 cycles and 10,000 thermocycling tests (a), (b) are quite clean, hence show adhesive failure. On the contrary, there were some traces of glass-ceramic liner retained on the zirconia surfaces of LLi950D at both 5,000 and 10,000 cycles. However, the mean shear bond strengths of these two groups are quite close.

The specimens with the highest mean shear bond strength, VLi850D group, was selected to run thermocyling tests to comparison with the VG980D group. The results are shown in **Figure 4.15**

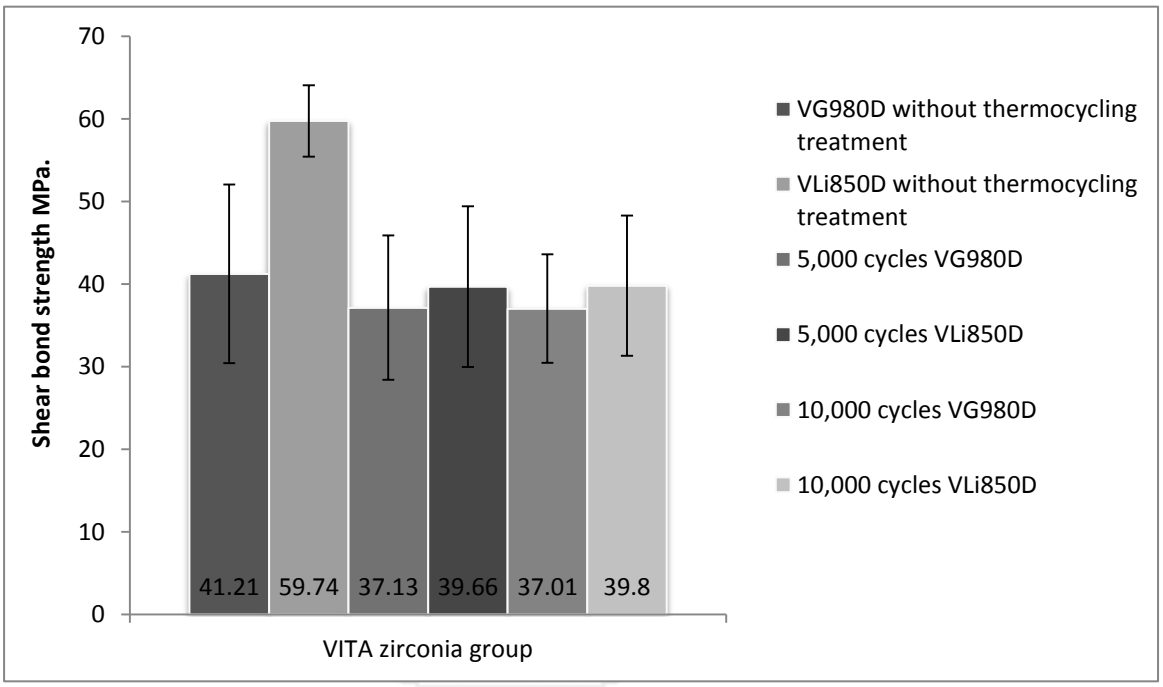

Figure 4.15 Mean shear bond strengths of VLi850D after thermocycling at 5,000 cycles and 10,000 cycles.

Fracture surfaces of specimens from the VG980D and VLi850D groups before and after thermocycling treatment at 5,000 and 10,000 cycles were imaged. It was found that the mean shear bond strength of VG980D was not affected by thermocycling. In contrast, it was found that in the VLi850D group, the mean shear bond strength at 5,000 cycles (39.66 MPa) and 10,000 cycles (37.01MPa.) had significantly decreased from that before thermocycling treatment (59.74 MPa). However, it is worth noting here that the mean shear bond strengths of specimens in the VLi850D group after thermocycling tests were well over 25 MPa.

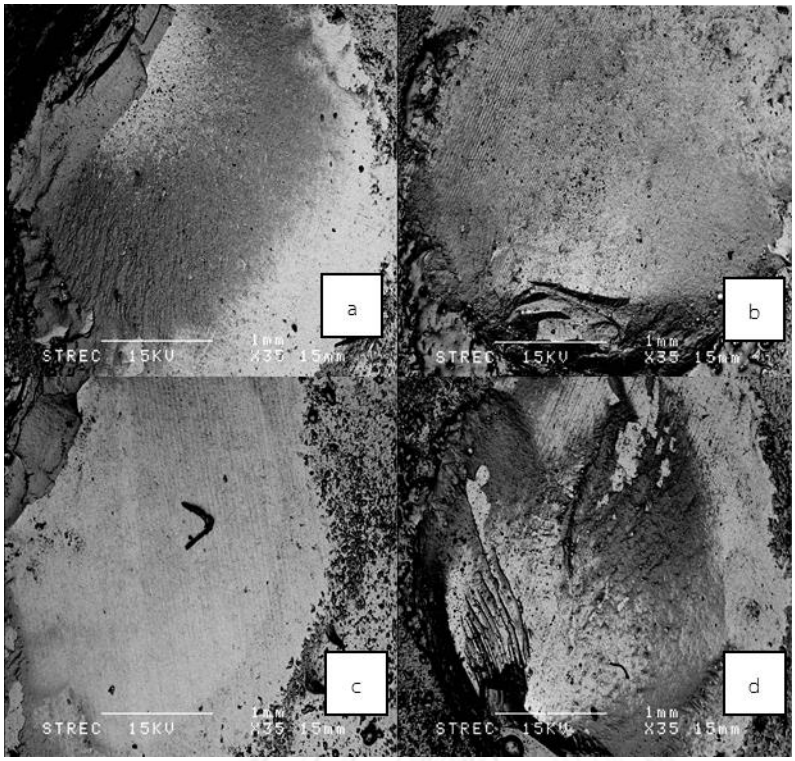

Figure 4.16 Fracture surfaces of VG980D after thermocycling treatment at 5,000 cycles(a), 10,000 cycles (b), 5,000 VLi850D at 5,000 cycles (c), and VLi850D at 10,000 cycles (d).

From the SEM micrographs, there are some traces of the glass-ceramic interlayer retained on zirconia surfaces of all the samples. It was noted that despite the insignificant decrease in the mean shear bond strength from the treatment at 5,000 cycles, the fracture surfaces of the samples after 10,000 test cycles became more porous, cracked and spalling was observed due to severe corrosion.

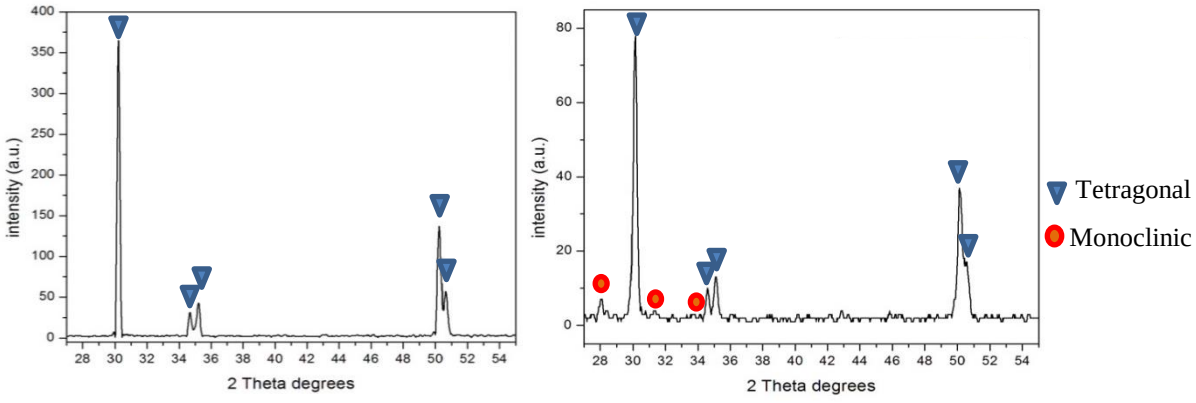

(a) (b)

Figure 4.17 X-Ray Diffraction patterns of fully sintered VITA zirconia and VITALi850 (fracture surface) before thermocycling test(a) and after thermocycling test at 5,000 cycles (b).

c) Result of mineral phases and morphologies of lithium disilicate glass-ceramic liner after multiple firings

Multiple firings or repetitive firing of LLi950

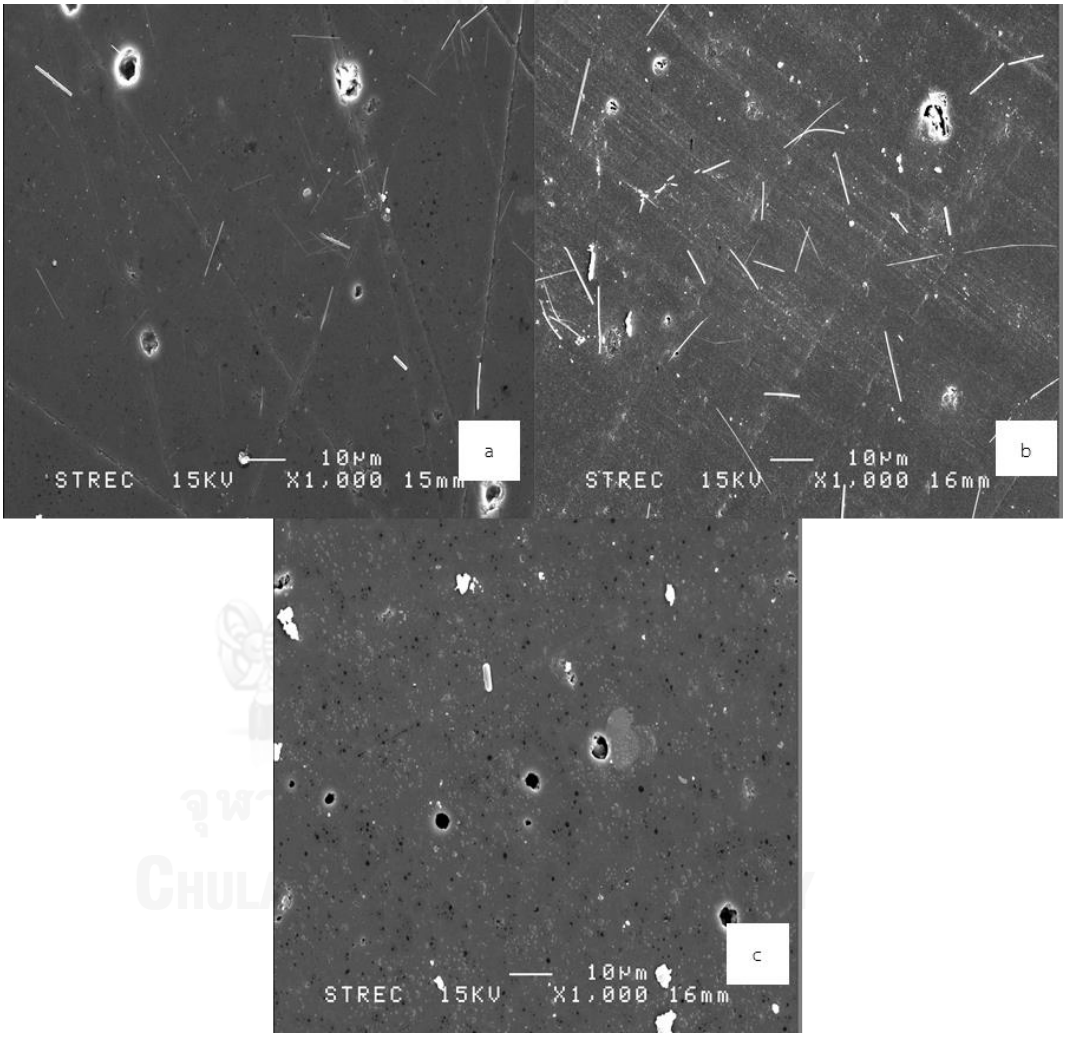

Figure 4.18 SEM micrographs of Lithium disilicate glass-ceramic under repetitive firing, first firing at 950°C (a), first firing at 950°C and 1ry dentin firing temperature at 810°C (b), first firing at 950°C, 1ry dentin firing temperature at 810°C and 2ry dentin firing temperature at 800°C (c)

The micrograph of the lithium disilicate glass-ceramic specimen first fired at a temperature of 950°C shows many pores and some short fiber-like crystals on the surface of specimens while more short and long fibers are formed and porosity is reduced during the second firing at the step of primary dentin firing of veneering porcelain at 810°C for 1 min. After the third firing (secondary dentin firing) at 800°C, the fiber-like crystals disappear, leaving small crystals dispersed as white spots in the glass matrix. However, some porosity is still remaining.

Multiple firings or repetitive firing of VLi850

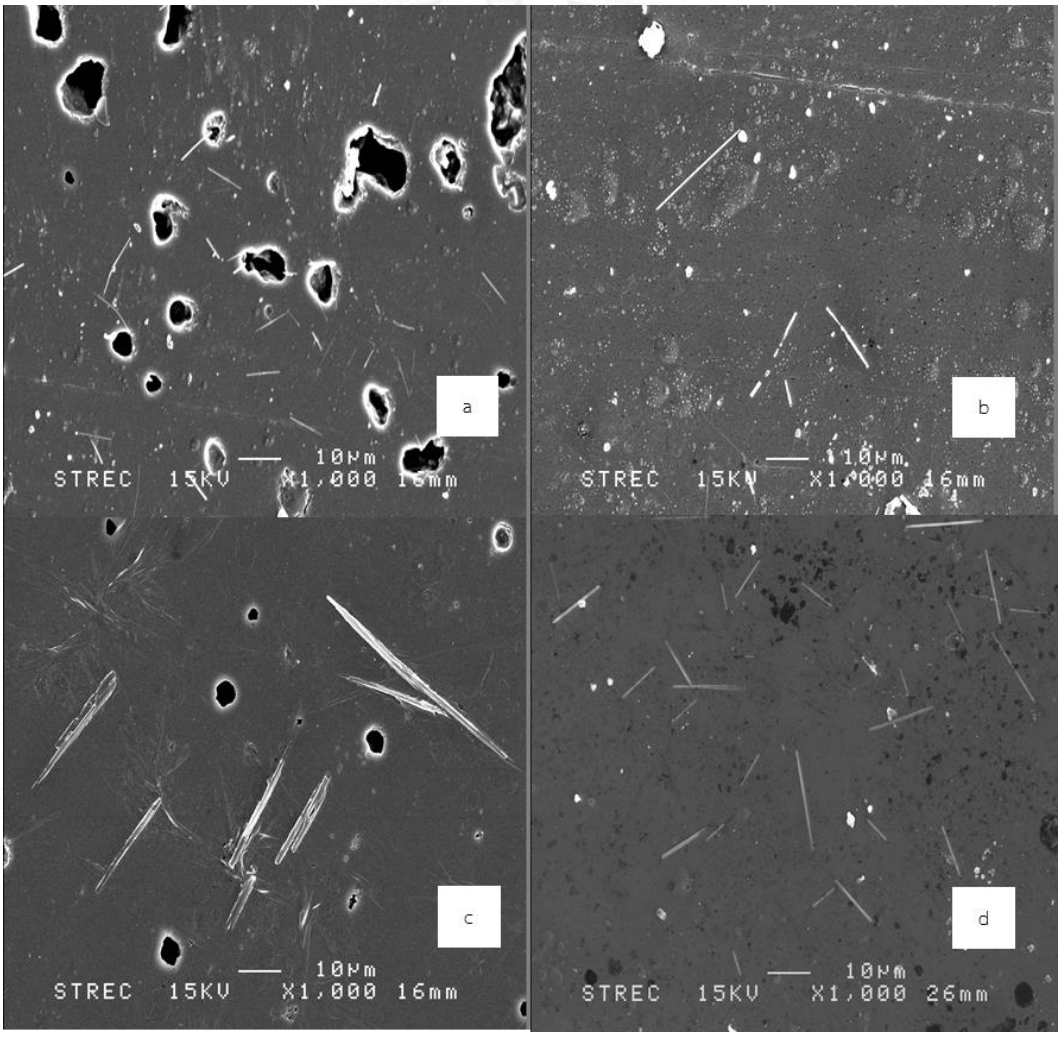

Figure 4.19 SEM micrographs of Lithium disilicate glass-ceramic after first firing at 850 °C (a), first firing at 850 °C and base dentin firing temperature at 930 °C (b), first firing at 850 °C, base dentin firing temperature at 930 °C and 1ry dentin

firing temperature at 910 °C (c), first firing at 850 °C and base dentin firing temperature at 930 °C and 1ry dentin firing temperature at 910 °C and 2ry dentin firing temperature at 900 °C (d)

After the first firing (850°C), it was found that there are many air bubbles and short crystals of lithium disilicate dispersed in the glass matrix. After the second firing (at 930°C), long fibers crystals and tiny round-shape were observed with porosity was reduced. After the third firing (at 910°C, as a step of primary dentin firing), large fibers were formed and there was a reduction in porosity in the matrix. After the fourth firing at 900°C, both short and long, fine fibers were formed throughout the glass matrix, but with remaining of small amounts of porosity

d) Result of Vickers microhardness and fracture toughness of glass-ceramic liner and interface between zirconia substrate and veneering porcelain

- Results of Vickers hardness and fracture toughness of bulk glass liner

Specimens of bulk glass-ceramic liners as well as lithium disilicate glass liners were prepared for mechanical property determination and the results are as followed:

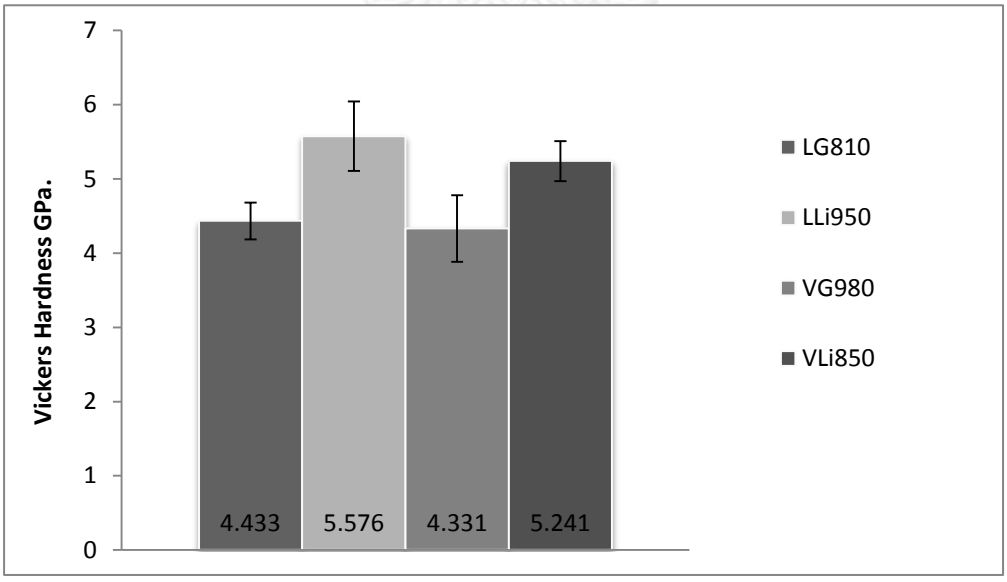

Figure 4.20 Vickers hardness of LG810, VG980, LLi950 and VLi850.

The prepared specimen was loaded with 300 gf on the surface for 10 seconds. It was found that LLi950 exhibits the highest Vickers hardness value (with statistically significance) followed by VLi850 (534.42 HV). In contrast, there was no statistic difference in the hardness between LG810 (451.02 Hv) and VG980 (441.6 Hv).

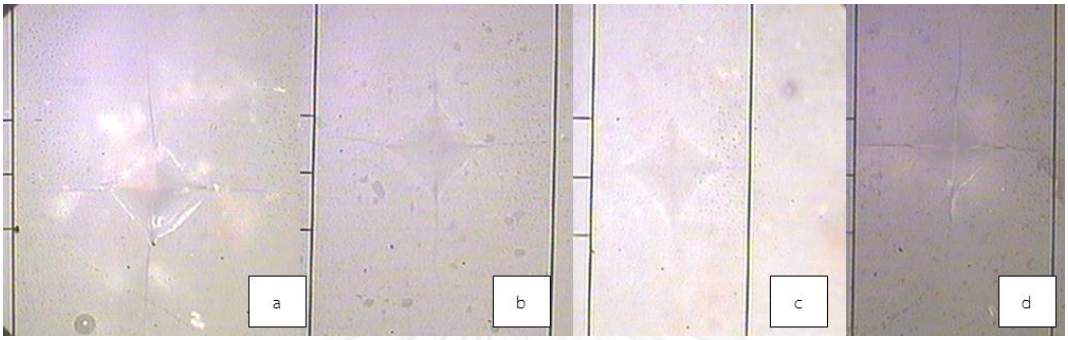

Figure 4.21 Interfacial Vickers indentation and microcracks from vertices of pyramid under stereomicroscope, LG810 (a), LLi950 (b), VG980 (c) and VLi850 (d).

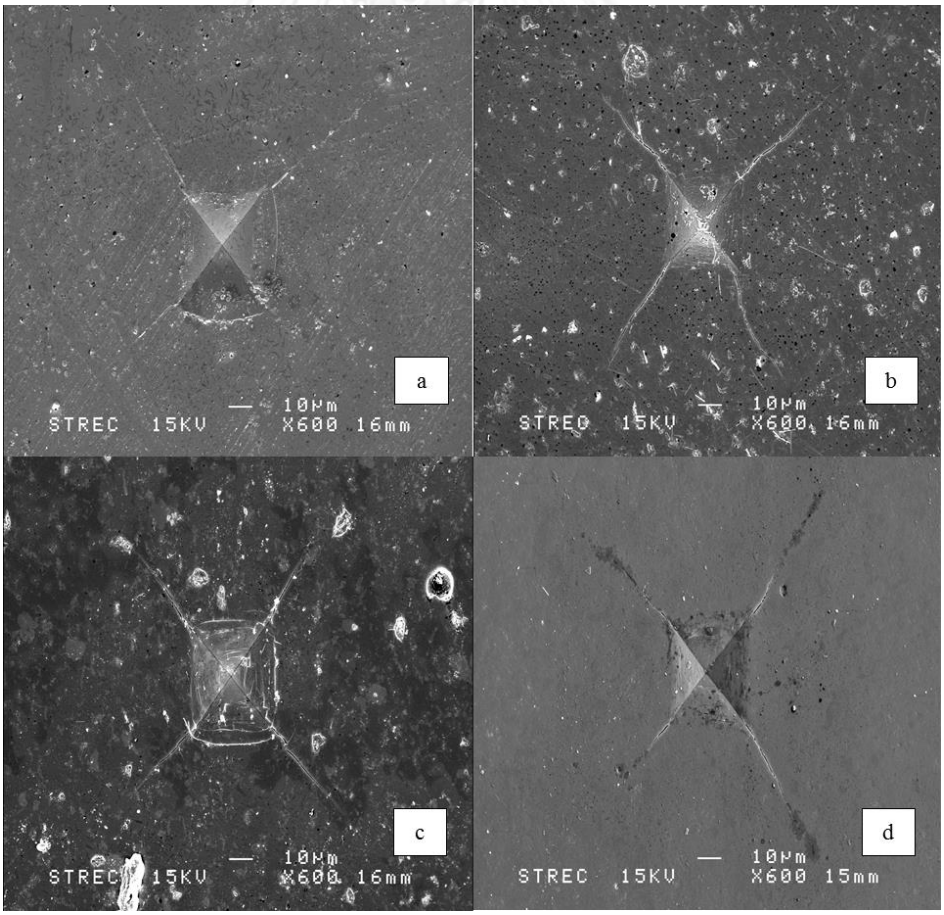

Figure 4.22 Vickers indentation and microcracks from vertices of identation observed by SEM, LG810 (a), LLi950 (b), VG980 (c) and VLi850 (d).

-Results of Vickers hardness and fracture toughness of bulk glass liner

Fracture toughness (K_{IC})

Fracture toughness values were calculated using the data from Vickers hardness and graphically presented in **Figure 4.23**

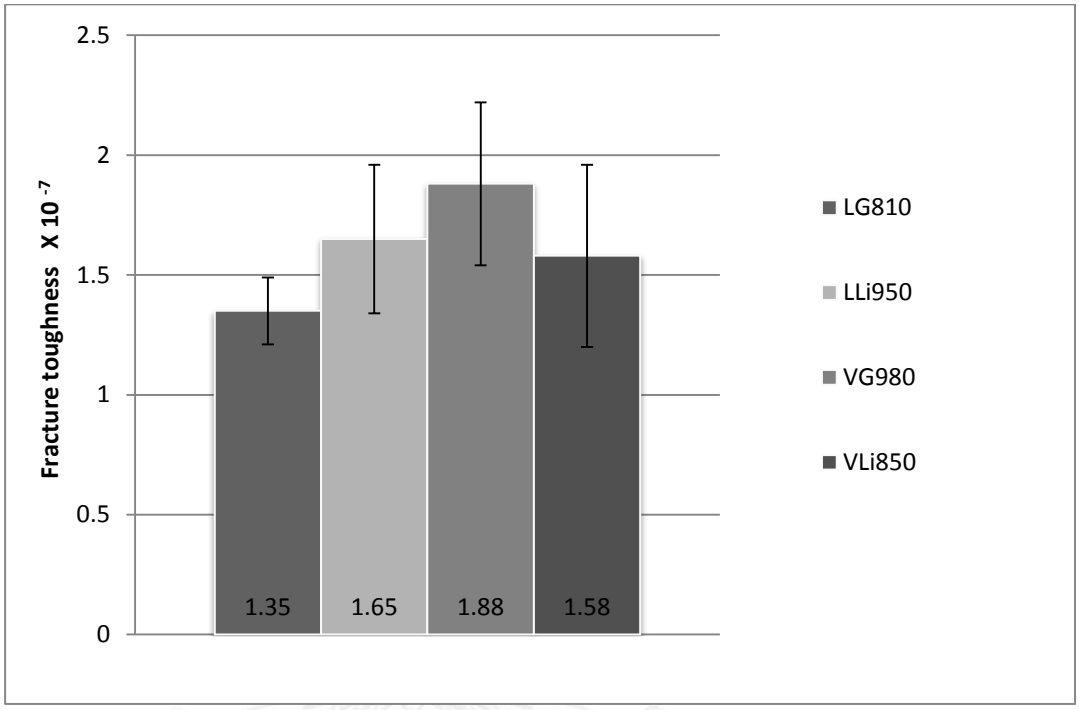

Figure 4.23 Fracture toughness type I (KIC) of LG810 and LLi950, VG980 and VLi850

VG980 gives the highest fracture toughness with statistical significance followed by LLi950 and VLi850 respectively.

e). Result of interface analysys between zirconia substructure and veneering porcelain

-Interface analysys by high resolution SEM

Figure 4.24 SEM images at the interface between zirconia substructure and glass-ceramic liner (x 20000), secondary electron mode in left column and back scattered mode in right column. LG810D (a, b), LLi950D (c, d), VG980D (e,f), VLi850D (g, h)

Figure 4.25 SEM images at the interface between zirconia substructure and glass-ceramic liner (x 50000), secondary electron mode in left column and back scattered mode in right column. LG810D (a, b), LLi950D (c, d), VG980D (e,f), VLi850D (g, h)

At the interfacial area between white color of opaque zirconia substrate and black color of translucency glass-ceramic, a thin gray layer of 0.2-0.5 is observed which may be the interdiffusion zone.

-Interface analysys by linear EDX

From the results of linear EDX at the interface, it is found that Si^{+4} ion clearly diffuses from high concentration (glass-ceramic layer) to the low concentration region (zirconia substrate). From the zirconia side, Y^{+3} ions diffuses into the glass side, but Zr^{+4} ion did not.

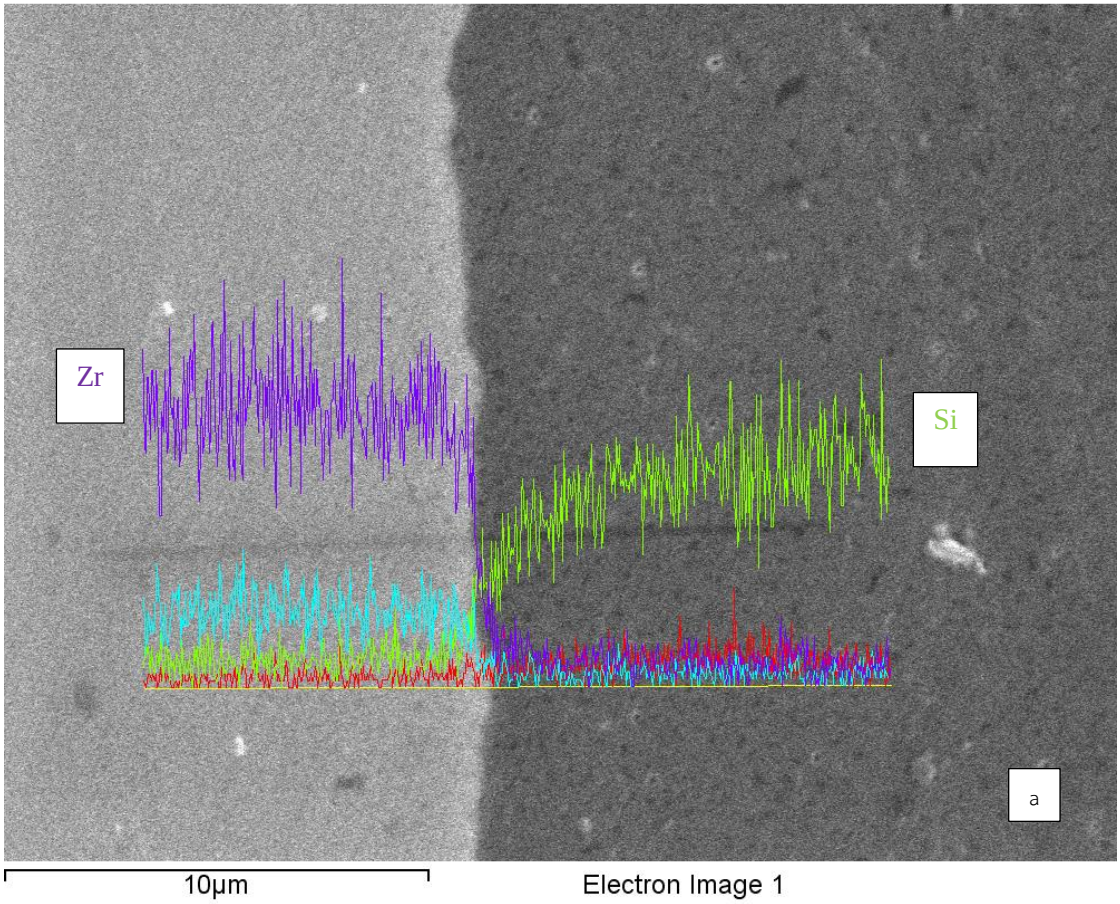

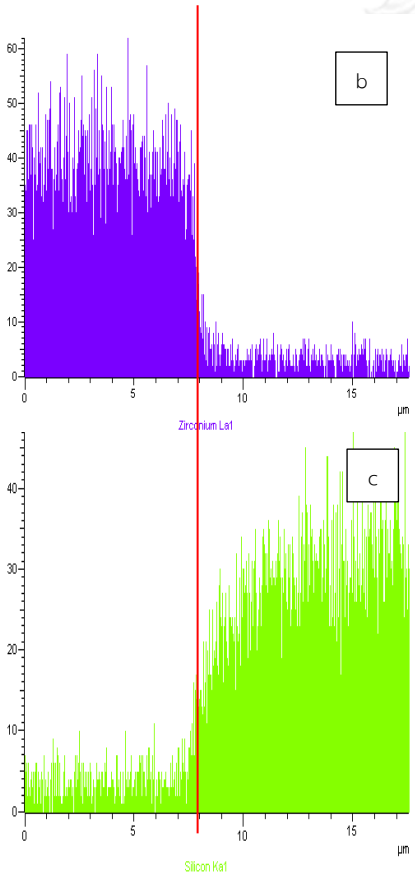

Figure 4.26

shows SEM with linear EDX of LG810D at the interface (a), intensity and distance of zirconia (b) and silicon (c) at the interface

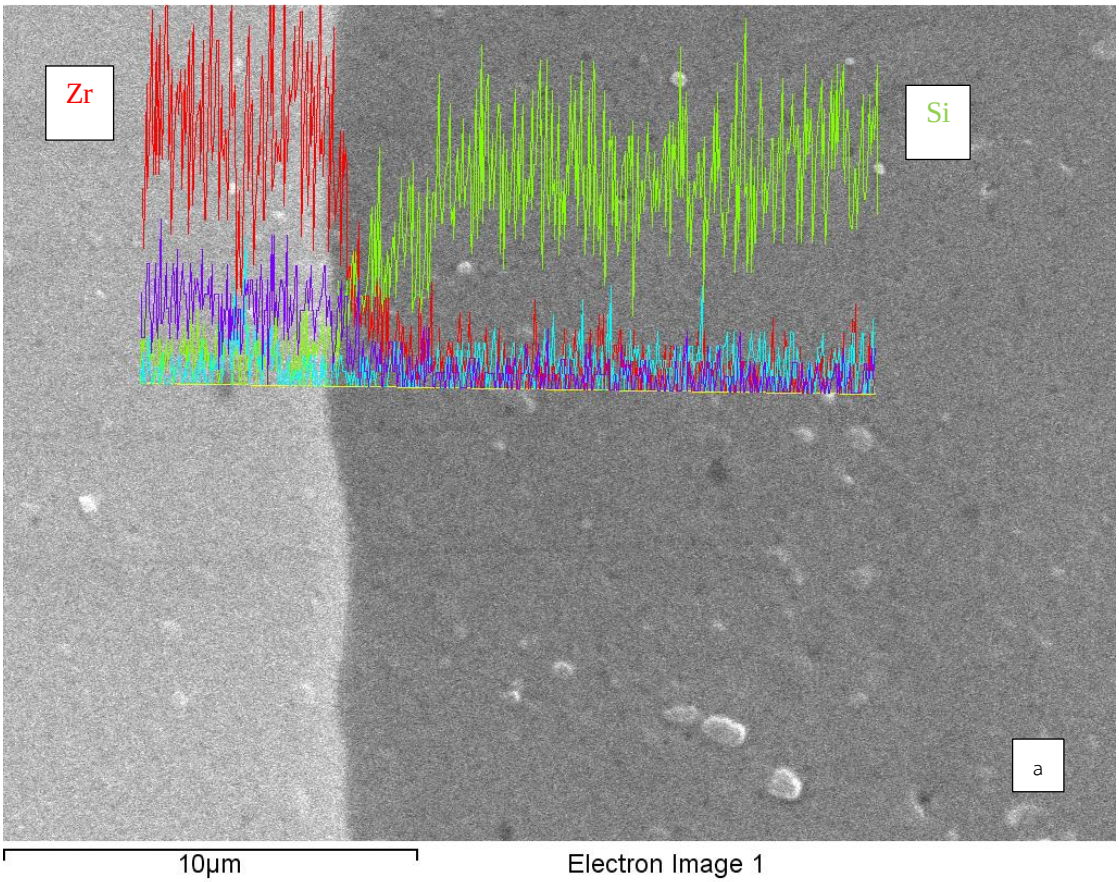

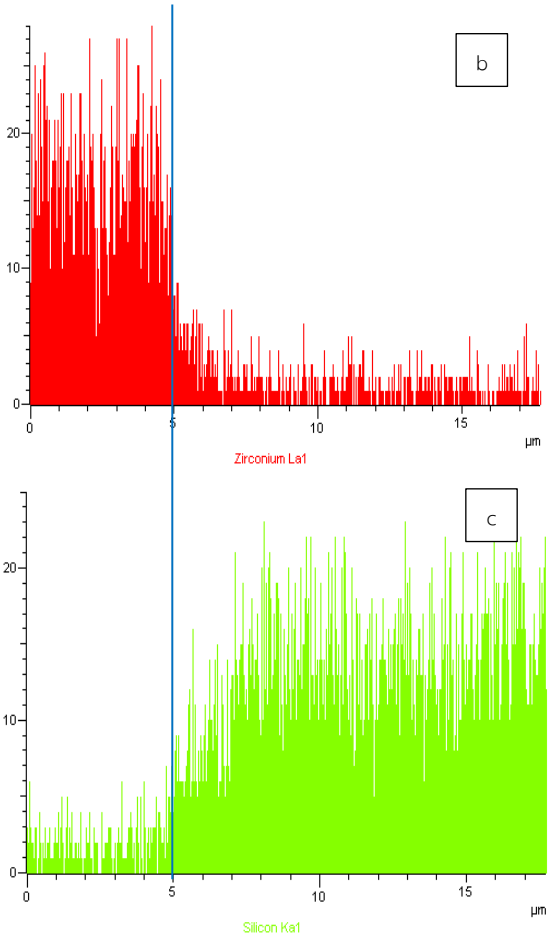

Figure 4.27

SEM with linear EDX of LLi950D at the interface (a), intensity and distance of zirconia (b) and silicon (c) at the interface

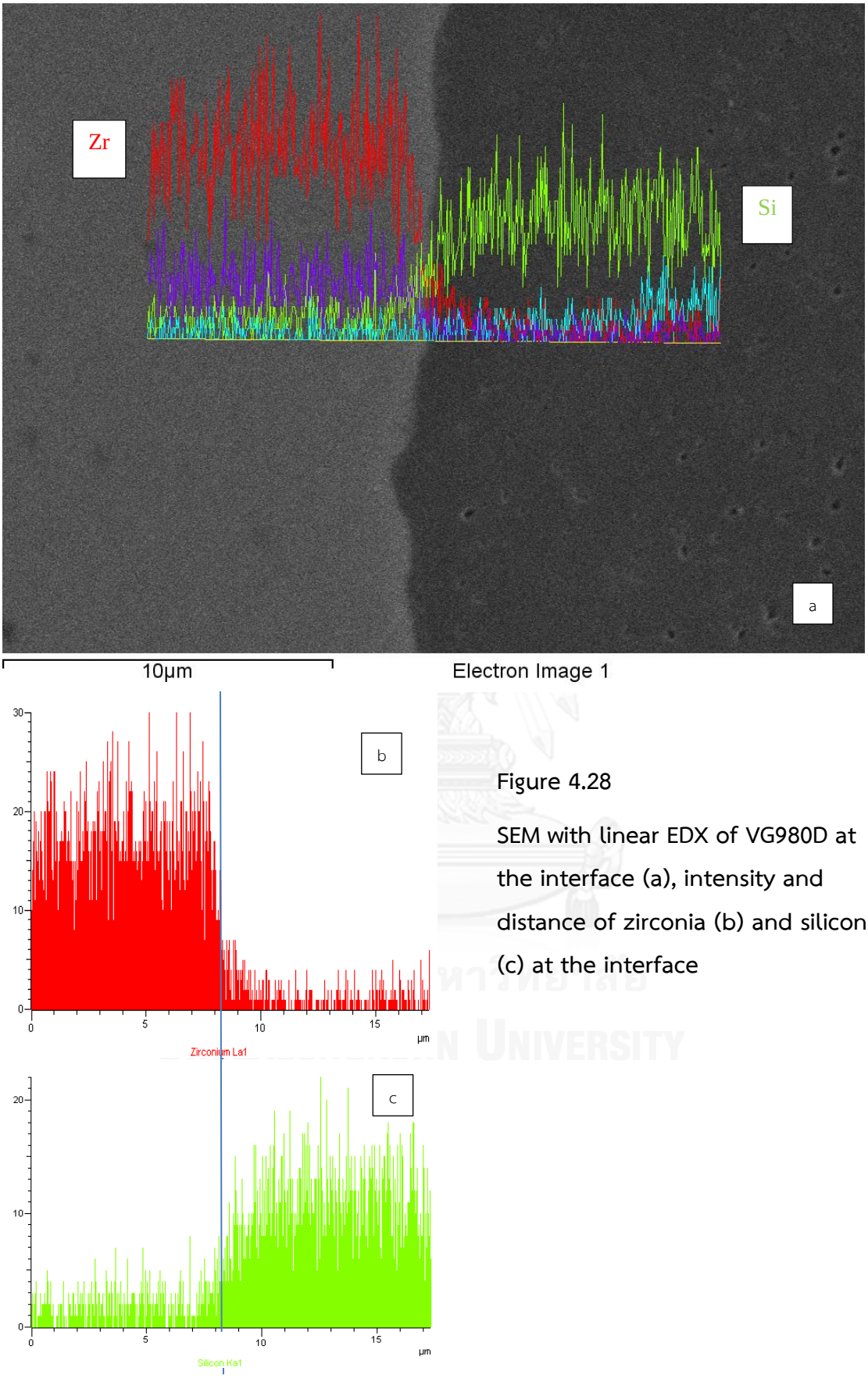

Figure 4.28

SEM with linear EDX of VG980D at the interface (a), intensity and distance of zirconia (b) and silicon (c) at the interface

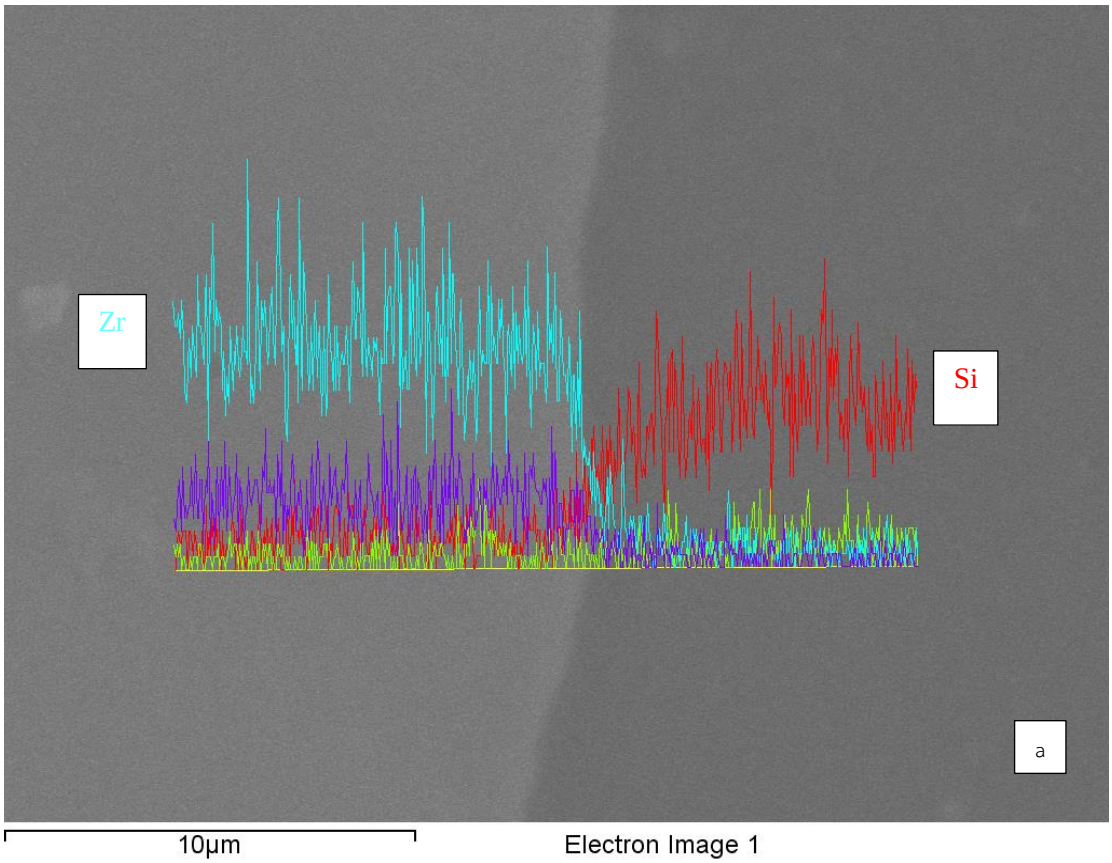

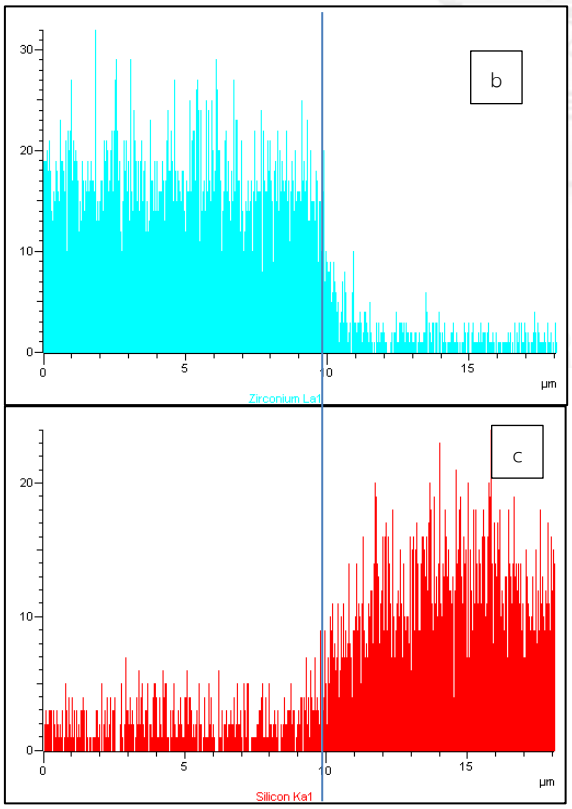

Figure 4.29

SEM with linear EDX of VLi850D at the interface (a), intensity and distance of zirconia (b) and silicon (c) at the interface

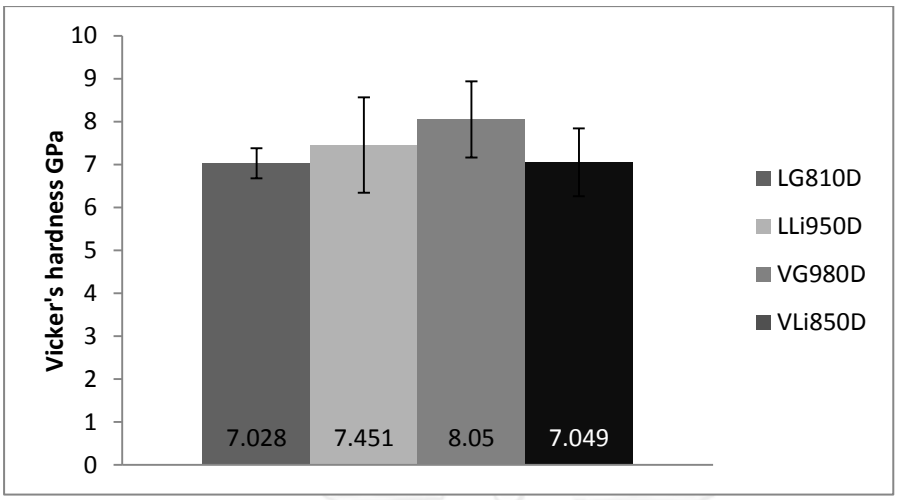

Figure 4.30 Vickers hardness at interface between zirconia substrate and veneering porcelain (with glass-ceramic interlayer).

It was found that specimens in the VG980D displayed the highest Vickers hardness significantly different from the other groups and this is followed by LLi950D, VLi850D and LG810D respectively.

Fracture toughness

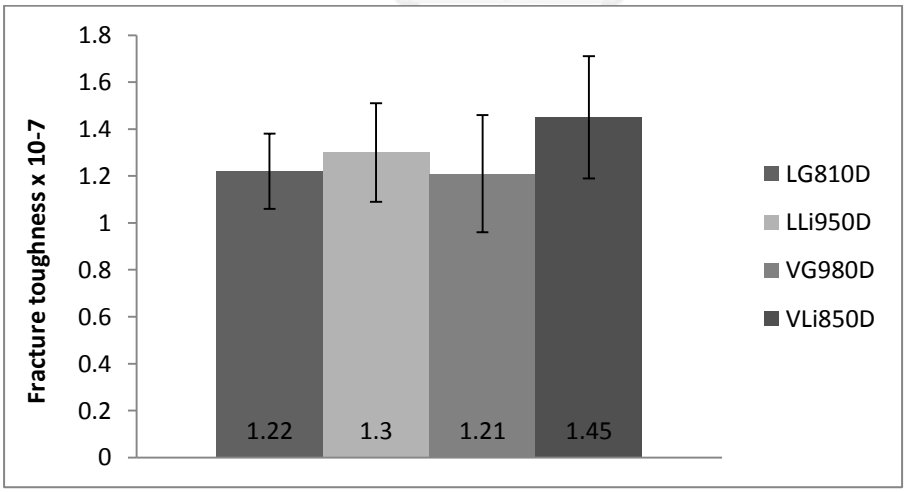

Figure 4.31 Fracture toughness at the interface between zirconia substructure and veneering porcelain (with glass-ceramic interlayer)

In contrast to the results of Vickers hardness, VLi850D shows the highest fracture toughness, followed by LLi950D and there is no significant difference between those of LG810D and VG980D.

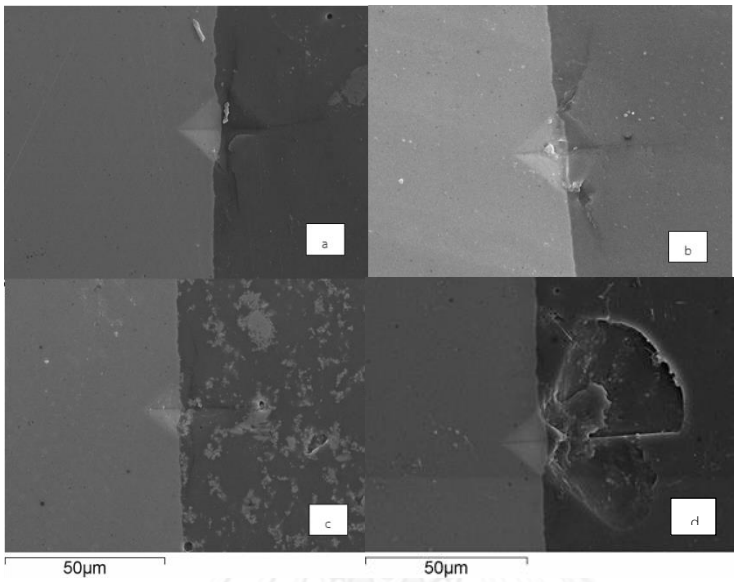

Figure 4.32 SEMs of indentations at the interface between zirconia substructure and glass-ceramic liner, LG810D (a), LLi950D (b), VG980D (c), VLi850D (d)

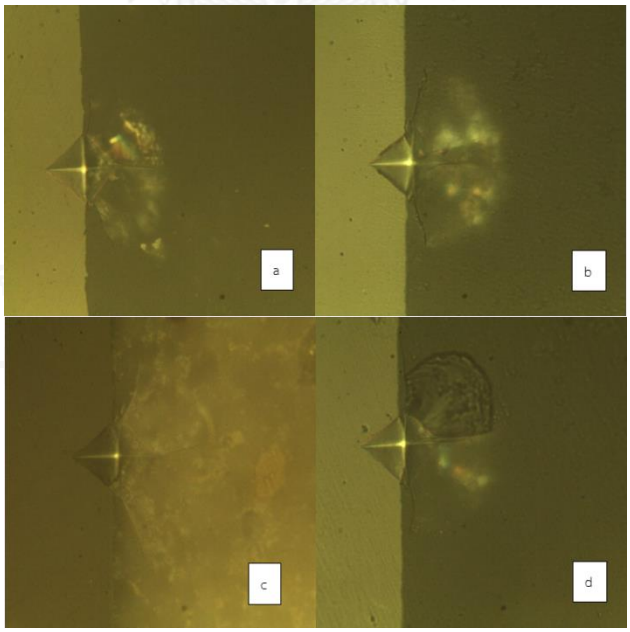

Figure 4.33 Stereomicrographs of indentations between zirconia and glass-ceramic at the interfaces. LG810D (a), LLi950D (b), VG980D (c), VLi850D (d)

From the SEM micrographs and stereomicrographs, it was found that there were no cracks propagating into the zirconia surface, but cracks were revealed in the veneering porcelain side. Therefore, the measurement of only 3 crack lines with lengths of C1, C2 and C3 was possible. C1 and C3 of each indentation were merged together. The average crack length was calculated to measure the length that form along the interface between zirconia substrate and glass-ceramic the results are shown in **Figure 4.33**. Moreover, it was note that there were no gaps and pores visible along the interface which confirm that glass-ceramic liner perfectly wets both zirconia and porcelain surfaces. However, according to M. Ferraris, the resistance to cracks propagation provides a qualitative measurement of the strength of a brittle material, especially when the indentation is performed at the substrate–coating interface, with one of the diagonals near or just on the border line between the two materials (brittle coating on brittle substrate). The pattern of crack propagation gives qualitative information about the fracture energy of the two joined materials and also about the fracture energy of their interface, thus comparative results for similar materials (brittle coatings on brittle substrates) can be obtained. If the interface is strongly bonded, the crack paths will propagate into the weaker material, glass-ceramic. As shown in Figure 4.32 and 4.33, the crack paths in the glass-ceramic coatings readily stop by the crystalline phases. Some small cracks propagate **p**arallel to the interface without any detachment of the coating from the substrate.

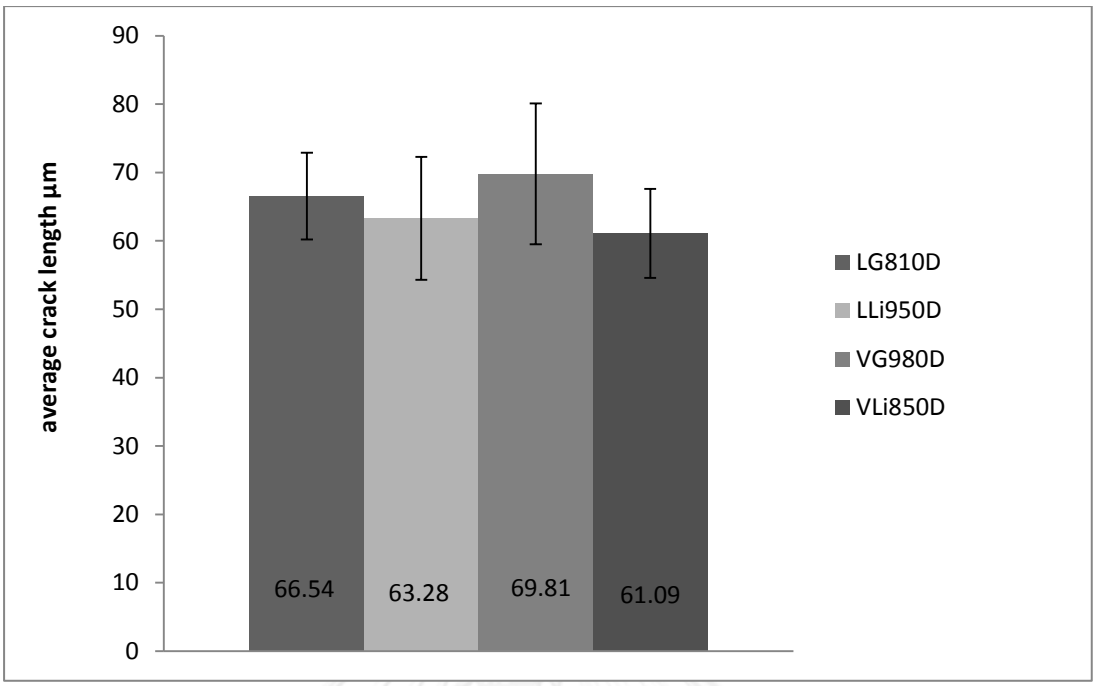

Figure 4.34 Average crack length along interface of bonding area

From the data, it was found that VG980D showed the highest average crack length along the interface (C1-C3), and was significantly different from another group. Both, VLi850D and LLi950D showed lower crack lengths when compared to those of commercial glass-ceramic.

C2, the crack length which was measured perpendicular to the interface of each indentation and the average C2 of these 4 groups was calculated and displayed in Figure 4.34

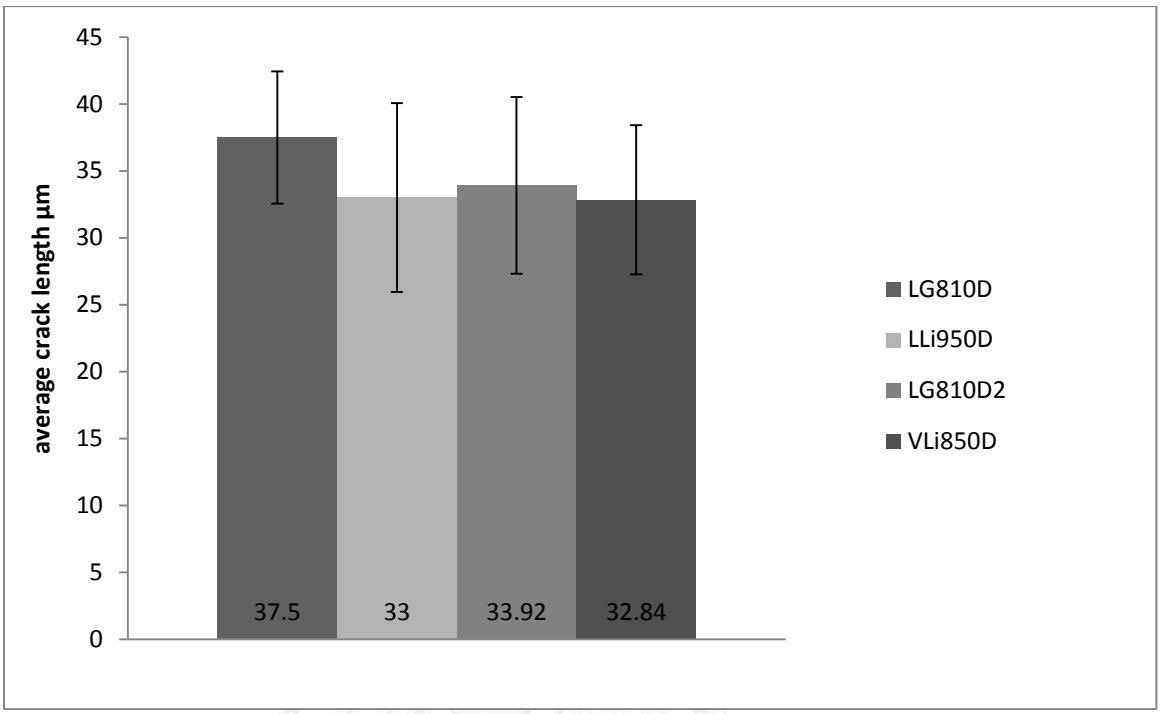

Figure 4.35 Average crack length perpendicular to the interface area: C2

From the data, it was found that LG810D showed the highest average C2 crack length that penetrates into the veneering porcelain and this result was significantly different from the other groups.

4.3 Result of biocompatibility test of lithium disilicate glass-ceramic

a) Result of MTT assay

A standard curve was plotted to investigate and determine the relationship between cell number of human gingival fibroblast cells (in a 24-well plate) and absorbance. The results are shown in **Figure 4.36**

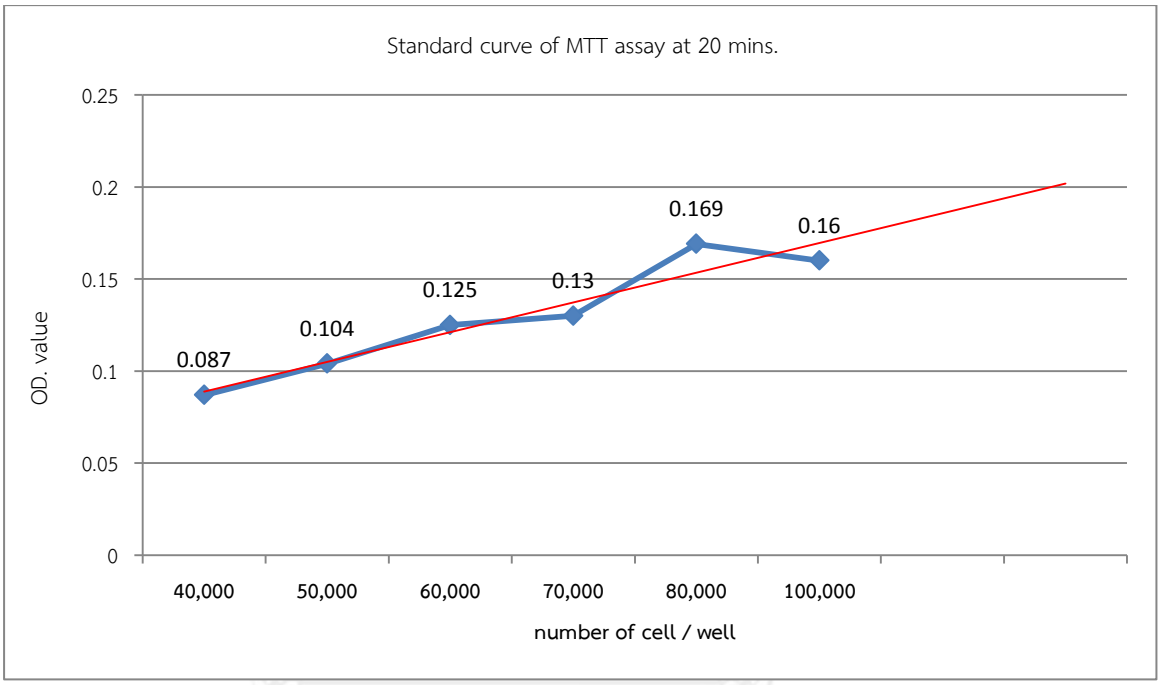

Figure 4.36 Standard curve of MTT assay of gingival fibroblast cell at 20 mins.

It was found that for all numbers of 40,000 cells/well , 50,000 cells/well and 60000 cells/well, the curve is still linear. Thus a OD. value of 40,000 cells/well, MTT at 20 mins was selected for this study.

The extracted media from LG810 and VG980, LLi950 and VLi850 glass-ceramic groups were dropped into 48-well microliter plates at 20,000 cells/well with varied time and concentration. Then OD values of all plates were measured. The results are shown in **Figure 4.37**

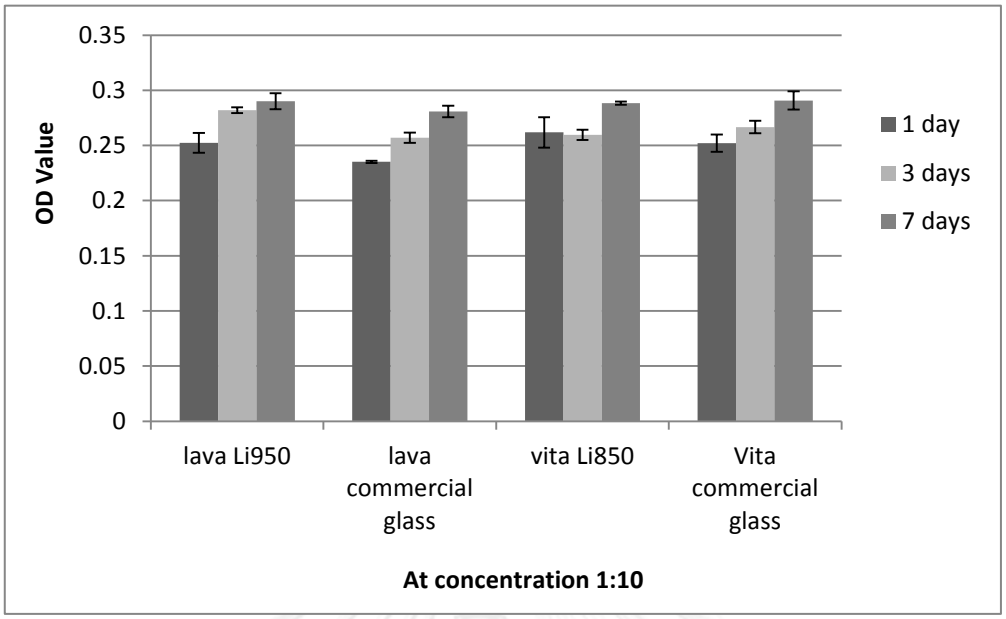

Figure 4.37 OD values of gingival fibroblast cells tested with 4 types of glass stored in medium for 1, 3 and 7 days, at concentration (solution per total medium volume) of 1:10

From the data for 1 day of cell culture, no difference was observed in statistical analysis of one-way ANOVA between the 4 glass-ceramic liners. But after 3 days, it was found that LLi950 gave the highest OD (oxygen demand) value, significantly different from the other glass liners but the results after 7 day show no statistically different between 4 groups of glass-ceramic liner.

b) Result of Direct contact technique

It was found that gingival fibroblast cells adhered to all types of glasses. After 24 hours incubation, cells were still alive and had propagated on all 4 groups of glass-ceramic as seen under stereomicroscope in the left column. In addition, under SEM, they are clearly observed through the cover glass surface as shown on the right column.

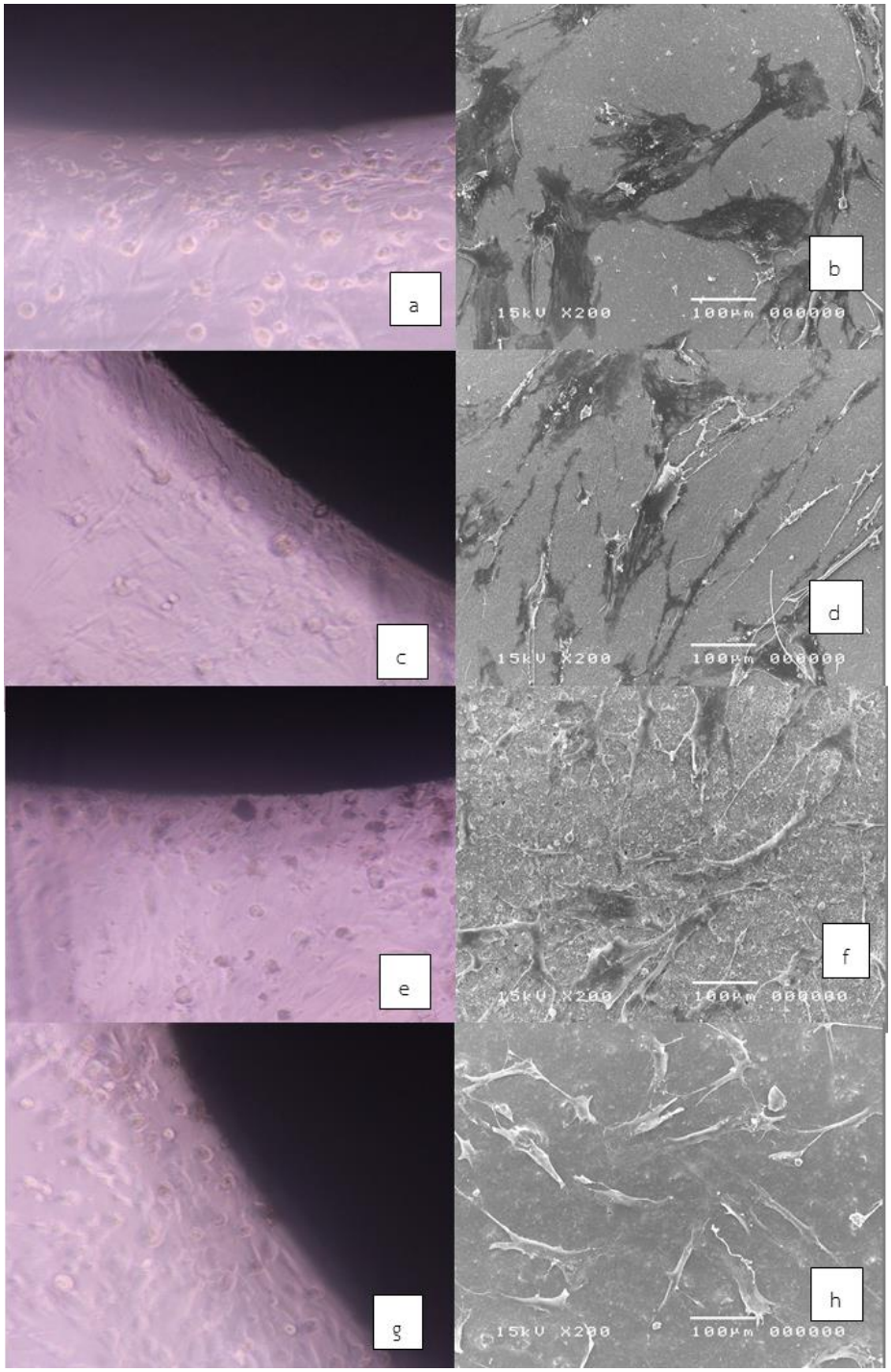

Figure 4.38 Cell direct contact on surfaces of glass-ceramic liners after plating for 24 hours under observed by stereomicroscope and SEM. LLi810 (a, b), LLi950 (c, d), VG980 (e, f) and VLi850 (g, h)

Chapter 5
Discussion

The effect of the glass interlayer on the shear bond strengths between the zirconia substrates and feldspartic veneering porcelain of the two zirconia systems at various firing temperatures and durations was investigated. In each zirconia system, the group with the highest mean shear bond strength was selected for further thermocycling tests. It was found that the shear bond strengths of all the groups in VITA zirconia system were higher than those of Lava zirconia system and higher than acceptable critical limit (25 MPa). This may have resulted from the difference in composition and crystal morphology after firing of the two zirconia systems. VITA zirconia contains 3 w% Hafnium Oxide (HfO_2)[61], (as shown in **Table 3.1 and the XRD results Figure 4.1**) while Lava zirconia does not, hence a chemical bond between zirconia substrate and glass-ceramic interlayer or veneering porcelain might be formed as a Hf-Si bond [62]. In addition, the VITA zirconia had a higher alumina content (<1 w%) than the Lava zirconia (<0.25%) which affects surface irregularities (surface roughness)[63]. From the SEM micrographs, (**Figure. 4.2**) a different fired grain size is visible, VITA zirconia shows smaller average grain size (measured according to ASTM E112-10)[59] with high surface roughness (VITA = 0.04714 μm, Lava = 0.05419 μm). Then, the fluid glass liner was able flow into the irregularities on the zirconia surface, forming micro-mechanical interlocking. Accordingly, this may be the explanation for the higher mean shear bond strength of specimens from the VITA zirconia system over that of there in the Lava system. Moreover it was found that no significant difference between the mean shear bond strengths of specimens between VD group and VG980D group. This result was similar to that of the Lava zirconia group where the mean shear bond strength of the LD group was just slightly lower than that of LG810D group. Referring to previous studies, this finding was consistent with Aboushelib [51] that the glass interlayer had no significant improvement on shear bond strength, but inconsistent with Fischer et al.[50] and Mosharraf et al. [64].

VLi850D gave the highest mean shear bond strength because the recommended veneer firing schedule of VITA zirconia system was performed in 4 steps starting from 980°C for the commercial glass-ceramic liner layer followed by 930°C for the base dentin and 910°C down to 900°C for the 2nd and 3rd dentin layers, respectively. After firing the first layer of glass-ceramic liner at 850°C, the SEM micrographs (**Figure. 4.6**) revealed many pores in the glass matrix of VLi850. Thus the first layer of porcelain (base dentin) could have later penetrated into the pores and fused together with

lithium disilicate glass-ceramic while it was subjected to the rest of veneering steps at high temperatures ranging from 930 to 900°C, These temperature should have been high enough for the first layer of lithium disilicate glass-ceramic to melt and penetrate into the irregularities on VITA zirconia surface, forming micromechanical interlocking, and, thus the lithium disilicate glass-ceramic liner forms strong bonds with both sides.

On the contrary, the recommended veneer firing schedule for specimens in the Lava zirconia system was performed in 3 steps starting from 810°C for the layer of glass-ceramic liner and 810°C down to 800°C for the 1st and 2nd dentin layers, respectively. For the specimen with the highest mean shear bond strength in this group, LLi950D, the lithium disilicate glass-ceramic liner layer was fired at 950°C followed respectively with primary dentin firing at 810°C and secondary dentin firing at 800°C. Accordingly, it is obvious that 950°C is the highest temperature that the specimens in this group experience and should be possible for lithium disilicate glass-ceramic to melt and penetrate into the irregularities of Lava zirconia surface, stress generating micromechanical interlocking between glassy interlayer and surface of zirconia substrate, hence resulting in stronger bonding on the zirconia side compared to LLi800D and LLi850D groups because the highest temperatures for these 2 groups were 810°C and 850°C, respectively, would have been too low for the glass-ceramic to melt and form lithium disilicate crystals with a homogeneous glass matrix[65]. Consequently, large pore spaces remained and formed a weak glass interlayer which could be broken easily, hence cohesive failure in glass layer is the major mode of failure in LLi800D and LLi850D groups as shown in **Figure 4.10(d-f)** while that of LLi950D group was a combination failure mode between adhesive and cohesive(**Figure 4.10 (g-i).).**

The results of fractography of the specimens in VITA zirconia groups, **Figure 4.12 (g-l)** illustrate combination failure mode between adhesive and cohesive. The fracture surface shows remaining of the glass-ceramic interlayer on both zirconia substrate and veneering porcelain sides which supports the results of their high shear bond strength.

From the XRD results, it can be explained why the specimens of LG810D and VG980D gave lower mean shear bond strengths than those using lithium disilicate glass-ceramic. The most important reason is the difference in chemical composition or type of the glass employed which after heat treatment, each will yield different

crystal phases and morphology. Lava glass and VITA glass-ceramic liners are composed mainly of non-crystalline glass and leucite (potash feldspar) with plate-like crystals **(Figure 4.7),** respectively, while those of lithium disilicate glass-ceramic are short needle-like crystals of Li_3PO_4 and long needle-like crystals of $Li_2Si_2O_5$ which fill and interlock in the surface irregularities of zirconia substrate, enhancing adherence and crack propagation resistance[66-68]. After firing, potash feldspar in the VITA glass-ceramic liner contributes plate-like leucite crystals which may cause an increase in the coefficient of thermal expansion (CTE) of the glass-ceramic interlayer and the porcelain as well[69]. To complete a veneering process, specimens have to be fired about 4-5 cycles at least. Every firing cycle, content of leucite crystals is changed in both glass-ceramic liner and veneering felspathic porcelain, unavoidably resulting in decreasing or an increase in the CTE[70]. Thus it is possible why finally, the CTE of glass-ceramic liner and veneering porcelain may be higher than those of the starting commercial glass-ceramic liner and porcelain powders and cause a mismatch with the zirconia substrate[71] while lithium disilicate glass-ceramic shows high thermal shock resistance and low thermal expansion[65]. To an extent, the stress generated by the CTE mismatch at the interface between the zirconia substrate and veneering porcelain can chip the porcelain off the zirconia substrate[37]. This has been thought to be a major clinical failure that occurred after the restoration received masticatory force in the oral cavity for a period of time[71].

Thermocycling testing was selected to evaluate durability of the specimens under many cycles of sudden change in temperature (from $5^{\circ}C$ to $55^{\circ}C$) under wet conditions. The shear bond strengths of all the groups under test droped significantly. The sudden change in temperature caused stresses to be generated at the interface between the veneering porcelain and zirconia substrate when combined with hydrolysis of the glass-ceramic interlayer can weaken the bond between the interfaces.

From the backscattered SEM images of the fracture surfaces, (**Figure 4.14**) the bonding area can be separated into outer zone and inner zone areas. In the outer zone area, pits and grooves in the remaining glass are clearly observed that may be from hydrolysis of glass phenomena[72]. During the thermocycling process, the Si-O-Si bond linkage would have been broken by the sudden change of temperature which promotes the hydrolysis of glass, H^+ ion from H_2O molecule diffuses and binds to the Si-O to form Si-OH group at the surface of glass [73]. Hydrolysis, a well-known mechanism of glass corrosion, is progressive with number of thermal cycles, hence

the reduction of bond strength depends on the degree of corrosion. This finding is inconsistent with a previous research that shear bond strength between zirconia substrate and veneering porcelain was not affected by thermocycling[74]. However, the size of specimen in the mentioned research was larger than ours and the contrast might have resulted from the different sizes of the bonding area. Moreover the drop in shear bond strength may be also affected by phase transformation of tetragonal zirconia to monoclinic zirconia as shown in **Figure 4.17**

When reheating the lithium disilicate glass-ceramic bulk according to the veneering process (base dentin , primary dentin and secondary dentin firings), it was found that crystal content and morphology depended on temperature, duration and cycles of firing[70]. At low temperature many crystals were found in the glassy matrix because under high viscosity, diffusion in the melt is limited, then most of the original crystals of the glass-ceramic liner still remain. At higher temperatures more flow able glass is form on the expense of crystals, thus larger and longer crystals are able to form[58]. As a result, the melted glass penetrates and forms diffusive adhesion to the zirconia substrate and chemical bond with porcelain.

The cross section of bonding interfaces **in Figure 4.23 and 4.24** SEM images (x20000 and x50000 resolution), show a thin, gray layer (0.2-0.5 μm) lying between the opaque, white zirconia substrate and the translucent, black glass-ceramic which might be the inter-diffusion zone. From the results of linear EDX, the plots show that Zr^{4+} ion did not diffuse into the glass-ceramic surface but Y^{3+} did. Si^{4+} and $Al^{3+}$from the glass-ceramic clearly penetrate into zirconia surface. Therefore it is possible that the thin gray layer results from the inter-diffusion of Si^{4+} and the other ions across the interface, forming glassy bond. In addition to the glassy bond, a chemical bond, Hf-Si, might also exist in VITA veneering system[62]. Therefore, the high shear bond strength of VLi850D can be explained from the combination of good properties of VITA zirconia system and lithium disilicate glass-ceramic.

Vickers hardness indentation results at the bonding interface show that VG980 gaves the longest C1&C3 crack lengths, hence has the highest Vickers hardness followed by LLi950D and VLi850D, respectively. In contrast, VLi850D shows the highest fracture toughness significantly different from the other groups. Equation showing the relation between hardness and toughness[75] is as follows:

$$K_c = \alpha\sqrt{\frac{E}{H}}\frac{P}{c^{\frac{3}{2}}}$$

Where P is the applied load, E is Youngs modulus, H is the hardness, and c is the length of the surface trace of the half penny crack measured from the center of the indentand **α** is an empirically determined calibration constant.

From the equation, when Vickers hardness and crack length are increased, fracture toughness will be decreased. It is interesting that the VLi850D group showed moderate Vickers hardness but the highest fracture toughness and shear bond strength. However according to M. Ferraris et al., it was well known that the indentation method at the interface of different materials was a qualitative method and it gave comparative results for similar materials (brittle coatings on brittle substrates)[76]. Since there were no detachments of the porcelain coatings from the zirconia substrate in all the experimented samples, the coatings were adhering well to the substrates, thus the bonding at the interface was stronger than the coating.

Chapter 6
Conclusion

From the experimental results obtained, bonding between the zirconia substrate and the veneering porcelain is improved by using glass-ceramic liners. The better CTE stability, mean shear bond strength and fracture toughness over those of the current commercial leucite glass-ceramic liners and good biocompatibility have proved lithium disilicate glass-ceramic a potent glass-ceramic liner for porcelain veneer. It has been also found that the performance depends on the mechanical property (high hardness and fracture toughness) and morphology of lithium disilicate glass-ceramic during firing, i.e. content, shape and size of crystals formed as well as porosity. These are dependent on firing schedule which is specific for each zirconia system. Additionally, it has been found that the firing temperature has an effect on the melting properties and crystal structure of lithium disilicate glass-ceramic. At high temperature, more melted glass was formed on the expense of crystals and porosity, resulting in better diffusive adhesion with the zirconia and better chemical reaction with the veneering porcelain. As well as leucite, the content of lithium disilicate in the glass-ceramic is also changed with firing temperature and multiple firings. However, due to its much lower CTE than leucite, the effect on the CTE mismatch generated between zirconia and felspathic veneering porcelain should be less. Referring to the durability, the mean shear bond strength of the veneering specimens using lithium disilicate glass-ceramic under thermocycling treatment was reduced by a hydrolysis phenomenon in glass corrosion but able to attain well over 25 MPa. The EDX and SEM results revealed the diffusive adhesion leading to micro mechanical interlocking of glassy bond with zirconia surface and combined failure fracture under shearing force. Accordingly, from the Vickers indentation test at the interface no crack propagation in the zirconia surface was observed but some crack paths were clearly evident in the glass-ceramic vicinity. The higher shear bond strength of VLi850D over that of LLi950D was possibly due to its higher firing temperature schedule which favors the melted glass formation from the lithium disilicate glass-ceramic as well as

chemical bond from the additional 3%wt HfO_2 and the high Al_2O_3 content in Vita zirconia system.

Future suggestions:

Besides using lithium disilicate glass as liner, due to its color being similar to natural teeth and excellent mechanical properties, it is very interesting to exploit lithium disilicate glass-ceramic as crowns, bridges and veneers by developing glass formulations of lithium disilicate glass-ceramic with high hardness, fracture toughness and controlled morphology, and investigating the crystalline phases and microstructure of the material by controlling the heat-treatment schedule.

REFERENCES

[1] Sailer I, Feher A, Filser F, Luthy H, Gauckler L, Scharer P, et al. Prospective Clinical Study of Zirconia Posterior Fixed Partial Denture: 3-Year Follow-up. . Quintessence Int. 2006;37:685-93.

[2] Ban S. Reliability and Properties Of Core Materials For all-ceramic dental restorations Review. Japanese Dental Science. 2008;44:3-21.

[3] Vult Von Steyern P, Carlson P, Nilner K. All-ceramic fixed partial dentures designed according to the DC-Zirkon technique. A 2-year clinical study. Journal of Oral Rehabilitation. 2005;32:180-7.

[4] Al-Dohan H, Yaman P, Dennison J, Razzoog M, Lang R. Shear strength of core-veneer interface in bi-layered ceramics. J Prosthet Dent. 2004;91:349-55.

[5] Fischer J, Grohmann P, Stawarczyk B. Effect of Zirconia Surface Treatments on the Shear Strength of Zirconia/Veneering Ceramic Composites. Dental Materials Journal. 2008:448-54.

[6] Kohal R, Klaus G. A Zirconia Implant-Crown System: A Case Report The International Journal of Periodontics & Restorative Dentistry. 2004;24:147-53.

[7] Manicone PF, Rossi Iommetti P, Raffaelli L. An overview of zirconia ceramics: Basic properties and clinical applications. J Dent. 2007;35:819-26.

[8] Piconi C, Maccauro G. Zirconia as a ceramic biomaterial. Biomaterials. 1999;20:1-25.

[9] Christel P, Meunier A, Dorlot JM. Biomechanical compatbility and design of ceramic implants for orthopaedic surgery. Biomechanic:material charaateristic versus in vivo behavior. Ann NY Acad Sci. 1988;523:234-56.

[10] Swain M, Hannink R. Metastability of the Martensitic Transformation in a 12 mol% Ceria-Zirconia Alloy: II, Grinding Studies. Journal of the American Ceramic Society. 1989;72:1358-64.

[11] Ruff O, Ebert F, Stephen E. Contribution to the ceramics of highly refractory materials:II. System zirconia-lime. Z anorg All Chem. 1992;180:215-24.

[12] Garvie RC, Nicholson P. Structure and Thermomechanical Properties of Partially Stabilized Zirconia in the CaO-ZrO2 System. Journal of the American Ceramic Society. 1972;55:152-7.

[13] Fabris S, Paxton A, Finnis MW. A Stabilizedzation mechanism of zirconia base on oxygen vacancy only. Acta Materialia. 2002;50:5171-8.

[14] Lawson S. Environmental Degradation of Zirconia Ceramics. Journal of the European Ceramic Society. 1995;15:485-502.

[15] Chevalier J. What future for zirconia as a biomaterial? Biomaterials. 2006; 27:535-43.

[16] Lilley E. . In: Tressler RE MH, editors. Ceramics transactions, , . Westerville, : . Review of low temperature degradation of tetragonal zirconia ceramics. Corrosion and corrosive degradation of ceramics. 1990;10:387-406.

[17] Swab J. Low temperature degradation of Y-TZP materials. Journal Of Matriaks Science. 1991;26:6706- 14.

[18] Haraguchi K, Sugano N, Nishii T, Miki H, Oka K, Yoshikawa H. Phase transformation of a zirconia ceramic head after total hip arthroplasty. THE JOURNAL OF BONE AND JOINT SURGERY 2001;83-B:996-1000.

[19] Catledge S A., Monique C, Vohra Y K, Santos E M, McClenny M D, Moore K D. Surface crystalline phases and nanoindentation hardness of explanted zirconia femeral heads. J Mater Sci-mater M. 2003;14:863-7.

[20] Denry I, Kelly J. State of the art of zirconia for dental applications. Dent Mater. 2008;24:299-307.

[21] Deville S, Chevalier J, Fantozzi G, Bartolome J, Requena J, Moya J, et al. Low-temperature ageing of zirconia-toughened alumina ceramics and its implication in biomedical implants. Journal of the European Ceramic Society. 2003;23:2975-82.

[22] Tanaka K, Tamura J, Kawanabe K, Nawa M, Oka M, Uchida M, et al. Ce-TZP/Al2O3 nanocomposite as a bearing material in total joint replacement. Journal of Biomedical Materials Research Part B. 2002;63:262-70.

[23] Fantozzi G, Chevalier J, Guilhot B. Processing microstructure and thermochemical behavior of ceramics. Adv Eng Mater. 2001;3:563-9.

[24] Sundh A, SjÖgren G. Fracture resistance of all-ceramic zirconia bridges with differing phase stabilizers and quality of sintering. Dental Materials. 2006;22:778-84.

[25] Filser F, Kocher P, Gauckler L. Net-shaping of ceramic components by direct ceramic machining. Assembly Automation. 2003;23:382-90.

[26] Chevalier J, Deville S, MÜnch E, Jullian R, Lair F. Critical effect of cubic phase on aging in 3mol% yttria-stabilized zirconia ceramics for hip replacement prosthesis. Biomaterials. 2004;25:5539-45.

[27] Ruiz L, Readey M. Effect of Heat Treatment on Grain Size, Phase Assemblage, and Mechanical Properties of 3 mol% Y-TZP. Journal of the American Ceramic Society. 1996;79:2331-40.

[28] Scott H. Phase relationships in the zirconia-yttria system Journal Of Matrials Scince. 1975;10:1527-35.

[29] Cottom BA, Mayo MJ. Fracture toughness of nanocrystalline ZrO_2-3mol% Y_2O_3 determined by Vickers indentation. Scripta Mater. 1996;34:809-14.

[30] Gupta TK, Bechtold JH, Kuznicki RC, Cadoff LH, Rossing BR. Stabilization of tetragonal phase in polycrystalline zirconia. J Mater Sci. 1977;12:2421-6.

[31] Witkowski S. (CAD-)/CAM in Dental Technology. Quintessence Dent Technol. 2005:169-84.

[32] McLaren E, Giordano R. Zirconia-Based Ceramics: Material Properties, Esthetics, and Layering Techniques of a New Veneering Porcelain, VM9 Quintessence Dent Technol. 2005:99- 111.

[33] Blue DS, Griggs JA, Woody RD, Miller BH. Effect of bur abrasiveparticle size and abutment composition on preparation of ceramic implant abutments. J Prosthet Dent. 2003;90:247-54.

[34] Kosmač T, Oblak Č, Jevnikar P, Funduk N, Marion L. The effect of surface grinding and sandblasting on flexural strength and reliability of Y-TZP zirconia ceramic. Dental Materials. 1999;15:426-33.

[35] Mackert J.R., Jr., TwiggsS.W., Williams A.L. High-temperature X-ray Diffraction Measurement of Sanidine Thermal Expansion. J Dent Res. 2000;79:1590-5.

[36] Bagby M, Marshall SJ, Marshall GW. Metal Ceramic Compatibility: A Review Of The Literature. J Prosthet Dent. 1990;63:21-5.

[37] Guazzato M, Proos K, Quach L, Swain M. Strength, reliability and mode of fracture of bilayered porcelain/zirconia (Y-TZP) dental ceramics. Biomaterials. 2004;25:5045-52.

[38] Saito A, Komine F, Blatz M, Matsumura H. A comparison of bond strength of layered veneering porcelains to zirconia and metal. J Prosthet Dent. 2010;104:247-57.

[39] Pjetursson B. E, Sailer I, Zwahlen M, Ha¨mmerle C. H. F. A systematic review of the survival and complication rates of all-ceramic and metal-ceramic reconstructions after an observation period of at least 3 years. Part I: single crowns Clin Oral Impl Res. 2007;18 73-85.

[40] Quinn J. B, Sundarb V, ParryaE. E, Quinna D.G. Comparison of edge chipping resistance of PFM and veneered zirconia specimens. dental materials. 2010;2 6:13-20.

[41] Yin JY, Zhang ZT, Ai HJ, Si WJ, Bao Y. Study on the compatibility of yttria-stabilized zirconia framework bonded to the corresponding veneering ceramic. Hua Xi Kou Qiang Yi Xue Za Zhi. 2009;27 669-72.

.

[42] Özkurt Z, KazazoĞlue E, Ünal A. In vitro evaluation of shear bond strength of veneering ceramics to zirconia. Dental Materials Journal. 2010;29:138-46.

[43] Garvie RC, Hannink RH, Pascoe RT. Ceramic steel? Nature. 1975;258:703-4.

[44] Reed JS, Lejus AM. Effect of grinding and polishing on near-surface phase transformations in zirconia. Mater Res Bull. 1977;12:949-54.

[45] Kitano Y, Mori Y, Ishitani A, Masaki T. Rhombohedral phase in Y_2O_3-partially-stabilized ZrO_2. J Am Ceram Soc. 1988;71:C34-C6.

[46] Denry IL, Peacock JJ, Holloway JA. Effect of heat treatment after accelerated aging on phase transformation in 3Y-TZP. J Biomed Mater Res Part B. 2010;93B:236-43

[47] Guazzato M, Quach L, Albakry M, Swain M. Influence of surface and heat treatments on the flexural strength of Y-TZP dental ceramic. J Dent. 2005;33:9-18.

[48] Nakamura T, Wakabayashi K, Zaima C, Nishida H, Kinuta S, Yatani H. Tensile bond strength between tooth-colored porcelain and sandblasted zirconia framework. Journal of Prosthodontic Research. 2009;53:116-9

[49] Alnasar H A, Giordano R, Pober R. Bond strength of pressed and conventional porcelain to zirconia. 2008.

[50] Aboushelib M, Kleverlaan C, Feilzer A. Microtensile Bond Strength Of Different Component Of Core Veneered All-Ceramic Restorations. Part 3: Double Veneer Technique. J Prosthodont. 2008;17:9-13.

[51] Aboushelib M. N, Kleverlaan C. J, Feilzer A. J. Microtensile bond strength of different components of core veneered all-ceramic restorations: Part II: Zirconia veneering ceramics. Dent Mater. 2006;22:857-63.

[52] Aboushelib M. N, Mirmohamadi H, Matinlinna J. P, Kukk E, Ounsi H. F, Salameh Z. Innovations in bonding to zirconia-based materials. Part II: Focusing on chemical interactions. Dent Mater. 2009;25:989-93.

[53] Zhang Y, Kim J-W. Graded structures for damage resistant and aesthetic all-ceramic restorations. Dental materials. 2009;25:781-90.

[54] Höland W, Rheinberger V, Schweiger M. Control of nucleation in glass ceramics. The Royal Society. 2003;361: 575-89.

[55] Höland W, Rheinberger V, Apel E, Hoen C. Principles and phenomena of bioengineering with glass-ceramics for dental restoration. Journal of the European Ceramic Society. 2007;27:1521-6.

[56] Headley T J, Loehman R E. Crystallization of a glass-ceramic by epitaxial growth. J Am Ceram Soc. 1984;67:620-5.

[57] Ntala P, Chen X, Niggli J, Cattell M. Development and testing of multi-phase glazes for adhesive bonding to zirconia substrates. J Dent. 2010;38:773-81.

[58] Monmaturapoj N, Lawita P, Thepsuwan W. Characterisation and Properties of Lithium Disilicate Glass Ceramics in the SiO2-Li2O-K2O-Al2O3 System for Dental Applications. Advances in Materials Science and Engineering. 2013;2013:1-11.

[59] 10 AE. Standard Test Methods for Determining Average Grain Size. 2010.

[60] 08 AC-. Standard Test Method for Vickers Indentation Hardness of Advanced Ceramics. 2008.

[61] VITA In-Ceram® YZ for inLab®.

[62] Hakala M. H., Foster A. S., Gavartin J. L., Havu P., Puska M. J., Nieminen R. M. Interfacial oxide growth at silicon/high-k oxide interfaces: First principles modeling of the Si–HfO2 interface. J Appl Phys. 2006;100:043708-1- -7

[63] Srdic ´ V. V., Winterer M, Hahn H. Sintering Behavior of Nanocrystalline Zirconia Doped with Alumina Prepared by Chemical Vapor Synthesis. J Am Ceram Soc. 2000;83:1853-60.

[64] Mosharraf R., Rismanchian M., Savabi O., Ashtiani A. H. Influence of surface modification techniques on shear bond strength between different zirconia cores and veneering ceramics. J Adv Prosthodont. 2011;3:221-8.

[65] El-Meliegy E., Noort R.V. Lithium Disilicate Glass Ceramics. Glasses and Glass Ceramic for Medical Applications. 1 ed. London: Springer Science+Business Media; 2012. p. 209-28.

[66] Höland W, Rheinberger V, Apel E, Ritzberger C, Rothbrust F, Kappert H, et al. Future perspectives of biomaterials for dental restoration. Journal of the European Ceramic Society. 2009; 29:1291-7.

[67] Belyakov A.V., Bakunov V.S. Development of rugged and crack-resistant structures in ceramics (review). Glass Ceram+. 1998;55:13-8.

[68] Shenoy A., Shenoy N. Dental ceramics: An update. J Conserv Dent 2010;13:195-203.

[69] Rosentiel S. F., Land M. F., Fujimoto J. Contemporary Fixed Prosthodontics. Third edition ed. St. Louis: Mosby, Inc; 2001.

[70] Tang X, Nakamura T, Usami H, Wakabayashi K, Yatani H. Effects of multiple firings on the mechanical properties and microstructure of veneering ceramics for zirconia frameworks. J Dent. 2012;40:372-80.

[71] Thompson J. Y., Stoner B. R., Piascik J.R., Smith R. Adhesion/cementation to zirconia and other non-silicate ceramics: Where are we now? Dent Mater 2011;27:71-82.

[72] ElBatal F. H., Azooz M. A., Hamdy Y. M. Preparation and characterization of some multicomponent silicate glasses and their glass–ceramics derivatives for dental applications. Ceram Int. 2009;35:1211-8.

[73] Esquivel-Upshaw J.F., Dieng F.Y., Clark A.E., Neal D., Anusavice K.J. surface Degradation of Dental ceramics as a Function of Environmental ph. J Dent Res 2013;92:467-71.

[74] Guess P. C., Kulis A., Witkowski S., Wolkewitzb M., Zhangc Y., Strub J.R. Shear bond strengths between different zirconia cores and veneering ceramics and their susceptibility to thermocycling. Dent Mater. 2008 24 1556-67.

[75] Kruzic J.J., Kim D.K., Koester K.J., Ritchie R.O. Indentation techniques for evaluating the fracture toughness of biomaterials and hard tissues. Journal Of The Mechanical Behavior Of Biomedical Matrials. 2009 2:384-95.

[76] Ferraris M., Verne E., Appendino P., Moisescu C., Krajewsk A., Ravaglioli A., et al. Coatings on zirconia for medical applications. Biomaterials. 2000;21: 765-73.

APPENDIX

SEM of VITA Zirconia

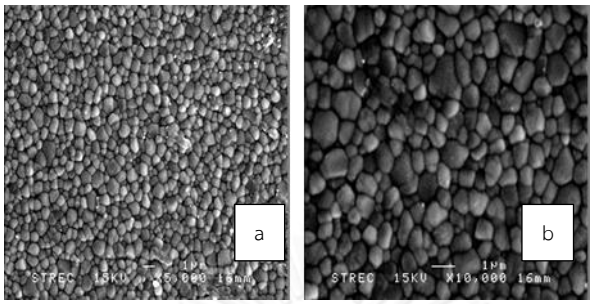

Figure 7.1 SEM of VITA Zirconia without thermocycling x5000 (a) and x10000 (b)

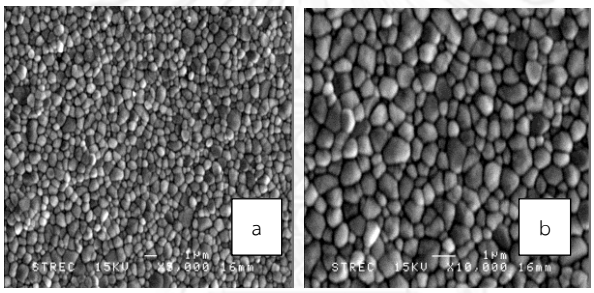

Figure 7.2 SEM of VITA Zirconia with thermocycling 5,000 cycles x5000 (a) and x10000 (b)

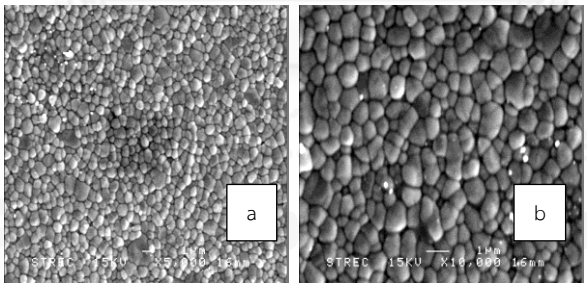

Figure 7.3 SEM of VITA Zirconia with thermocycling 10,000 cycles x5000 (a) and x10000 (b)

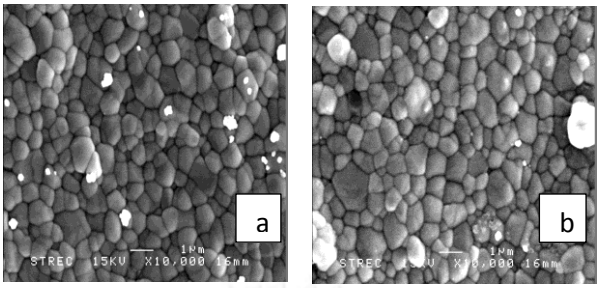

Figure 7.4 SEM of Lava Zirconia without thermocycling x10,000 (a) and with thermocycling 5,000 cycles x10,000 (b)

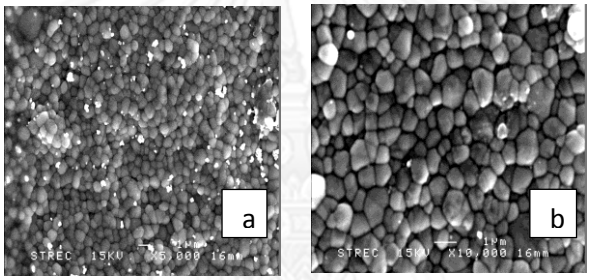

Figure 7.5 SEM of Lava Zirconia with thermocycling 10,000 cycle x 5000 (a) and x10,000 (b)

Mineral phase analysis by EDX of glass-ceramic bulk analysis

Table7.1 EDX Result of VG980 group

group	VG980			
Matrix	Elmt	Spect Type%	Element%	Atomic
	O K	ED	51.56	65.34
	Na K	ED	3.46	3.05
	Al K	ED	5.84	4.39
	Si K	ED	34.10	24.61
	K K	ED	4.54	2.35
	Ca K	ED	0.51	0.26
		Total	100.00	100.00
crystal	O K	ED	97.87	99.61
	Y K	ED	2.13*	0.39*
		Total	100.00	100.00

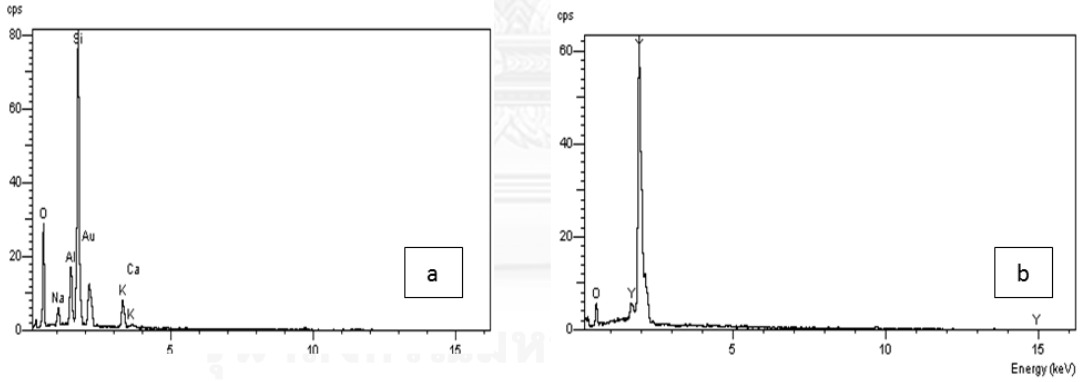

Figure 7.6 EDX of matrix area of VG980 (a), EDX of crystal of VG980 (b)

Table 7.2 EDX Result of LG810 group

	LG810			
Matrix	Elmt	Spect Type%	Element%	Atomic
	O K	ED	49.38	62.89
	Na K	ED	8.18	7.25
	Al K	ED	5.91	4.46
	Si K	ED	31.18	22.62
	K K	ED	3.98	2.08
	Ca K	ED	1.37	0.07
		Total	100.00	100.00
crystal	O K	ED	50.63	64.08
	Na K	ED	7.71	6.79
	Al K	ED	5.88	4.41
	Si K	ED	30.53	22.01
	K K	ED	3.96	2.05
	Ca K	ED	1.3	0.66
		Total	100	100.00

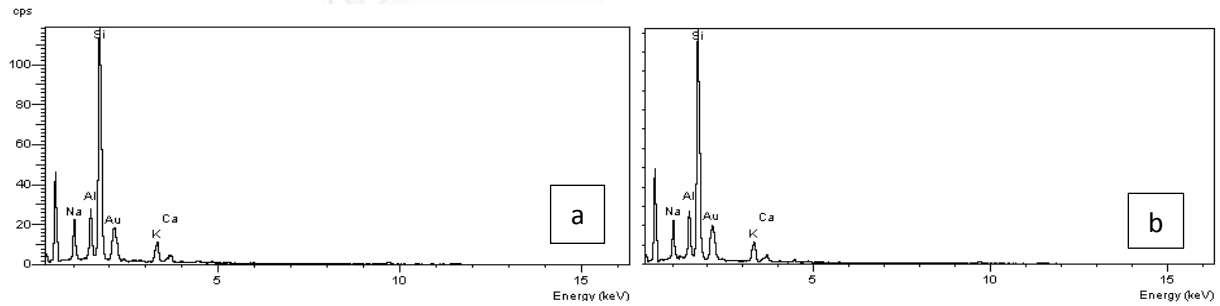

Figure 7.7 EDX of matrix area of LG (a), EDX of crystal of LG810 (b)

Table 7.3 EDX Result of LLi950 group after 2^{yr} dentin firing

	LLi950			
Matrix	Elmt	Spect Type%	Element%	Atomic
	C K	ED	44.61	57.74
	O K	ED	28.11	27.32
	Na K	ED	0.23*	0.15*
	Al K	ED	1.44	0.83
	Si K	ED	24.21	13.40
	K K	ED	0.54	0.22
	Ca K	ED	0.86	0.33
		Total	100.00	100.00
crystal	C K	ED	38.31	51.19
	O K	ED	31.97	32.08
	Na K	ED	0.68	0.48
	Al K	ED	2.01	1.19
	Si K	ED	24.69	14.11
	K K	ED	1.34	0.55
	Ca K	ED	1.00	0.40
		Total	100	100.00

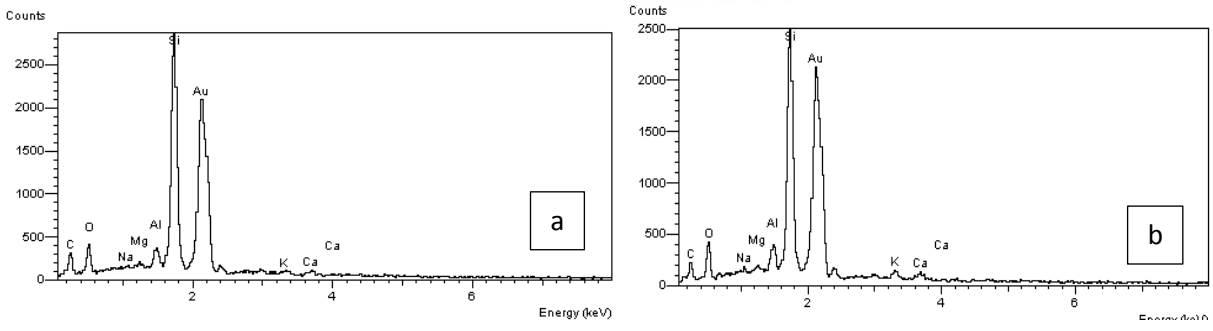

Figure 7.8 EDX of matrix area of LLi950 (a), EDX of crystal of LLi950 (b)

Table7.4 **Results of raw data of VITA zirconia shear bond strength (MPa.)**

	VD	VG980D	VLi800D	VLi850D	Vli900D
1	34.29	43.12	27.2	62.37	20.96
2	36.39	30.93	49.1	52.94	26.43
3	49	31.46	44.9	54.65	50.36
4	25.48	33.05	49.22	61.11	26.68
5	38.23	48.25	51.63	63.68	24.56
6	53.34	39.61	36.33	65.47	42.51
7	57.27	52.39	41.57	58.19	34.78
8	36.16	36.98	55.51	59.47	21.98

Table7.5 Test distribution of **VITA zirconia shear bond strength**

One-Sample Kolmogorov-Smirnov Test

		Shear
N		40
Normal Parameters[a,,b]	Mean	43.1888
	Std. Deviation	12.70165
Most Extreme Differences	Absolute	.105
	Positive	.088
	Negative	-.105
Kolmogorov-Smirnov Z		.663
Asymp. Sig. (2-tailed)		.771

a. Test distribution is Normal.

b. Calculated from data.

Table7.6 **Descriptive Statistics of Shear bond strength of VITA zirconia group**

	N	Mean	Std. Deviation	Std. Error	95% Confidence Interval for Mean		Minimum	Maximum
					Lower Bound	Upper Bound		
1	8	41.2700	10.81434	3.82345	32.2290	50.3110	25.48	57.27
2	8	39.4738	7.94503	2.80899	32.8315	46.1160	30.93	52.39
3	8	44.4325	9.18261	3.24654	36.7556	52.1094	27.20	55.51
4	8	59.7350	4.33876	1.53398	56.1077	63.3623	52.94	65.47
5	8	31.0325	10.58808	3.74345	22.1806	39.8844	20.96	50.36
Total	40	43.1888	12.70165	2.00831	39.1266	47.2509	20.96	65.47

Table7.7 Homogeneity of Variances of Shear bond strength of VITA zirconia group

Levene Statistic	df1	df2	Sig.
1.924	4	35	.128

Table7.8 One-way ANOVA of Shear bond strength of VITA zirconia group

	Sum of Squares	df	Mean Square	F	Sig.
Between Groups	3524.660	4	881.165	11.145	.000
Within Groups	2767.284	35	79.065		
Total	6291.945	39			

Table7.9 **Multiple Comparisons of Shear bond strength of VITA zirconia group**

Multiple Comparisons							
(I) 1=VD,2=VG980D,3=VLi800D,4=VLi850D,5=Vli900D		(J) 1=VD,2=VG980D,3=VLi800D,4=VLi850D,5=Vli900D	Mean Difference (I-J)	Std. Error	Sig.	95% Confidence Interval	
						Lower Bound	Upper Bound
Tukey HSD	1	2	1.79625	4.44593	.994	-10.9861	14.5786
		3	-3.16250	4.44593	.953	-15.9448	9.6198
		4	-18.46500*	4.44593	.002	-31.2473	-5.6827
		5	10.23750	4.44593	.168	-2.5448	23.0198
	2	1	-1.79625	4.44593	.994	-14.5786	10.9861
		3	-4.95875	4.44593	.797	-17.7411	7.8236
		4	-20.26125*	4.44593	.001	-33.0436	-7.4789
		5	8.44125	4.44593	.337	-4.3411	21.2236
	3	1	3.16250	4.44593	.953	-9.6198	15.9448
		2	4.95875	4.44593	.797	-7.8236	17.7411
		4	-15.30250*	4.44593	.012	-28.0848	-2.5202
		5	13.40000*	4.44593	.036	.6177	26.1823
	4	1	18.46500*	4.44593	.002	5.6827	31.2473
		2	20.26125*	4.44593	.001	7.4789	33.0436
		3	15.30250*	4.44593	.012	2.5202	28.0848
		5	28.70250*	4.44593	.000	15.9202	41.4848
	5	1	-10.23750	4.44593	.168	-23.0198	2.5448
		2	-8.44125	4.44593	.337	-21.2236	4.3411

		3	-13.40000*	4.44593	.036	-26.1823	-.6177
		4	-28.70250*	4.44593	.000	-41.4848	-15.9202
Tamhane	1	2	1.79625	4.74439	1.000	-14.1834	17.7759
		3	-3.16250	5.01586	1.000	-19.8646	13.5396
		4	-18.46500*	4.11969	.014	-33.5080	-3.4220
		5	10.23750	5.35091	.548	-7.4976	27.9726
	2	1	-1.79625	4.74439	1.000	-17.7759	14.1834
		3	-4.95875	4.29308	.956	-19.2397	9.3222
		4	-20.26125*	3.20055	.001	-31.4511	-9.0714
		5	8.44125	4.68016	.630	-7.2900	24.1725
	3	1	3.16250	5.01586	1.000	-13.5396	19.8646
		2	4.95875	4.29308	.956	-9.3222	19.2397
		4	-15.30250*	3.59070	.017	-28.1204	-2.4846
		5	13.40000	4.95515	.161	-3.0814	29.8814
	4	1	18.46500*	4.11969	.014	3.4220	33.5080
		2	20.26125*	3.20055	.001	9.0714	31.4511
		3	15.30250*	3.59070	.017	2.4846	28.1204
		5	28.70250*	4.04556	.000	13.9717	43.4333
	5	1	-10.23750	5.35091	.548	-27.9726	7.4976
		2	-8.44125	4.68016	.630	-24.1725	7.2900
		3	-13.40000	4.95515	.161	-29.8814	3.0814
		4	-28.70250*	4.04556	.000	-43.4333	-13.9717

*. The mean difference is significant at the 0.05 level.

Table7.10 **Homogeneous Subsets of Shear bond strength of VITA zirconia group**

Shear

	1=VD,2=VG980D,3=VLi800D,4=VLi850D,5=Vli900D	N	Subset for alpha = 0.05		
			1	2	3
Tukey HSD[a]	5	8	31.0325		
	2	8	39.4738	39.4738	
	1	8	41.2700	41.2700	
	3	8		44.4325	
	4	8			59.7350
	Sig.		.168	.797	1.000

Means for groups in homogeneous subsets are displayed.

a. Uses Harmonic Mean Sample Size = 8.000.

Mode of failure of VITA zirconia

	Porcelain side	Zirconia side	Back scatter
VG980D	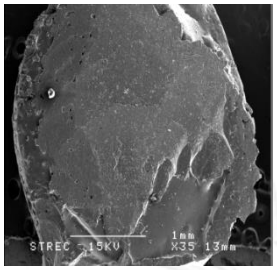	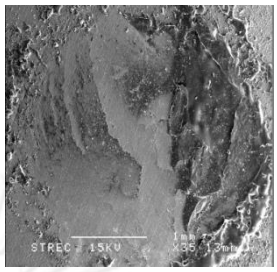	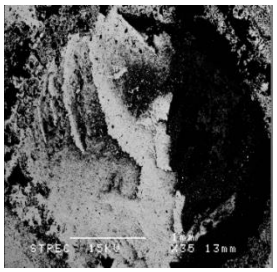
VLi800D	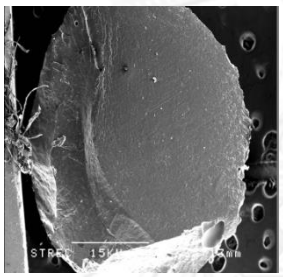	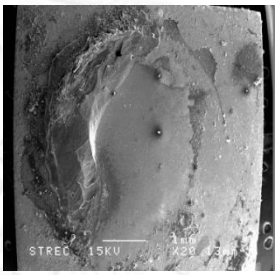	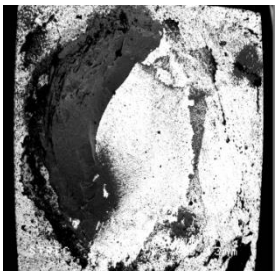

Figure 7.9 SEM micrographs showing modes of failure of VITA groups porcelain side of VG980D (a), zirconia side of VG980D (b), zirconia side of VG980D (back scattered) (c), porcelain side of VLi8000D (d), zirconia side of VLi800D (e) zirconia side of VLi800D (back scattered) (f)

VLi850D	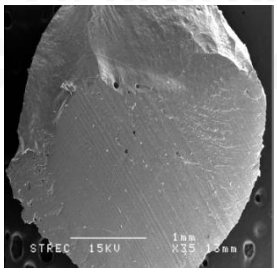	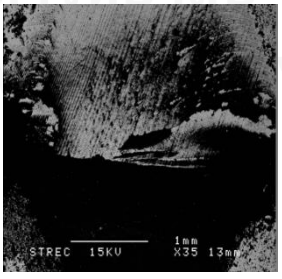

Figure 7.10 SEM micrographs showing modes of failure of porcelain side of VLi850D (a) and zirconia side of VLi850D (back scattered) (b)

VD	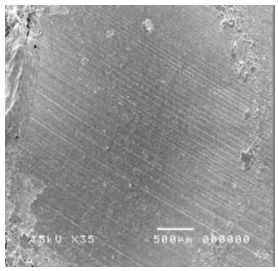	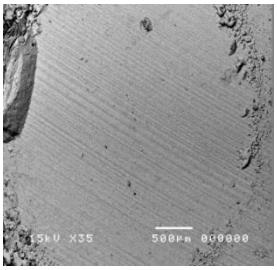

Figure 7.11 SEM micrographs showing modes of failure of porcelain side of VD (j), zirconia side of VD (k), zirconia side of VD (back scattered) (l).

Table7.11 Results of raw data of Lava zirconia shear bond strength (MPa.)

	LD	LG810D	LLi800D	LLi850D	LLi900D	LLi950D
1	10.62	14.1	10.97	6.54	21.91	25.45
2	12.32	23.78	4.64	4.61	15.23	35.41
3	15.91	18.32	15.03	5.51	20.64	18.64
4	17.39	30.49	10.17	19.08	15.44	24.9
5	30.48	14.68	5.83	9.46	22.78	26.61
6	17.23	25.78	5.65	4.79	18.89	20.48
7	19.13	20.16	3.29	18.4	18.87	24.26
8	12.71	10.99	14.19	5.9	21.51	25.1

Table7.12 Test distribution of **Lava zirconia shear bond strength**

One-Sample Kolmogorov-Smirnov Test

		shear
N		48
Normal Parameters[a,,b]	Mean	16.3653
	Std. Deviation	7.76310
Most Extreme Differences	Absolute	.089
	Positive	.089
	Negative	-.067
Kolmogorov-Smirnov Z		.608
Asymp. Sig. (2-tailed)		.854

a. Test distribution is Normal.

b. Calculated from data.

Table7.13 Descriptive Statistics of Shear bond strength of Lava zirconia group

	N	Mean	Std. Deviation	Std. Error	95% Confidence Interval for Mean		Minimum	Maximum
					Lower Bound	Upper Bound		
1	8	16.9738	6.19500	2.19026	11.7946	22.1529	10.62	30.48
2	8	19.7875	6.59563	2.33191	14.2734	25.3016	10.99	30.49
3	8	8.7213	4.48506	1.58571	4.9716	12.4709	3.29	15.03
4	8	9.2862	6.02803	2.13123	4.2467	14.3258	4.61	19.08
5	8	19.4087	2.86169	1.01176	17.0163	21.8012	15.23	22.78
6	8	25.1071	5.36221	2.02673	20.1479	30.0664	18.64	35.41
Total	48	16.3653	7.76310	1.13237	14.0860	18.6447	3.29	35.41

Table7.14 **Homogeneity of Variances of Shear bond strength of Lava zirconia group**

Levene Statistic	df1	df2	Sig.
.846	5	41	.525

Table7.15 One-way ANOVA of Shear bond strength of VITA zirconia group

ANOVA

	Sum of Squares	df	Mean Square	F	Sig.
Between Groups	1574.048	5	314.810	10.772	.000
Within Groups	1198.178	41	29.224		
Total	2772.226	46			

Table7.16 Multiple Comparisons of Shear bond strength of Lava zirconia group

Multiple Comparisons							
(I) 1=LD,2=LG810D,3=LLi800,4=LLi850D, 5=LLi900D,6=LLi950D		(J) 1=LD,2=LG810D,3=LLi800,4=LLi850D, 5=LLi900D,6=LLi950D	Mean Difference (I-J)	Std. Error	Sig.	95% Confidence Interval	
						Lower Bound	Upper Bound
Tukey HSD	1	2	-2.81375	2.70295	.901	-10.8919	5.2644
		3	8.25250*	2.70295	.043	.1743	16.3307
		4	7.68750	2.70295	.070	-.3907	15.7657
		5	-2.43500	2.70295	.944	-10.5132	5.6432
		6	-8.13339	2.79782	.061	-16.4951	.2283
	2	1	2.81375	2.70295	.901	-5.2644	10.8919
		3	11.06625*	2.70295	.003	2.9881	19.1444
		4	10.50125*	2.70295	.005	2.4231	18.5794
		5	.37875	2.70295	1.000	-7.6994	8.4569
		6	-5.31964	2.79782	.416	-13.6814	3.0421
	3	1	-8.25250*	2.70295	.043	-16.3307	-.1743
		2	-11.06625*	2.70295	.003	-19.1444	-2.9881
		4	-.56500	2.70295	1.000	-8.6432	7.5132
		5	-10.68750*	2.70295	.004	-18.7657	-2.6093
		6	-16.38589*	2.79782	.000	-24.7476	-8.0242
	4	1	-7.68750	2.70295	.070	-15.7657	.3907
		2	-10.50125*	2.70295	.005	-18.5794	-2.4231
		3	.56500	2.70295	1.000	-7.5132	8.6432
		5	-10.12250*	2.70295	.007	-18.2007	-2.0443
		6	-15.82089*	2.79782	.000	-24.1826	-7.4592
	5	1	2.43500	2.70295	.944	-5.6432	10.5132
		2	-.37875	2.70295	1.000	-8.4569	7.6994
		3	10.68750*	2.70295	.004	2.6093	18.7657
		4	10.12250*	2.70295	.007	2.0443	18.2007
		6	-5.69839	2.79782	.340	-14.0601	2.6633

	6	1	8.13339	2.79782	.061	-.2283	16.4951
		2	5.31964	2.79782	.416	-3.0421	13.6814
		3	16.38589*	2.79782	.000	8.0242	24.7476
		4	15.82089*	2.79782	.000	7.4592	24.1826
		5	5.69839	2.79782	.340	-2.6633	14.0601
Tamhane	1	2	-2.81375	3.19922	.999	-14.0760	8.4485
		3	8.25250	2.70402	.133	-1.4441	17.9491
		4	7.68750	3.05604	.313	-3.0640	18.4390
		5	-2.43500	2.41266	.998	-11.6725	6.8025
		6	-8.13339	2.98410	.231	-18.7908	2.5240
	2	1	2.81375	3.19922	.999	-8.4485	14.0760
		3	11.06625*	2.81997	.028	.8777	21.2548
		4	10.50125	3.15910	.073	-.6288	21.6313
		5	.37875	2.54194	1.000	-9.4481	10.2056
		6	-5.31964	3.08956	.823	-16.3629	5.7236
	3	1	-8.25250	2.70402	.133	-17.9491	1.4441
		2	-11.06625*	2.81997	.028	-21.2548	-.8777
		4	-.56500	2.65643	1.000	-10.0628	8.9328
		5	-10.68750*	1.88099	.002	-17.5415	-3.8335
		6	-16.38589*	2.57334	.001	-25.7789	-6.9929
	4	1	-7.68750	3.05604	.313	-18.4390	3.0640
		2	-10.50125	3.15910	.073	-21.6313	.6288
		3	.56500	2.65643	1.000	-8.9328	10.0628
		5	-10.12250*	2.35920	.023	-19.1169	-1.1281
		6	-15.82089*	2.94105	.002	-26.3261	-5.3157
	5	1	2.43500	2.41266	.998	-6.8025	11.6725
		2	-.37875	2.54194	1.000	-10.2056	9.4481
		3	10.68750*	1.88099	.002	3.8335	17.5415
		4	10.12250*	2.35920	.023	1.1281	19.1169
		6	-5.69839	2.26523	.398	-14.6563	3.2595
	6	1	8.13339	2.98410	.231	-2.5240	18.7908
		2	5.31964	3.08956	.823	-5.7236	16.3629
		3	16.38589*	2.57334	.001	6.9929	25.7789

		4	15.82089*	2.94105	.002	5.3157	26.3261
		5	5.69839	2.26523	.398	-3.2595	14.6563
*. The mean difference is significant at the 0.05 level.							

Table7.17 Homogeneous Subsets of Shear bond strength of Lava zirconia group

1=LD,2=LG810D,3=LLi800,4=LLi850D,5=LLi900D,6=LLi950D		N	Subset for alpha = 0.05		
			1	2	3
Tukey HSD[a,,b]	3	8	8.7213		
	4	8	9.2862	9.2862	
	1	8		16.9738	16.9738
	5	8			19.4087
	2	8			19.7875
	6	8			25.1071
	Sig.		1.000	.076	.052

Means for groups in homogeneous subsets are displayed.

a. Uses Harmonic Mean Sample Size = 7.814.

..The group sizes are unequal. The harmonic mean of the group sizes is used. Type I error levels are not guaranteed

Mode of failure of Lava zirconia

	Porcelain side	Zirconia side	Back scatter
LG810D	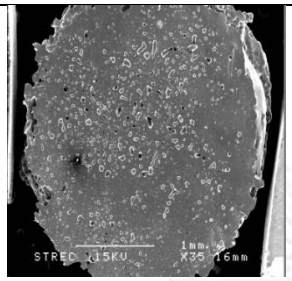	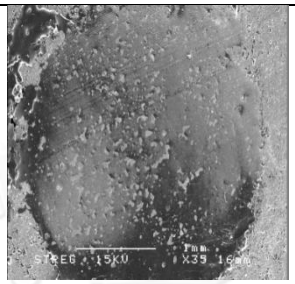	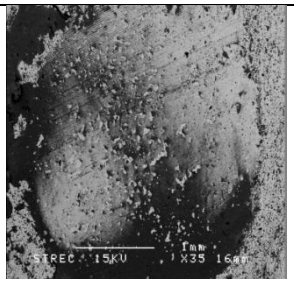
LLi800D	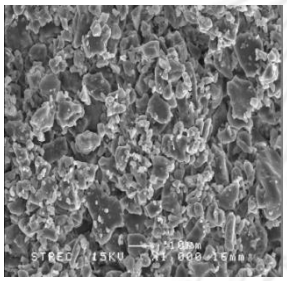	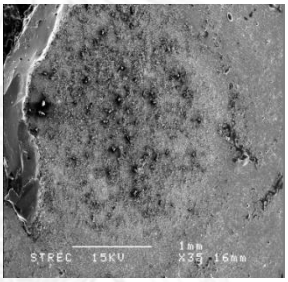	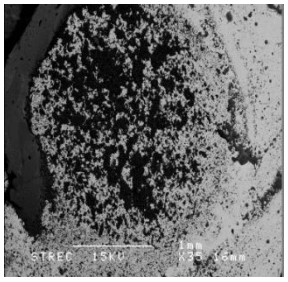
LLi950D	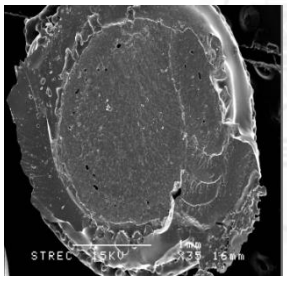	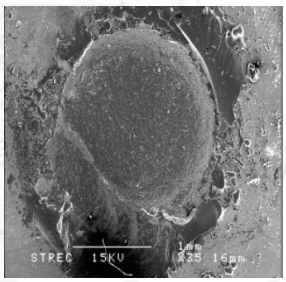	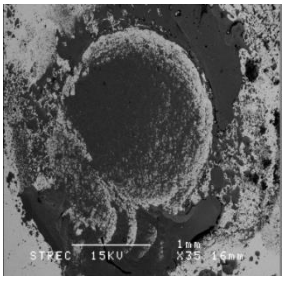

Figure 7.12 **SEM micrographs showing modes of failure of Lava groups Porcelain side of LG810D (a), zirconia side of LG810D (b), zirconia side of LG810D (back scattered mode) (c), porcelain side of LLi800D (d), and zirconia side of LLi800D (e), zirconia side of LLi800D (back scattered mode) (f), porcelain side of LLi950D (g), and zirconia side of LLi950D (h), zirconia side of LLi950D (back scattered mode) (i).**

Table7.18 **Results of raw data of VITA Zirconia before and after thermocycling treatment (MPa.)**

	VG980D	VG980D 5000 cycle	VG980D 10000 cycle	VLi850D	VLi850D 5000 cycle	VLi850D 10000 cycle
1	43.12	40.32	28.84	62.37	34.02	33.52
2	30.93	22.56	34.97	52.94	48.99	26.58
3	31.46	41.03	33.43	54.65	49.05	36.34
4	33.05	43.03	20.57	61.11	26.41	47.4
5	48.25	29.74	51.7	63.68	41.86	37.36
6	39.61	29.12	40.38	65.47	40.68	55.53
7	52.39	47.16	35.17	58.19	49.76	40.26
8	36.98	44.07	51.03	59.47	26.53	41.43

Table7.19 Test distribution of VITA zirconia before and after 5000 and 10,000 cycles thermocycling test

One-Sample Kolmogorov-Smirnov Test

		shear
N		48
Normal Parameters[a,,b]	Mean	42.13563
	Std. Deviation	11.425541
Most Extreme Differences	Absolute	.072
	Positive	.072
	Negative	-.045
Kolmogorov-Smirnov Z		.500
Asymp. Sig. (2-tailed)		.964

a. Test distribution is Normal.

b. Calculated from data.

Table7.20 **Descriptive Statistics of VITA zirconia before and after 5000 and 10,000 cycles thermocycling test**

	N	Mean	Std. Deviation	Std. Error	95% Confidence Interval for Mean		Minimum	Maximum
					Lower Bound	Upper Bound		
1	8	39.47375	7.945034	2.808994	32.83154	46.11596	30.930	52.390
2	8	37.12875	8.783244	3.105346	29.78577	44.47173	22.560	47.160
3	8	37.01125	10.563410	3.734730	28.18002	45.84248	20.570	51.700
4	8	59.73500	4.338756	1.533982	56.10771	63.36229	52.940	65.470
5	8	39.66250	9.731248	3.440516	31.52697	47.79803	26.410	49.760
6	8	39.80250	8.784673	3.105851	32.45833	47.14667	26.580	55.530
Total	48	42.13563	11.425541	1.649135	38.81799	45.45326	20.570	65.470

Table7.21 **Homogeneous Subsets of Shear bond strength of VITA zirconia before and after 5,000 and 10,000 cycles thermocycling test**

Levene Statistic	df1	df2	Sig.
1.145	5	42	.352

Table7.22 **Multiple Comparisons of VITA zirconia before and after 5,000 and 10,000 cycles thermocycling test**

Multiple Comparisons

Dependent Variable:shear

	(I) 1=VG980D, 2=VG980Dx5000, 3= VG980Dx100000, 4=VLi850D, 5=VLi850Dx5000, 6=VLi850Dx10000	(J) 1=VG980D, 2=VG980Dx5000, 3= VG980Dx100000, 4=VLi850D, 5=VLi850Dx5000, 6=VLi850Dx10000	Mean Difference (I-J)	Std. Error	Sig.	95% Confidence Interval	
						Lower Bound	Upper Bound
Tukey HSD	1	2	2.345000	4.294119	.994	-10.47401	15.16401
		3	2.462500	4.294119	.992	-10.35651	15.28151
		4	-20.261250*	4.294119	.000	-33.08026	-7.44224
		5	-.188750	4.294119	1.000	-13.00776	12.63026
		6	-.328750	4.294119	1.000	-13.14776	12.49026
	2	1	-2.345000	4.294119	.994	-15.16401	10.47401
		3	.117500	4.294119	1.000	-12.70151	12.93651
		4	-22.606250*	4.294119	.000	-35.42526	-9.78724
		5	-2.533750	4.294119	.991	-15.35276	10.28526
		6	-2.673750	4.294119	.989	-15.49276	10.14526
	3	1	-2.462500	4.294119	.992	-15.28151	10.35651
		2	-.117500	4.294119	1.000	-12.93651	12.70151
		4	-22.723750*	4.294119	.000	-35.54276	-9.90474
		5	-2.651250	4.294119	.989	-15.47026	10.16776
		6	-2.791250	4.294119	.986	-15.61026	10.02776

	4	1	20.261250*	4.294119	.000	7.44224	33.08026
		2	22.606250*	4.294119	.000	9.78724	35.42526
		3	22.723750*	4.294119	.000	9.90474	35.54276
		5	20.072500*	4.294119	.000	7.25349	32.89151
		6	19.932500*	4.294119	.000	7.11349	32.75151
	5	1	.188750	4.294119	1.000	-12.63026	13.00776
		2	2.533750	4.294119	.991	-10.28526	15.35276
		3	2.651250	4.294119	.989	-10.16776	15.47026
		4	-20.072500*	4.294119	.000	-32.89151	-7.25349
		6	-.140000	4.294119	1.000	-12.95901	12.67901
	6	1	.328750	4.294119	1.000	-12.49026	13.14776
		2	2.673750	4.294119	.989	-10.14526	15.49276
		3	2.791250	4.294119	.986	-10.02776	15.61026
		4	-19.932500*	4.294119	.000	-32.75151	-7.11349
		5	.140000	4.294119	1.000	-12.67901	12.95901
Tamhane	1	2	2.345000	4.187316	1.000	-12.41324	17.10324
		3	2.462500	4.673184	1.000	-14.22733	19.15233
		4	-20.261250*	3.200554	.001	-32.19728	-8.32522
		5	-.188750	4.441576	1.000	-15.93599	15.55849
		6	-.328750	4.187691	1.000	-15.08840	14.43090
	2	1	-2.345000	4.187316	1.000	-17.10324	12.41324
		3	.117500	4.857096	1.000	-17.08011	17.31511
		4	-22.606250*	3.463564	.001	-35.72866	-9.48384
		5	-2.533750	4.634687	1.000	-18.87016	13.80266
		6	-2.673750	4.391979	1.000	-18.12297	12.77547
	3	1	-2.462500	4.673184	1.000	-19.15233	14.22733
		2	-.117500	4.857096	1.000	-17.31511	17.08011
		4	-22.723750*	4.037487	.004	-38.46065	-6.98685
		5	-2.651250	5.077928	1.000	-20.53689	15.23439
		6	-2.791250	4.857419	1.000	-19.98981	14.40731

4	1	20.261250*	3.200554	.001	8.32522	32.19728
	2	22.606250*	3.463564	.001	9.48384	35.72866
	3	22.723750*	4.037487	.004	6.98685	38.46065
	5	20.072500*	3.766995	.006	5.57021	34.57479
	6	19.932500*	3.464016	.003	6.80803	33.05697
5	1	.188750	4.441576	1.000	-15.55849	15.93599
	2	2.533750	4.634687	1.000	-13.80266	18.87016
	3	2.651250	5.077928	1.000	-15.23439	20.53689
	4	-20.072500*	3.766995	.006	-34.57479	-5.57021
	6	-.140000	4.635025	1.000	-16.47750	16.19750
6	1	.328750	4.187691	1.000	-14.43090	15.08840
	2	2.673750	4.391979	1.000	-12.77547	18.12297
	3	2.791250	4.857419	1.000	-14.40731	19.98981
	4	-19.932500*	3.464016	.003	-33.05697	-6.80803
	5	.140000	4.635025	1.000	-16.19750	16.47750

Table7.23 **Homogeneous Subsets of Shear bond strength of VITA zirconia before and after 5000 and 10000 cycles thermocycling test**

	1=VG980D, 2=VG980Dx5000, 3= VG980Dx100000, 4=VLi850D, 5=VLi850Dx5000, 6=VLi850Dx10000	N	Subset for alpha = 0.05	
			1	2
Tukey HSD[a]	3	8	37.01125	
	2	8	37.12875	
	1	8	39.47375	
	5	8	39.66250	
	6	8	39.80250	
	4	8		59.73500
	Sig.		.986	1.000

Means for groups in homogeneous subsets are displayed.

a. Uses Harmonic Mean Sample Size = 8.000.

Table7.24 **Result of raw data of shear bond strength of Lava Zirconia before and after 5000 and 10000 cycles thermocycling treatment (MPa.)**

	LG810D	LG810D 5,000 cycles	Lg810D 10,000 cycles	LLi950D	LLi950D 5,000 cycles	LLi950 10,000 cycles
1	14.1	13.46	22.1	25.45	18.37	16
2	23.78	16.22	17.74	35.41	32.77	15.44
3	18.32	27.52	19.48	18.64	17.4	18.15
4	30.49	15.74	15.42	24.9	31.5	20.21
5	14.68	11.09	17.95	26.61	17.65	12.43
6	25.78	20.53	17.04	20.48	24	21.2
7	20.16	22.37	21.03	24.26	19.75	16.84
8	10.99	16.92	14.52	25.1	28	19.13

Table7.25 **Homogeneity of Variances of shear bond strength of Lava Zirconia before and after 5000 and 10,000 cycles thermocycling treatment**

One-Sample Kolmogorov-Smirnov Test

		shear
N		48
Normal Parameters[a,,b]	Mean	19.4702
	Std. Deviation	5.45329
Most Extreme Differences	Absolute	.122
	Positive	.122
	Negative	-.062
Kolmogorov-Smirnov Z		.843
Asymp. Sig. (2-tailed)		.477

a. Test distribution is Normal.

b. Calculated from data.

Table 7 26 Descriptive Statistics of Lava Zirconia before and after 5000 and 10,000 cycles thermocycling treatment

	N	Mean	Std. Deviation	Std. Error	95% Confidence Interval for Mean		Minimum	Maximum
					Lower Bound	Upper Bound		
1	8	19.7875	6.59563	2.33191	14.2734	25.3016	10.99	30.49
2	8	17.9813	5.26345	1.86091	13.5809	22.3816	11.09	27.52
3	8	18.1600	2.61138	.92326	15.9768	20.3432	14.52	22.10
4	8	19.7875	6.59563	2.33191	14.2734	25.3016	10.99	30.49
5	8	23.6800	6.34694	2.24398	18.3738	28.9862	17.40	32.77
6	8	17.4250	2.84612	1.00625	15.0456	19.8044	12.43	21.20
Total	48	19.4702	5.45329	.78711	17.8867	21.0537	10.99	32.77

Table 7.27 **Homogeneity of Variances of Lava Zirconia before and after 5000 and 10,000 cycles thermocycling treatment**

Levene Statistic	df1	df2	Sig.
2.663	5	42	.035

Table 7.28 **One-way ANOVA of Shear bond strength of Lava Zirconia before and after 5000 and 10,000 cycles thermocycling treatment**

	Sum of Squares	df	Mean Square	F	Sig.
Between Groups	208.322	5	41.664	1.471	.220
Within Groups	1189.383	42	28.319		
Total	1397.705	47			

Table 729. Multiple Comparisons of Lava Zirconia before and after 5,000 and 10,000 cycles thermocycling treatment

Multiple Comparisons

Dependent Variable:shear

	(I) 1=LG810D, 2=LG810D x5000, 3=Lg810Dx100000, 4=LLi950D, 5=LLi950Dx5000, 6=LLi950x10000	(J) 1=LG810D, 2=LG810D x5000, 3=Lg810Dx100000, 4=LLi950D, 5=LLi950Dx5000, 6=LLi950x10000	Mean Difference (I-J)	Std. Error	Sig.	95% Confidence Interval	
						Lower Bound	Upper Bound
Tukey HSD	1	2	1.80625	2.66076	.983	-6.1368	9.7493
		3	1.62750	2.66076	.990	-6.3155	9.5705
		4	.00000	2.66076	1.000	-7.9430	7.9430
		5	-3.89250	2.66076	.689	-11.8355	4.0505
		6	2.36250	2.66076	.947	-5.5805	10.3055
	2	1	-1.80625	2.66076	.983	-9.7493	6.1368
		3	-.17875	2.66076	1.000	-8.1218	7.7643
		4	-1.80625	2.66076	.983	-9.7493	6.1368
		5	-5.69875	2.66076	.286	-13.6418	2.2443
		6	.55625	2.66076	1.000	-7.3868	8.4993
	3	1	-1.62750	2.66076	.990	-9.5705	6.3155
		2	.17875	2.66076	1.000	-7.7643	8.1218
		4	-1.62750	2.66076	.990	-9.5705	6.3155
		5	-5.52000	2.66076	.320	-13.4630	2.4230
		6	.73500	2.66076	1.000	-7.2080	8.6780
	4	1	.00000	2.66076	1.000	-7.9430	7.9430
		2	1.80625	2.66076	.983	-6.1368	9.7493
		3	1.62750	2.66076	.990	-6.3155	9.5705
		5	-3.89250	2.66076	.689	-11.8355	4.0505
		6	2.36250	2.66076	.947	-5.5805	10.3055
	5	1	3.89250	2.66076	.689	-4.0505	11.8355
		2	5.69875	2.66076	.286	-2.2443	13.6418

		3	5.52000	2.66076	.320	-2.4230	13.4630
		4	3.89250	2.66076	.689	-4.0505	11.8355
		6	6.25500	2.66076	.197	-1.6880	14.1980
	6	1	-2.36250	2.66076	.947	-10.3055	5.5805
		2	-.55625	2.66076	1.000	-8.4993	7.3868
		3	-.73500	2.66076	1.000	-8.6780	7.2080
		4	-2.36250	2.66076	.947	-10.3055	5.5805
		5	-6.25500	2.66076	.197	-14.1980	1.6880
Tamhane	1	2	1.80625	2.98342	1.000	-8.7904	12.4029
		3	1.62750	2.50803	1.000	-8.2003	11.4553
		4	.00000	3.29781	1.000	-11.6004	11.6004
		5	-3.89250	3.23624	.986	-15.2796	7.4946
		6	2.36250	2.53975	.999	-7.4640	12.1890
	2	1	-1.80625	2.98342	1.000	-12.4029	8.7904
		3	-.17875	2.07735	1.000	-8.0438	7.6863
		4	-1.80625	2.98342	1.000	-12.4029	8.7904
		5	-5.69875	2.91521	.672	-16.0226	4.6251
		6	.55625	2.11555	1.000	-7.3456	8.4581
	3	1	-1.62750	2.50803	1.000	-11.4553	8.2003
		2	.17875	2.07735	1.000	-7.6863	8.0438
		4	-1.62750	2.50803	1.000	-11.4553	8.2003
		5	-5.52000	2.42649	.522	-14.9753	3.9353
		6	.73500	1.36563	1.000	-4.0757	5.5457
	4	1	.00000	3.29781	1.000	-11.6004	11.6004
		2	1.80625	2.98342	1.000	-8.7904	12.4029
		3	1.62750	2.50803	1.000	-8.2003	11.4553
		5	-3.89250	3.23624	.986	-15.2796	7.4946
		6	2.36250	2.53975	.999	-7.4640	12.1890
	5	1	3.89250	3.23624	.986	-7.4946	15.2796
		2	5.69875	2.91521	.672	-4.6251	16.0226

		3	5.52000	2.42649	.522	-3.9353	14.9753
		4	3.89250	3.23624	.986	-7.4946	15.2796
		6	6.25500	2.45927	.365	-3.2044	15.7144
	6	1	-2.36250	2.53975	.999	-12.1890	7.4640
		2	-.55625	2.11555	1.000	-8.4581	7.3456
		3	-.73500	1.36563	1.000	-5.5457	4.0757
		4	-2.36250	2.53975	.999	-12.1890	7.4640
		5	-6.25500	2.45927	.365	-15.7144	3.2044

Table7.30 Homogeneous Subsets of Lava Zirconia before and after 5,000 and 10,000 cycles thermocycling treatment

shear

	1=LG810D, 2=LG810D x5000, 3=Lg810Dx100000, 4=LLi950D, 5=LLi950Dx5000, 6=LLi950x10000	N	Subset for alpha = 0.05
			1
Tukey HSD[a]	6	8	17.4250
	2	8	17.9813
	3	8	18.1600
	1	8	19.7875
	4	8	19.7875
	5	8	23.6800
	Sig.		.197

Means for groups in homogeneous subsets are displayed.

a. Uses Harmonic Mean Sample Size = 8.000.

Table7.31 Raw data of Vickers hardness of bulk glass

	LG810	LLi950	VG980	VLi850
1	3.522	5.892	4.239	5.511
2	4.761	6.1	3.638	5.388
3	4.304	5.464	4.175	5.154
4	4.461	5.952	3.537	4.967
5	4.49	5.483	3.717	5.217
6	4.516	5.31	5.453	5.135
7	4.256	5.461	5.578	5.125
8	4.733	5.114	4.182	5.644
9	4.367	5.192	4.213	5.585
10	4.514	4.951	4.582	5.212
11	4.51	5.085	4.278	5.017
12	4.403	5.104	4.233	5.115
13	4.347	6.057	4.16	4.833
14	4.345	5.468	4.338	5.04
15	4.329	5.511	4.192	4.975
16	4.548	5.285	4.239	5.102
17	4.751	6.567	4.057	5.044
18	4.522	5.812	4.517	5.448
19	4.584	6.089	4.371	5.667
20	4.416	5.561	4.496	5.938
21	4.658	6.135	4.272	5.373
22	3.997	5.009	4.239	5.015
23	4.489	5.163	4.611	5.242
24	4.559	6.48	4.288	4.944
25	4.461	5.165	4.663	5.336

Table 7.32 Test distribution of **Vickers hardness of bulk glass**

One-Sample Kolmogorov-Smirnov Test

		Vicker
N		100
Normal Parameters[a,,b]	Mean	498.9140
	Std. Deviation	65.95634
Most Extreme Differences	Absolute	.114
	Positive	.114
	Negative	-.069
Kolmogorov-Smirnov Z		1.136
Asymp. Sig. (2-tailed)		.151

a. Test distribution is Normal.

b. Calculated from data.

Table 7.33 One-way ANOVA of Vickers hardness of bulk glass

ANOVA

Vicker

	Sum of Squares	df	Mean Square	F	Sig.
Between Groups	292439.413	3	97479.804	67.697	.000
Within Groups	138234.227	96	1439.940		
Total	430673.640	99			

Table 7.34 Multiple Comparisons of **Vickers hardness** of bulk glass

Multiple Comparisons

Dependent Variable:Vicker

	(I) 1=Lavaframe, 2=LavaLi950, 3=Vitaeffect, 4=VitaLi850	(J) 1=Lavaframe, 2=LavaLi950, 3=Vitaeffect, 4=VitaLi850	Mean Difference (I-J)	Std. Error	Sig.	95% Confidence Interval	
						Lower Bound	Upper Bound
Tukey HSD	1	2	-117.58800*	10.73290	.000	-145.6503	-89.5257
		3	9.42800	10.73290	.816	-18.6343	37.4903
		4	-83.40000*	10.73290	.000	-111.4623	-55.3377
	2	1	117.58800*	10.73290	.000	89.5257	145.6503
		3	127.01600*	10.73290	.000	98.9537	155.0783
		4	34.18800*	10.73290	.010	6.1257	62.2503
	3	1	-9.42800	10.73290	.816	-37.4903	18.6343
		2	-127.01600*	10.73290	.000	-155.0783	-98.9537
		4	-92.82800*	10.73290	.000	-120.8903	-64.7657
	4	1	83.40000*	10.73290	.000	55.3377	111.4623
		2	-34.18800*	10.73290	.010	-62.2503	-6.1257
		3	92.82800*	10.73290	.000	64.7657	120.8903
Tamhane	1	2	-117.58800*	10.76760	.000	-147.5531	-87.6229
		3	9.42800	10.42574	.938	-19.5458	38.4018
		4	-83.40000*	7.43748	.000	-103.8174	-62.9826
	2	1	117.58800*	10.76760	.000	87.6229	147.5531
		3	127.01600*	13.23156	.000	90.7068	163.3252
		4	34.18800*	11.03152	.022	3.5938	64.7822
	3	1	-9.42800	10.42574	.938	-38.4018	19.5458
		2	-127.01600*	13.23156	.000	-163.3252	-90.7068
		4	-92.82800*	10.69809	.000	-122.4583	-63.1977
	4	1	83.40000*	7.43748	.000	62.9826	103.8174
		2	-34.18800*	11.03152	.022	-64.7822	-3.5938
		3	92.82800*	10.69809	.000	63.1977	122.4583

Multiple Comparisons

Dependent Variable:Vicker

	(I) 1=Lavaframe, 2=LavaLi950, 3=Vitaeffect, 4=VitaLi850	(J) 1=Lavaframe, 2=LavaLi950, 3=Vitaeffect, 4=VitaLi850	Mean Difference (I-J)	Std. Error	Sig.	95% Confidence Interval	
						Lower Bound	Upper Bound
Tukey HSD	1	2	-117.58800*	10.73290	.000	-145.6503	-89.5257
		3	9.42800	10.73290	.816	-18.6343	37.4903
		4	-83.40000*	10.73290	.000	-111.4623	-55.3377
	2	1	117.58800*	10.73290	.000	89.5257	145.6503
		3	127.01600*	10.73290	.000	98.9537	155.0783
		4	34.18800*	10.73290	.010	6.1257	62.2503
	3	1	-9.42800	10.73290	.816	-37.4903	18.6343
		2	-127.01600*	10.73290	.000	-155.0783	-98.9537
		4	-92.82800*	10.73290	.000	-120.8903	-64.7657
	4	1	83.40000*	10.73290	.000	55.3377	111.4623
		2	-34.18800*	10.73290	.010	-62.2503	-6.1257
		3	92.82800*	10.73290	.000	64.7657	120.8903
Tamhane	1	2	-117.58800*	10.76760	.000	-147.5531	-87.6229
		3	9.42800	10.42574	.938	-19.5458	38.4018
		4	-83.40000*	7.43748	.000	-103.8174	-62.9826
	2	1	117.58800*	10.76760	.000	87.6229	147.5531
		3	127.01600*	13.23156	.000	90.7068	163.3252
		4	34.18800*	11.03152	.022	3.5938	64.7822
	3	1	-9.42800	10.42574	.938	-38.4018	19.5458
		2	-127.01600*	13.23156	.000	-163.3252	-90.7068
		4	-92.82800*	10.69809	.000	-122.4583	-63.1977
	4	1	83.40000*	7.43748	.000	62.9826	103.8174
		2	-34.18800*	11.03152	.022	-64.7822	-3.5938
		3	92.82800*	10.69809	.000	63.1977	122.4583

*. The mean difference is significant at the 0.05 level.

Table 7.35 Homogeneous Subsets of Vickers hardness of bulk glass

Vicker

	1=Lavaf rame, 2=Lava Li950, 3=Vitaef fect, 4=VitaLi 850	N	Subset for alpha = 0.05		
			1	2	3
Tukey HSD[a]	3	25	441.5960		
	1	25	451.0240		
	4	25		534.4240	
	2	25			568.6120
	Sig.		.816	1.000	1.000

Means for groups in homogeneous subsets are displayed.

a. Uses Harmonic Mean Sample Size = 25.000.

Table7.32 Raw data of Fracture toughness of bulk glass

	LG810	LLi950	VG980	Vli850
1	1.33167176	1.15053071	1.33167176	1.48942551
2	1.22593217	1.49667906	1.22593217	1.48841804
3	1.17420136	0.92284433	1.17420136	1.67269612
4	1.47162804	1.12495581	1.47162804	1.68458973
5	1.0424717	1.94463673	1.0424717	1.46981849
6	1.63303164	1.80568604	1.63303164	1.91450437
7	1.38311102	2.24700359	1.38311102	1.68129469
8	1.44287501	1.59698391	1.44287501	1.40713903
9	1.19822714	1.81242266	1.19822714	1.55355161
10	1.36773681	1.91195419	1.36773681	2.10072946
11	1.43763252	1.5576157	1.43763252	1.77340649
12	1.35846109	1.43707836	1.35846109	1.27053993
13	1.31655111	1.49617109	1.31655111	1.34382219
14	1.41473778	1.59632365	1.41473778	1.87893906
15	1.63322752	1.47261663	1.63322752	1.63029341
16	1.34566424	2.12905773	1.34566424	1.46866889
17	1.42653844	1.8024488	1.42653844	1.89476209
18	1.22115043	1.98773575	1.22115043	1.84914986
19	1.33867269	1.8703116	1.33867269	1.78743084
20	1.2275736	1.84782547	1.2275736	1.80545449
21	1.29716427	1.88178828	1.29716427	1.51714946
22	1.21729936	1.49355115	1.21729936	1.83585771
23	1.37476309	1.50458951	1.37476309	0.00472397
24	1.27435216	1.63097725	1.27435216	1.50990194
25	1.56799109	1.49862895	1.56799109	1.58974605

Table 7.33 Test distribution of **Fracture toughness of bulk glass**

One-Sample Kolmogorov-Smirnov Test

		Fracture
N		100
Normal Parameters[a,,b]	Mean	1.6165
	Std. Deviation	.36163
Most Extreme Differences	Absolute	.092
	Positive	.092
	Negative	-.065
Kolmogorov-Smirnov Z		.917
Asymp. Sig. (2-tailed)		.369

a. Test distribution is Normal.

b. Calculated from data.

Table 7.34 **Homogeneity of Variances of Fracture toughness of bulk glass**

Levene Statistic	df1	df2	Sig.
3.649	3	96	.015

Table 7.35 One-way ANOVA of Fracture toughness of bulk glass

	Sum of Squares	df	Mean Square	F	Sig.
Between Groups	3.624	3	1.208	12.441	.000
Within Groups	9.322	96	.097		
Total	12.947	99			

Table 7.36 Multiple Comparisons of Fracture toughness of bulk glass

Multiple Comparisons

Dependent Variable:Fracture

	(I) 1=Lavaframe, 2=LavaLi950, 3=Vitaeffect, 4=VitaLi850	(J) 1=Lavaframe, 2=LavaLi950, 3=Vitaeffect, 4=VitaLi850	Mean Difference (I-J)	Std. Error	Sig.	95% Confidence Interval	
						Lower Bound	Upper Bound
Tamhane	1	2	-.29991*	.06838	.001	-.4911	-.1087
		3	-.53466*	.07533	.000	-.7461	-.3233
		4	-.23597*	.08226	.044	-.4675	-.0044
	2	1	.29991*	.06838	.001	.1087	.4911
		3	-.23475	.09365	.090	-.4919	.0224
		4	.06394	.09931	.988	-.2091	.3370
	3	1	.53466*	.07533	.000	.3233	.7461
		2	.23475	.09365	.090	-.0224	.4919
		4	.29869*	.10422	.036	.0126	.5848
	4	1	.23597*	.08226	.044	.0044	.4675
		2	-.06394	.09931	.988	-.3370	.2091
		3	-.29869*	.10422	.036	-.5848	-.0126

*. The mean difference is significant at the 0.05 level.

Table 7.37 Homogeneous Subsets of fracture toughness of bulk glass

Fracture

	1=Lavaframe, 2=LavaLi950, 3=Vitaeffect, 4=VitaLi850	N	Subset for alpha = 0.05		
			1	2	3
Tukey B[a]	1	25	1.3489		
	4	25		1.5849	
	2	25		1.6488	
	3	25			1.8836

Means for groups in homogeneous subsets are displayed.

a. Uses Harmonic Mean Sample Size = 25.000.

VITA

Miss Kamolporn Wattanasirmkit was born in Bangkok, Thailand on December 26th, 1974. In 1999, she received the Degree of Doctor of Dental Surgery (D.D.S.) from the Faculty of Dentistry, Chulalongkorn University. After graduation, she work as a Dentist at Thepsathid Hospital, Chaiyaphom. In 2001, she started her post-graduated study for the Master of Science in Prosthodontics Program (M.Sc.) at Faculty of Dentistry, Chulalongkorn University. After she finished her Master degree in 2003, she has been work as a lecturer in Prosthodontics Department, Faculty of Dentistry, Chulalongkorn University. In 2008, She started her study for the Degree of Doctor of Philosophy Program in Dental-Biomaterials at Graduate School, Chulalongkorn University.